Estimating the capacity of a production well

Christopher J. Neville
S.S. Papadopulos & Associates, Inc.
Last update: February 17, 2026

Overview

These notes address one of the most basic, but also one of the most important, assignments of a hydrogeologist: the estimation of the capacity of a production well. Assessing the capacity of a well is not something a hydrogeologist wants to get wrong, but there are plenty of opportunities to do so. Estimating the long-term capacity of a well necessarily involves a large degree of extrapolation, so it is important to recognize from the outset that professional judgement is essential.

The notes begin with some definitions to distinguish between the capacity and the sustainable yield of a production well. The treatment of the capacity of a well is built up gradually, starting with simplified approaches that are appropriate when the water level in a well stabilizes during testing. The discussion then proceeds to consideration of tests during which the water levels in the pumping well do not stabilize. The role and interpretation of step tests will be highlighted.

A case study is presented to highlight the caution that is required when extrapolating from the observations during short-term tests to predictions of long-term well performance. The results of the analyses demonstrate the importance of selecting the appropriate conceptual model for the aquifer when making long-term predictions.

Table of Contents

1. Key definitions

We begin by distinguishing between two concepts that have been associated with the rate at which a well can be pumped: the *safe yield of a well* and the *sustainable yield of a well*.

The **safe yield of a well** is defined here as the average rate at which a well can be pumped without the water level in the well declining below a minimum specified level after a specified duration of pumping.

The **sustainable yield of a well** is defined here as the average rate at which a well can be pumped without there being unacceptable impacts. The definition of sustainable yield offered here is consistent with an inclusive definition of *sustainable water resource developments* proposed by the American Society of Civil Engineers as those developments that are designed and managed "to maintain ecological, environmental, and hydrological integrity" (ASCE, 1998).

The safe yield is the focus of our notes and to avoid any confusion between the terms "sustainable" and "safe" we will refer to the safe yield as the **long-term capacity of a well**.

Although our focus is limited to the capacity of a well, we recognize that an assessment of the yield of a well is <u>not</u> complete if it is assumed that the only potentially undesirable effect of pumping is the decline of the water level in the pumping well below a specified minimum level. A complete assessment of the yield of a well will generally require answering broader questions.

- Is there a possibility that pumping will cause declines in water levels in neighboring wells (private or municipal) that impair the ability of those wells to produce water?

- Is there a possibility that declines in groundwater discharge to streams, or induced leakage from streams, will be sufficient to affect the ecology of the streams, including the temperature regimes?

- Is there a possibility that pumping will induce the migration of water with undesirable characteristics? Specific cases might require assessments of the likelihood of upconing of brine or seawater intrusion.

2. Well design considerations

The focus of these notes is directed primarily towards the control that the aquifer exerts on the capacity of a production well. However, it is important to bear in mind that the well capacity is influenced by several design factors, including:

- The specification of the length of the screened or open interval of the well;
- The selection of the well screen diameter;
- The selection of the screen type;
- The specification of the filter pack (sand/gravel pack); and
- The choice of well development methods.

There is an extensive literature on well design. A list of selected references is appended to these notes. The must-have book is Groundwater and Wells (3rd edition: Sterrett et al., 2007). The third edition appears to be abbreviated compared to the second edition, but that is only because the appendices are included on an accompanying CD. In these notes we review briefly only three aspects of well design, the length of the open interval of the well, the screen transmitting capacity of a well and the development effort of the constructed well.

2.1. Length of the open interval of the well

Guidance regarding the length of the screened interval of a well is provided in Groundwater and Wells (pp. 429-430) and illustrated schematically in Figure 1.

a) Confined aquifer **b) Unconfined aquifer**

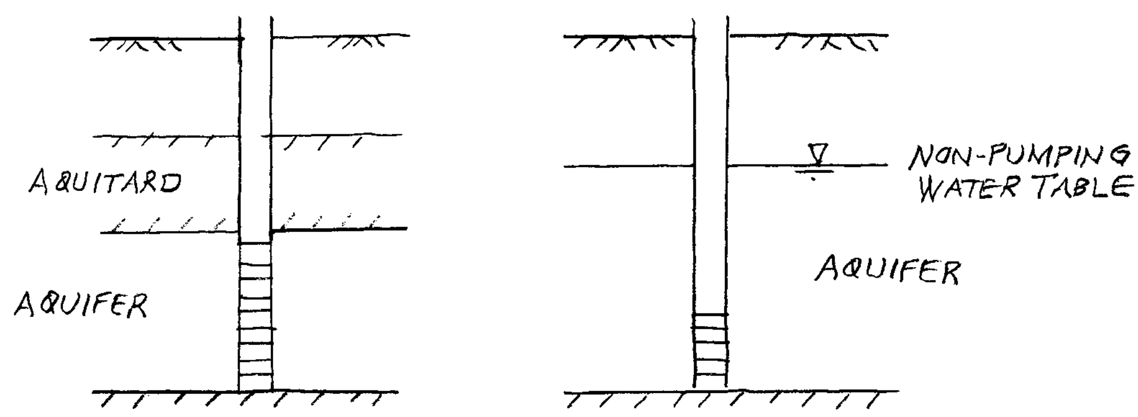

Figure 1. Recommended lengths of the open interval in homogenous aquifers

Confined aquifers

- When the aquifer is homogeneous, 80% to 90% of the aquifer thickness should be screened.
- When the aquifer is heterogeneous, 80% to 90% of the most permeable thickness should be screened.

Unconfined aquifers

- When the aquifer is homogeneous, screening the lower third to lower half of an aquifer "provides the optimum design".
- When the aquifer is heterogeneous, selectively placing screens across the most permeable layers of the lower portions of the aquifer "maximizes available drawdown and yield".

2.2. Screen transmitting capacity

The design details of a well screen control how much water can pass through the well screen efficiently. The maximum flow rate for an efficient well screen is referred to as the *well screen transmitting capacity* (Driscoll, 1986; p. 453). Driscoll (1986) makes the important point:

> *It should be recognized that the transmitting capacity of a well screen is a hydraulic characteristic of the screen itself at the assumed entrance velocity, and is not a measure of the yielding ability of the water-bearing formation in which the screen might be installed.*

The well screen transmitting capacity can be used to check whether the selected well screen will deliver the required pumping rate efficiently. The conceptual model for the estimation of the screen transmitting capacity is shown schematically in Figure 2.

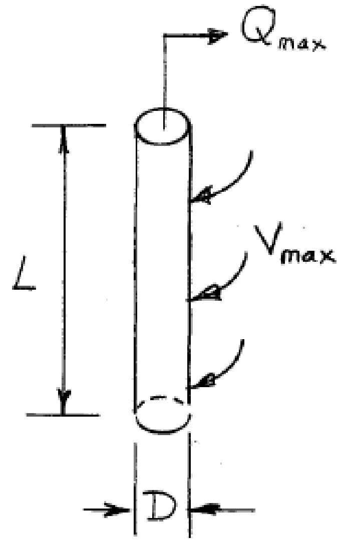

Figure 2. Conceptual model for the estimation of the screen transmitting capacity

In general terms, the inflow groundwater velocity across the well screen should be less than some maximum value for efficient performance:

$$v = \frac{Q}{A} < v_{max}$$

Here Q is the pumping rate and A is the screen open area. It is indicated in Groundwater and Wells that v_{max} for an efficient screened well is about **0.1 ft/s (0.03 m/s)**. This maximum velocity maintains laminar flow across the well screen.

The screen open area is calculated as:

$$A = \text{screen surface area} \times \text{fraction of open area}$$

The screen surface area is calculated as:

$$\text{screen surface area} = \pi\, D\, L$$

Here D and L are the screen diameter and length.

The screen transmitting capacity per unit length of screen is therefore given by:

$$\frac{Q_{max}}{L} = v_{max}\ \pi\, D \times \text{fraction of open area}$$

Example calculations:

- Screen type: 60-slot, wire-wrap (continuous slot)
- Well screen inner diameter, d = 8 inches

Referring to Groundwater and Wells (3rd edition; Table 9.15), the fraction of open area (% open area) of this particular screen is 41%.

The screen transmitting capacity per unit length of well screen is therefore:

$$\frac{Q_{max}}{L} = (0.1\ \text{ft/s})\ \pi\ (8\ \text{in}) \times (0.41) \left|\frac{\text{ft}}{12\ \text{in}}\right| \left|\frac{7.481\ \text{gal}}{\text{ft}^3}\right| \left|\frac{60\ \text{sec}}{\text{min}}\right| = \mathbf{38.5\ \frac{gpm}{ft}}$$

2.3. The influence of well development on well capacity

Development is an essential operation in the proper completion of any water well and the maximum specific capacity will rarely be reached without it. Driscoll (1986; p. 497-499) provides the following important advice regarding well development.

> *All new wells should be developed before being put into production to achieve sand-free water at the highest possible specific capacity. In addition, older wells often require periodic redevelopment to maintain or even improve the original yield and drawdown conditions.*

Data from Werner et al. (1980) reproduced in Figure 3 illustrate that the eventual specific capacity of a well depends to a great extent on what development method is used.

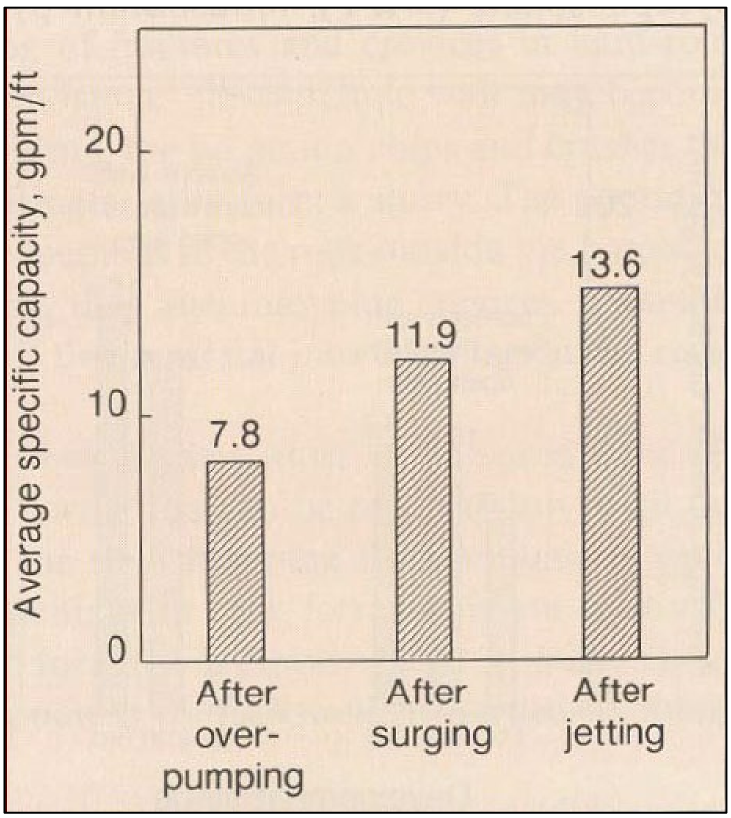

Figure 3. Specific capacity values for three development methods
Data from Werner et al. (1980)

Vonhof (1975) conducted sequential slug tests during well development to obtain an objective measure of the progress of well development. The results of the testing for Well G are plotted in Figure 4. After the well screen was installed, the well was developed with air until the discharge water was sand-free. Two more rounds of development were conducted. A slug test was conducted after each round of development. As shown in the plot of the results, the response time of the well decreased during each test, due to the removal of drilling mud in the aquifer immediate surrounding the well screen. These results translate directly to an increase in the capacity of the well.

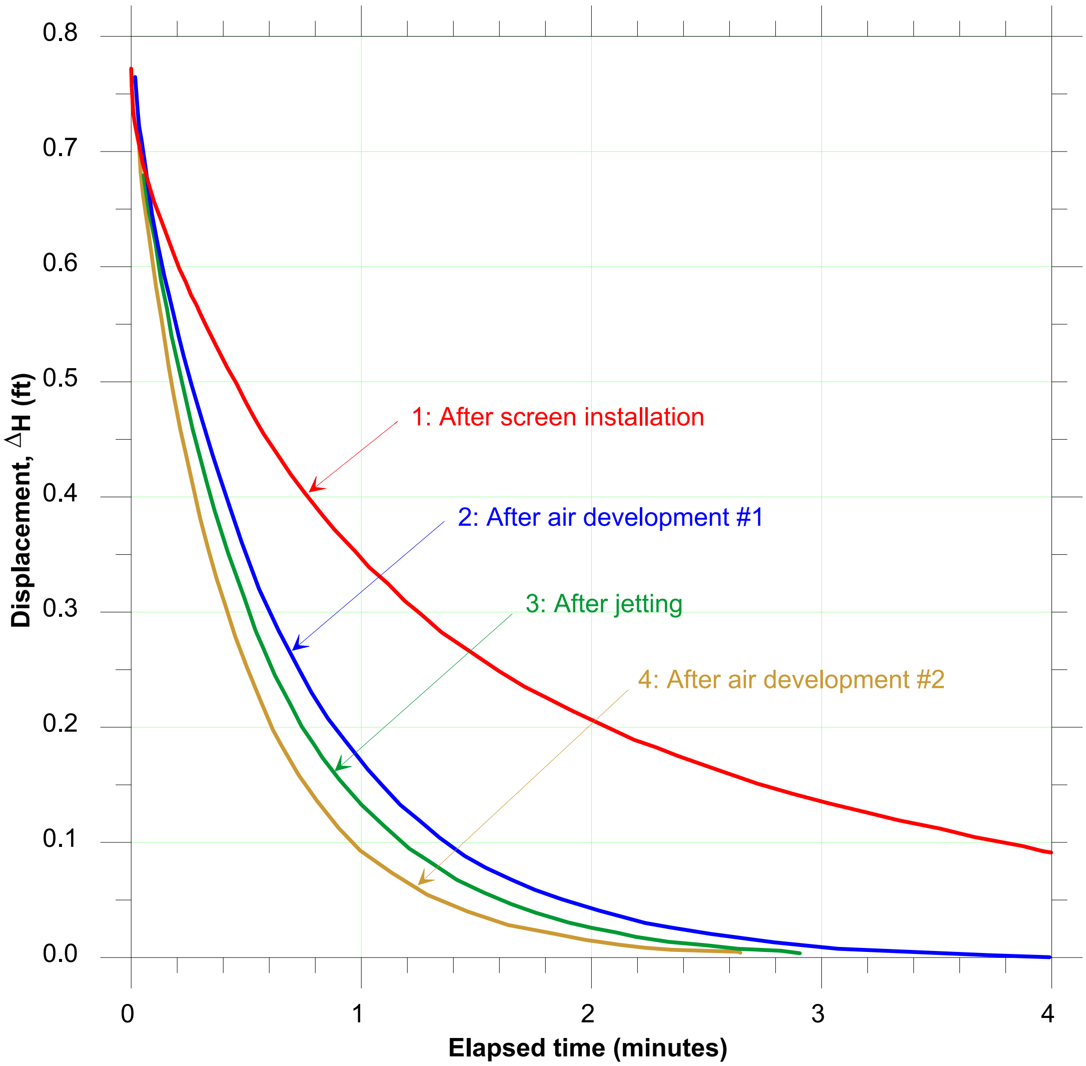

Figure 4. Well response during development
Data from Vonhof (1975)

3. Maximum allowable drawdown

The maximum allowable drawdown is defined as the difference between the non-pumping water level and the minimum allowable water level in the well.

Confined aquifer

According to the *Guide to Groundwater Authorization* (Alberta Environment, 2011), the maximum allowable drawdown for a production well in a confined aquifer is the difference between the non-pumping water level and the elevation of the top of the aquifer (Figure 5).

We can conceive of at least two other definitions:

- The difference between the non-pumping water level and the elevation of the top of the well screen; and
- The difference between the non-pumping water level and the elevation of the pump intake.

In light of the uncertainties inherent in estimating the long-term capacity of a well, we recommend that some margin of safety be added to the definition that is selected. For example, the maximum permissible drawdown might be defined as the difference between the non-pumping level and a point that is 5 feet above the topmost screen slot (1.5 m).

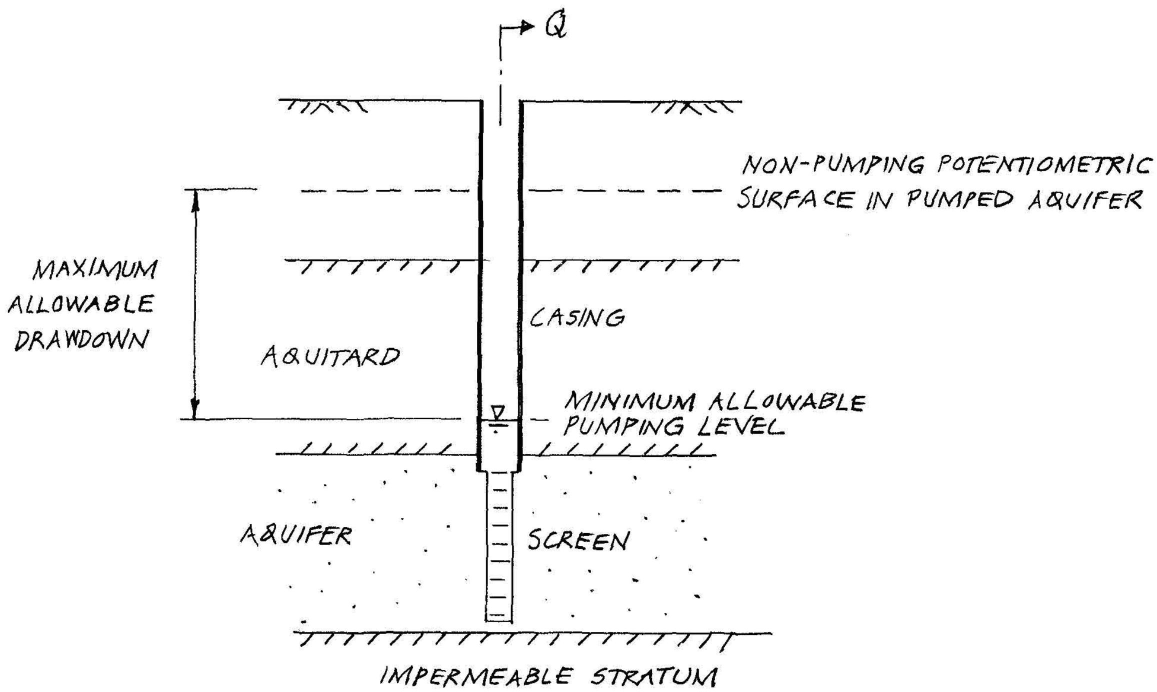

Figure 5. Schematic illustration of the maximum allowable drawdown

Unconfined aquifer

According to the *Guide to Groundwater Authorization* (Alberta Environment, 2011), the maximum allowable drawdown for a production well in an unconfined aquifer is two-thirds of the initial saturated thickness of the aquifer.

The Alberta Environment definition of the allowable drawdown in an unconfined aquifer is somewhat consistent with guidance presented in Groundwater and Wells (Driscoll, 1986; p. 433-434). It is indicated in Groundwater and Wells that for a homogeneous unconfined aquifer, screening of the bottom one-third to one-half of an aquifer less than 150 ft thick (45 m) is optimal. It is further indicated that an unconfined aquifer is usually pumped so that, at maximum capacity, the pumping water level is maintained slightly above the top of the screen. As shown in Figure 6, the combination of these two pieces of guidance leads to the definition of the allowable drawdown as ranging between two-thirds and one-half of the initial saturated thickness of the aquifer.

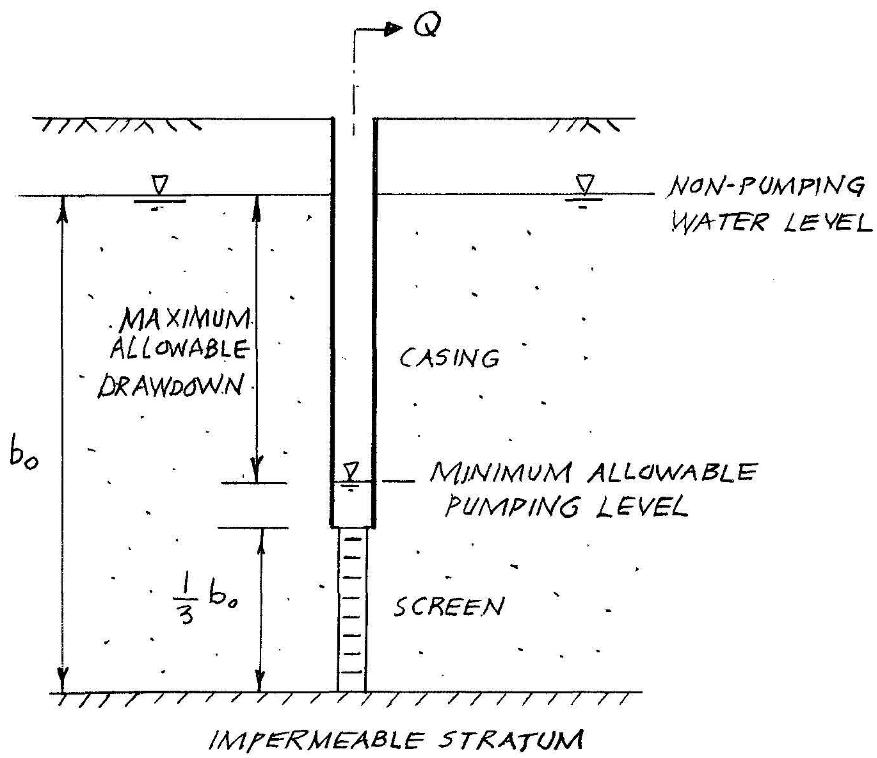

Figure 6. Definition of the maximum allowable drawdown for an unconfined aquifer

4. The simplest possible approach for estimating the well capacity

The specific capacity of a well is defined as the ratio of the pumping rate and the drawdown in te well:

$$SC = \frac{Q}{s_{\mathrm{w}}} \quad (1)$$

If it is assumed that the specific capacity is constant, the maximum yield of a well can be estimate directly from Equation (1):

$$Q_{\max} = SC \times s_{\mathrm{w-max}} \quad (2)$$

Here Q_{max} is the maximum pumping rate, $s_{\mathrm{w\text{-}max}}$ is the maximum allowable drawdown in the pumping well, and *SC* is the **specific capacity** of the well. The specific capacity is defined as the pumping rate per unit drawdown. Referring to Figure 7, for this ideal case, the specific capacity is the same whether we consider a single point (Q/s_{w}) or the slope of the plot of pumping rate against drawdown, ($\Delta Q/\Delta s_{\mathrm{w}}$).

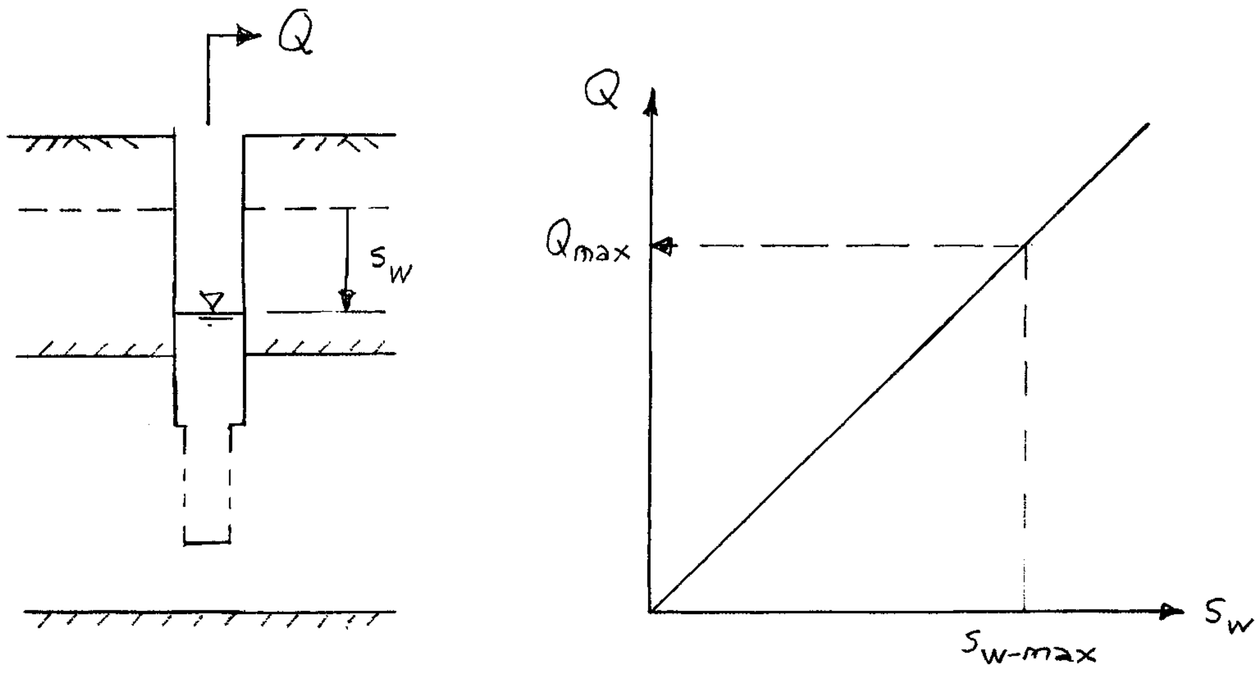

Figure 7. Estimation of the capacity of well with a constant specific capacity

<u>Example 1</u>

The results from a well performance test conducted on a municipal production well in Linnich (Ruhr Valley, Germany) are reproduced in Figure 8 (Langguth and Voigt, 1980). The top curve shows the pumping rate and the bottom curve shows the water level in the well. The data suggest that the water level in the well reaches a steady level during each pumping step.

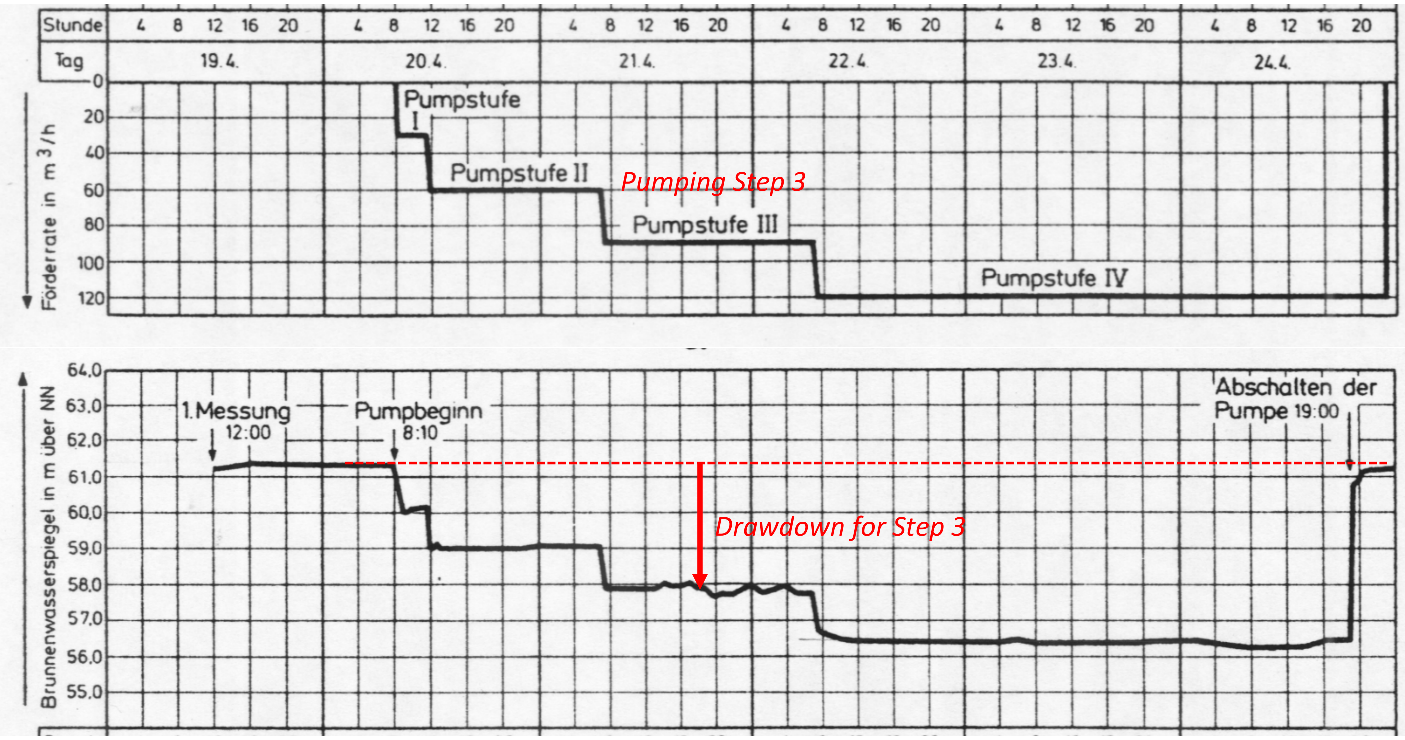

Figure 8. Data from municipal well testing, Linnich, Germany
(Data from Langguth and Voigt, 1980)

The pumping rates during the Linnich test are plotted against the stabilized drawdown in Figure 9. The results of the test approximate a straight line so we can estimate the specific capacity from either a single point or from the slope of the line of best fit through the data. For this example, the specific capacity is about 25 m^3/hr/m.

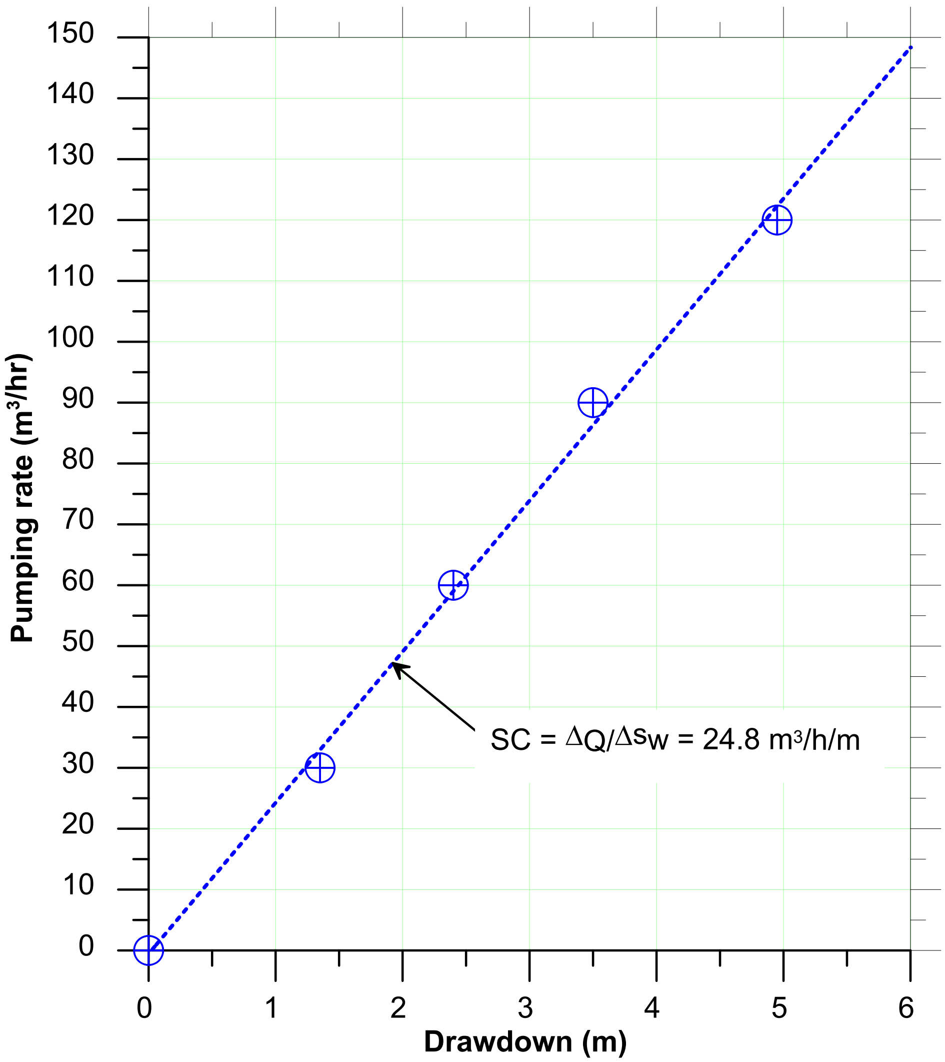

Figure 9. Reduced data from the Linnich step test

Example 2

The data in Figures 8 and 9 were obtained from a controlled test. To infer the specific capacity from the operating record of a production well generally requires additional data processing. The data from a well in Aberfoyle, Ontario are shown in Figure 10. As shown in the figure, the daily pumping varied substantially, and the water level fluctuated on a daily basis.

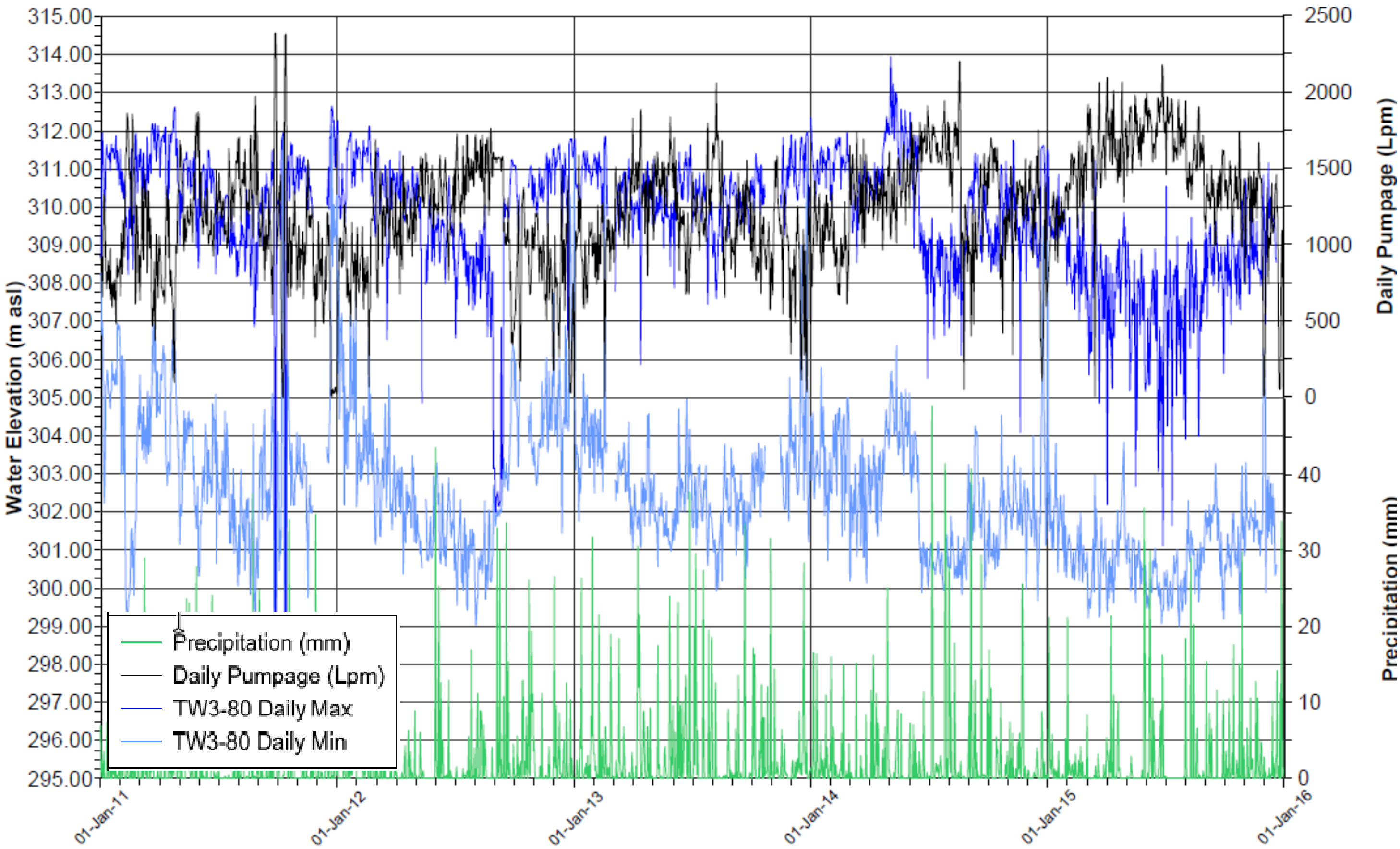

Figure 10. Performance record for an operating production well

The same data are plotted in Figure 11 but are averaged for each month of the record. In this form it is possible to estimate the long-term specific capacity of the well, about 160 L/min/m, and to assess whether the specific capacity changes through time.

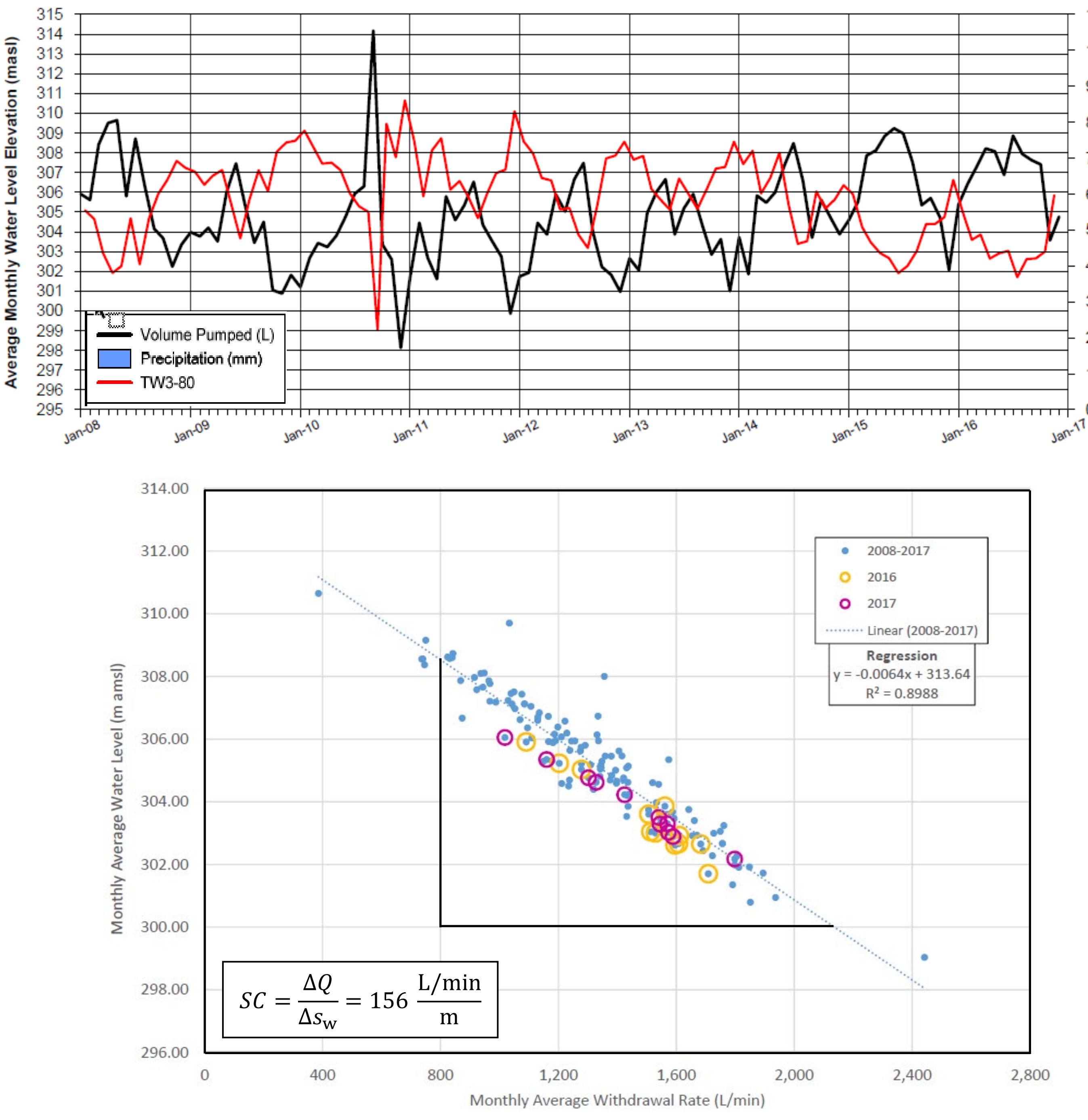

Figure 11. Monthly-average operating well performance data

5. Estimation of the specific capacity: Simplified approach for stabilized conditions

Confined aquifer

If it is assumed that all of the drawdown in the pumping well is attributable to head losses due to laminar flow in the formation, the discharge to a well under steady conditions in an ideal confined aquifer is given by the Thiem solution:

$$Q = 2\pi K b \frac{(h_R - h_w)}{ln\left\{\frac{R}{r_w}\right\}} = \frac{2\pi T}{ln\left\{\frac{R}{r_w}\right\}} s_w \tag{3}$$

Here K is the horizontal hydraulic conductivity, b is the aquifer thickness, T is the transmissivity ($K \times b$), R is radius of influence, r_w is the radius of the pumping well, and h_R and h_w are the hydraulic heads at radial distances R and r_w from the center of the well.

For this case, the specific capacity is a constant given by:

$$SC = \frac{Q}{s_w} = \frac{2\pi T}{ln\left\{\frac{R}{r_w}\right\}} \tag{4}$$

We can only guesstimate the radius of influence R. However, since the ratio R/r_w appears in the logarithm term, the estimate of the specific capacity is relatively insensitive to the assumed value of R. As indicated on the table below, for variations of the assumed radius of influence by a factor of 100, the estimate of the specific capacity varies only by a factor of about 2.

R/r_w	$\frac{SC}{T}$
50	1.61
100	1.36
200	1.19
500	1.01
1000	0.91
2000	0.83
5000	0.74

We also note from the tabulated values that the ratio of the specific capacity and the transmissivity is relatively close to 1.0. The results of these simple calculations lead us to a rule of thumb.

> If most of the head losses in a well are due to laminar flow in the formation, as a first approximation the specific capacity of a well in a confined aquifer is equal to the transmissivity.

Unconfined aquifer

Assuming again that all head losses occur in the formation, the discharge of a well in an unconfined aquifer is estimated with the Dupuit solution (see for example Bear, 1979: Hydraulics of Groundwater, p. 310):

$$Q = \pi K \frac{H^2 - h_\mathrm{w}^2}{ln\left\{\frac{R}{r_\mathrm{w}}\right\}} \tag{5}$$

Noting that $(h_\mathrm{R}^2 - h_\mathrm{w}^2) = (h_\mathrm{R} + h_\mathrm{w})(h_\mathrm{R} - h_\mathrm{w})$, the Dupuit solution can be expanded as:

$$Q = \pi K \frac{(h_\mathrm{R} + h_\mathrm{w})(h_\mathrm{R} - h_\mathrm{w})}{ln\left\{\frac{R}{r_\mathrm{w}}\right\}} = \frac{\pi K (h_\mathrm{R} + h_\mathrm{w})}{ln\left\{\frac{R}{r_\mathrm{w}}\right\}} s_\mathrm{w} = \frac{2\pi \frac{(h_\mathrm{R} + h_\mathrm{w})}{2}}{ln\left\{\frac{R}{r_\mathrm{w}}\right\}} s_\mathrm{w}$$

The specific capacity is given by:

$$SC = \frac{Q}{s_\mathrm{w}} = \frac{2\pi K \frac{(h_\mathrm{R} + h_\mathrm{w})}{2}}{ln\left\{\frac{R}{r_\mathrm{w}}\right\}} \tag{6}$$

This expression for the specific capacity of an unconfined aquifer is written in this form to highlight both its similarities and differences with respect to the Thiem solution for a confined aquifer.

In contrast to the results for an ideal confined aquifer, the specific capacity of a well in an unconfined aquifer varies with the drawdown. The dependence on the drawdown is illustrated with some example calculations.

Example calculations:

The conceptual models for the example calculations are shown schematically in Figure 10. The following parameter values are specified.

- $K = 0.864$ m/d
- $r_w = 0.1$ m
- $b = 20$ m
- $R = 500$ m
- $h_R = 20$ m

In Figure 11, the discharge rate is plotted against the drawdown. The corresponding specific capacities are plotted in Figure 12. The results for the unconfined aquifer show a marked decline in the specific capacity for increasing drawdown.

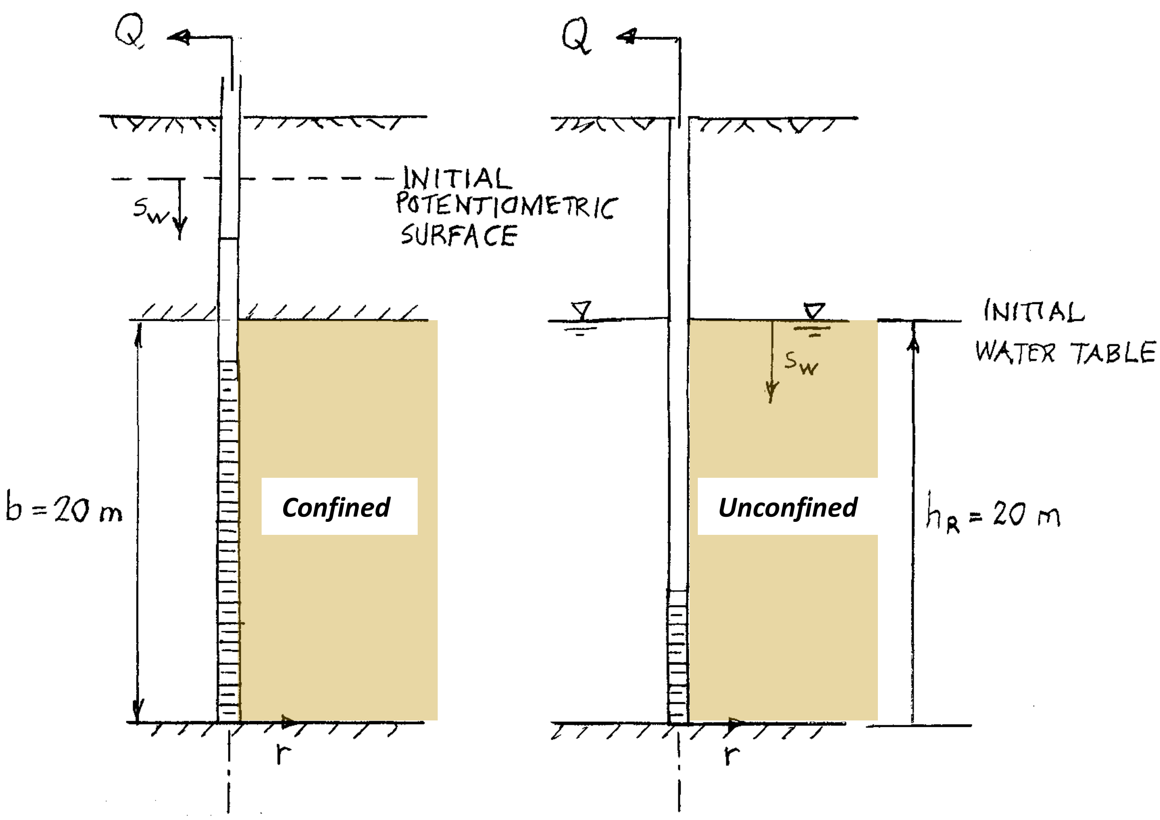

Figure 10. Conceptual model of wells in confined and unconfined aquifers

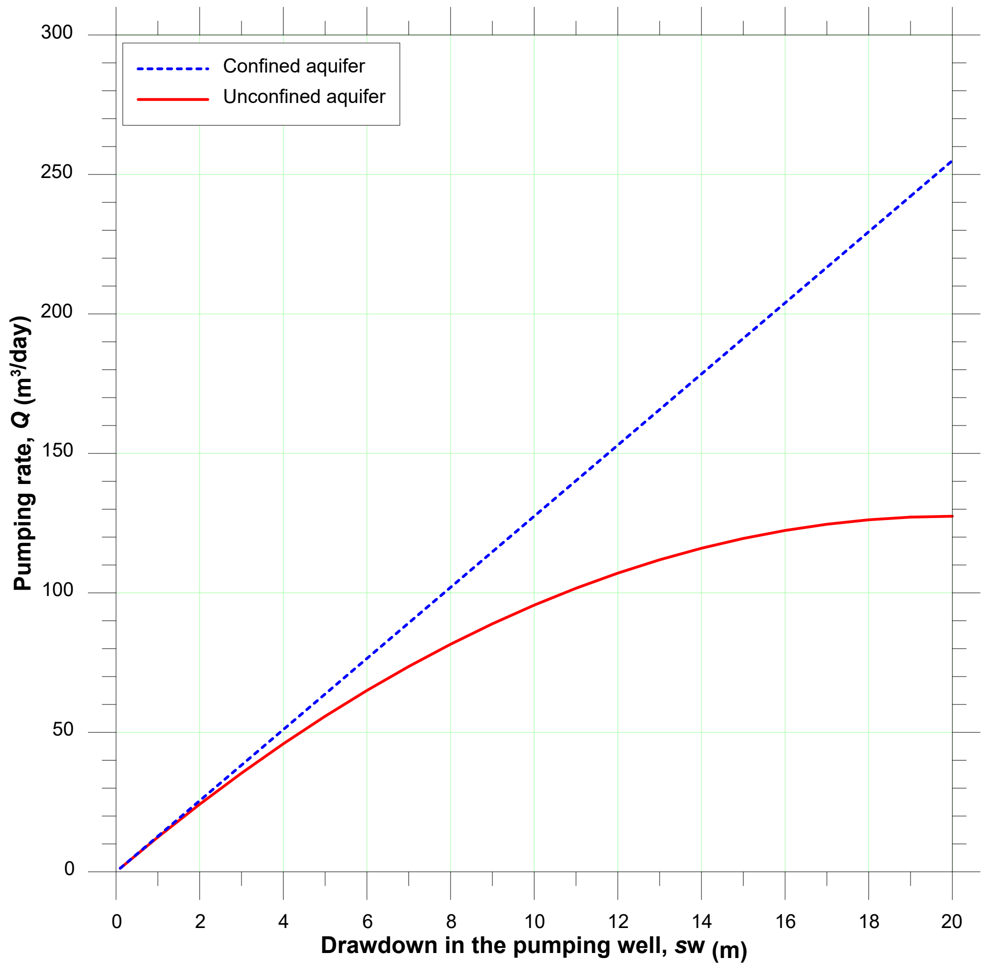

Figure 11. Example calculations of pumping rate vs. drawdown in the pumping well

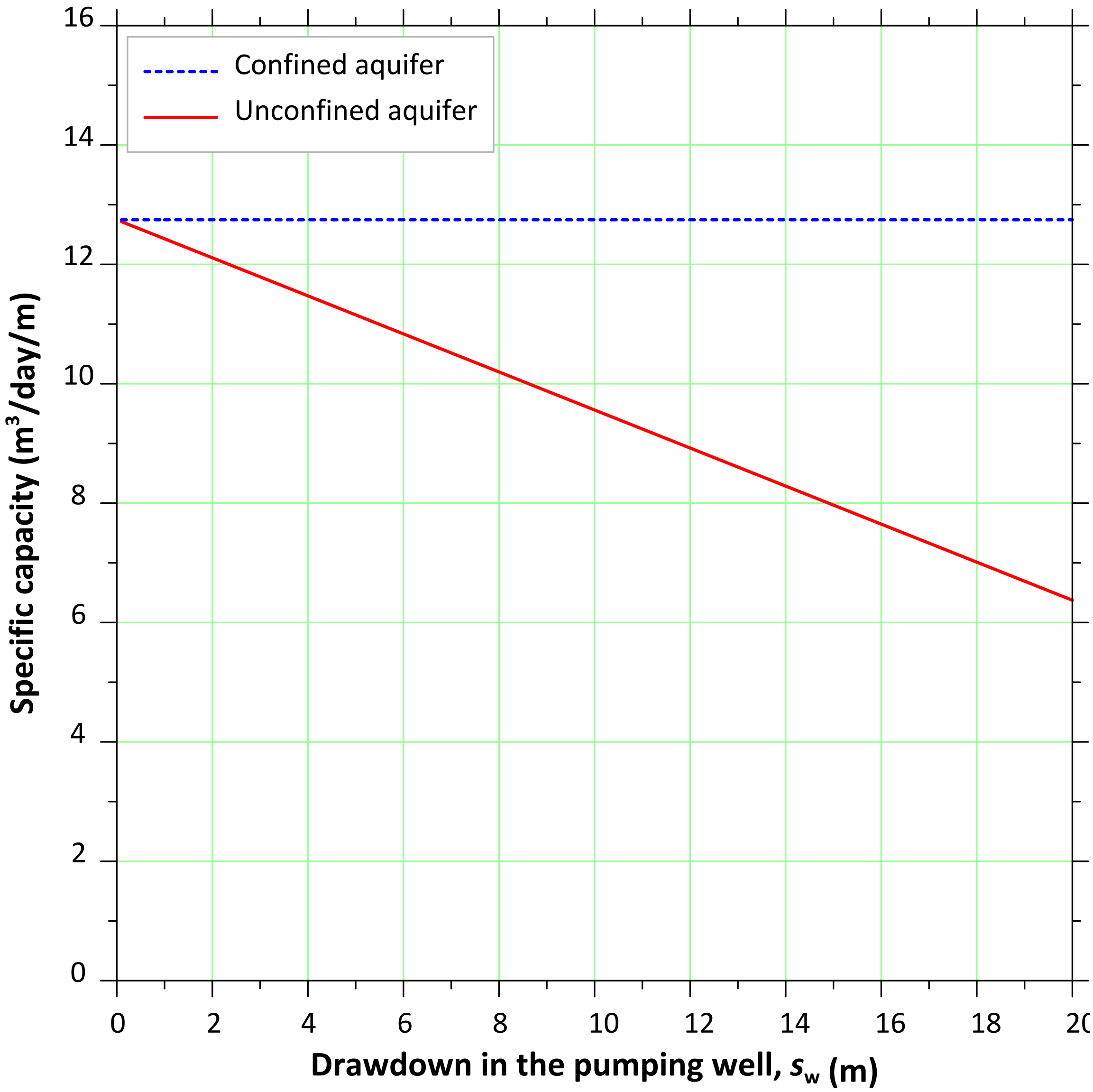

Figure 12. Example calculations of specific capacity vs. drawdown in the pumping well

6. The components of the drawdown in a pumping well

The drawdown in a pumping well is generally due to more than just head losses associated with laminar flow in the formation. To estimate the capacity of a well it is important to understand the sources of the drawdown. The area around a pumping well is shown schematically in Figure 13. The *total* drawdown in the pumping well is defined as the difference between the non-pumping (static) water level and the pumping level in the well. Following the general approach of Walton (1962, 1970) and Atkinson and others (1994), the total drawdown is idealized as consisting of five components. Moving inwards from the formation to the inner casing, the head losses are:

- s_a: the head loss due to *laminar* flow in the formation;
- s_t: the additional head loss due to *turbulent* flow in the formation;
- s_s: the additional head loss across a zone of reduced permeability around the well;
- s_e: the additional head loss across the well screen; and
- s_c: the additional head loss within the well casing itself.

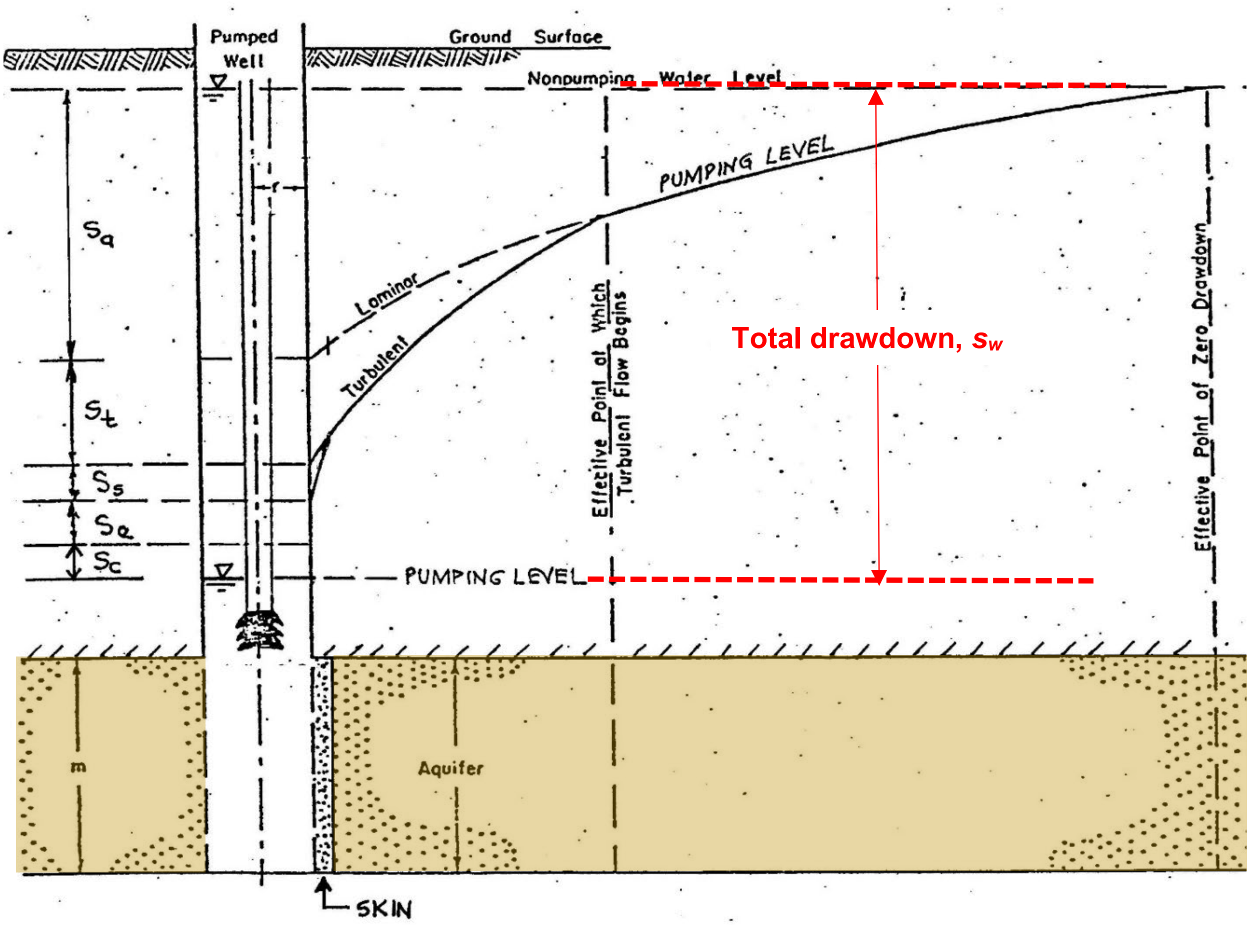

Figure 13. Components of drawdown in a pumping well
(adapted from Bruin and Hudson, 1955)

The components of the total drawdown in a pumping well are defined below.

1. s_a : Head loss due to *laminar* flow in the formation

The head losses due to laminar flow in the formation arise from friction losses as water is transmitted through the formation towards the pumping well. These head losses depend on the duration of pumping, the properties of the formation (transmissivity and storage coefficient), and the construction of the well (radius and extent of penetration).

2. s_t : Additional head loss due to *turbulent* flow in the formation

If the flow rate is sufficiently high, there may be additional head losses in the formation due to turbulent flow. If a well screened in a porous medium has been designed properly, there should be little possibility of turbulent flow in the formation. However, in fractured-rocks, pumping may induce velocities that are sufficiently high that flow is no longer laminar. Atkinson and others (1994) present an excellent treatment of turbulent flow in discrete fractures.

3. s_s: Additional head loss across a zone of reduced permeability around the well

Regardless of how carefully a well may be drilled, there is always the possibility that a zone of disturbed material may be created around it. The zone of disturbed material is usually referred to as a "skin", and the additional head losses due to its presence are referred to as a "skin effect". Skin effects may arise from the use of drilling mud in porous media, or by the closing off of fractures in rock. Skin effects may be mitigated to a certain extent by proper well development following drilling.

4. s_e: Additional head loss across the well screen

Head losses due to the flow of water across the well screen arise from the constriction in the flow as it passes through the openings of the well screen. These losses are generally referred to as entrance losses. If a well screen has been designed properly, these losses should not be significant. However, they may evolve through time if bacterial growth or mineral precipitates clog the well screen.

5. s_c: Additional head losses within the well itself

Additional head losses may occur within the well itself, due, for example, to turbulence arising from the constrictions around the pump appurtenances.

Simplification

The head losses in a pumping well are assumed to be additive. That is, the total drawdown in a pumping well is assumed to be the sum of drawdowns due to each of the components:

$$s_\mathrm{w}(t) = s_\mathrm{a} + s_\mathrm{t} + s_\mathrm{s} + s_\mathrm{e} + s_\mathrm{c} \tag{7}$$

Some researchers have attempted to quantify some or all of the five components of the drawdown indicated in Equation (1) (see for example Barker and Herbert, 1992a,b; and Atkinson et. al., 1994). However, on a practical level, it is generally not feasible to distinguish between all of them. To make the analysis of the drawdowns in a pumping well tractable, we will distinguish only between linear head losses in the formation, additional linear losses and head losses due to turbulent flow:

$$s_\mathrm{w} = s_\mathrm{formation} + \Delta s_\mathrm{skin} + \Delta s_\mathrm{turbulence} \tag{8}$$

The representation of these lumped components of the drawdowns are discussed in the following sections of the notes, starting with the representation of head losses in the formation.

6.1 Representation of head losses in the formation

The component of the drawdown due to head losses in the formation is shown schematically in Figure 14.

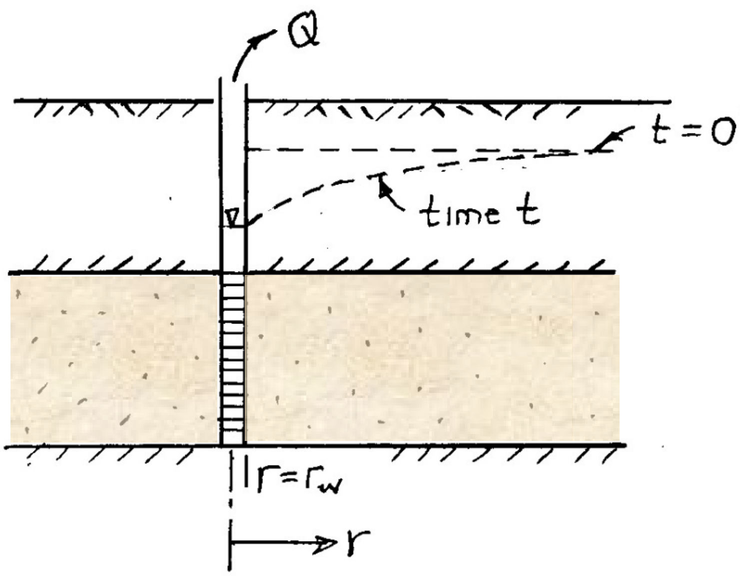

Figure 14. Idealization of the component of drawdown due to linear head losses in the formation

The head losses in the formation are the difference in the groundwater level in the aquifer under non-pumping conditions and the level at the outside edge of the well screen or borehole at any subsequent time:

$$s_{\text{formation}}(t) = h(r_{\text{w}})_{\text{non-pumping}} - h(r_{\text{w}}, t)_{\text{pumping}} \tag{9}$$

Here r_w is the effective radius of the pumping well and t is the elapsed time since the start of pumping. The effective radius is frequently assumed to be the full outside radius of the borehole.

The key aspect of linear formation losses is that, for either steady or transient flow, if flow in the formation is laminar, the change in the water level (drawdown) is a linear function of the flow rate from the formation:

$$s_{\text{formation}}(t) = Q \times F(r_{\text{w}}, t) \tag{10}$$

Here $F(r_w,t)$ denotes a particular aquifer model. Retaining, for the time being, the assumption that water levels in the pumping well have stabilized, for an ideal confined aquifer we have from the Thiem solution:

$$F(r_{\text{w}}) = \frac{1}{2\pi T} ln\left\{\frac{R}{r_{\text{w}}}\right\} \tag{11}$$

6.2 Representation of the additional linear head losses at the well

Drilling and installing a pumping well generally cause some alteration in the properties of the formation around the wellbore. The zone of altered material is referred to as the *skin*. If the hydraulic conductivity of the skin is reduced relative to the formation, there will be additional head losses across the skin, as shown schematically in Figure 15. The distance from the center of the well to the outer edge of the skin is designated r_s.

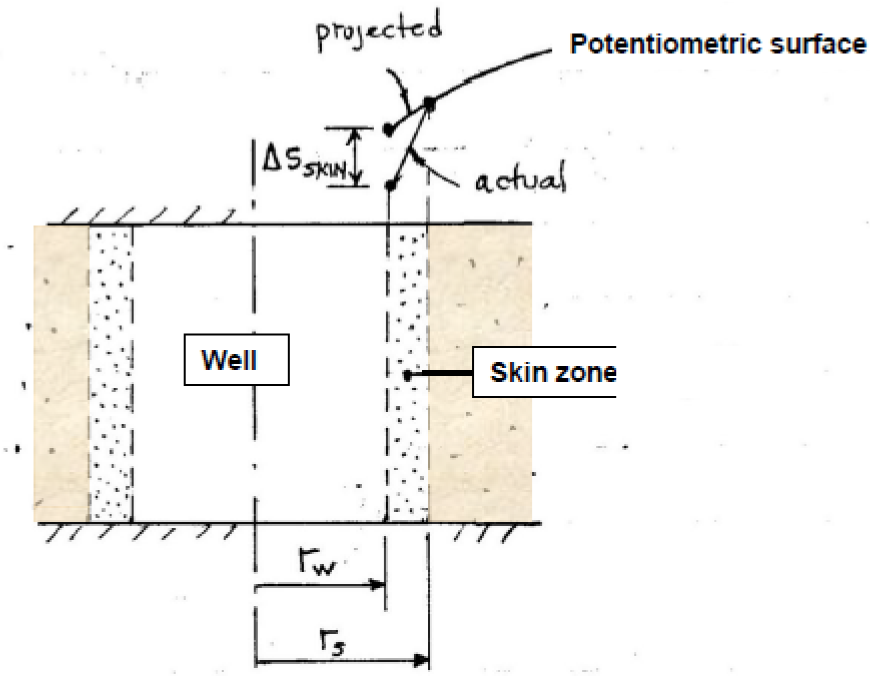

Figure 15. Schematic cross-section of a well surrounded by a skin zone

There are two key aspects of the additional head losses attributed to the skin:

- Skin losses are established relatively quickly after pumping starts; and
- Skin losses are proportional to the pumping rate.

Ramey (1982) proposed that the presence of a skin zone could be represented by a constant additional drawdown:

$$\Delta s_{\text{skin}} = \frac{Q}{4\pi T} 2S_{\text{w}} \tag{12}$$

Here S_{w} is referred to as the *dimensionless skin factor*.

Assuming that there is no storage within the skin zone it is possible to derive an analytical expression for the dimensionless skin factor (Hawkins, 1956):

$$S_w = \left(\frac{T - T_s}{T_s}\right) ln\left\{\frac{r_s}{r_w}\right\} \tag{13}$$

Here T and T_s are the transmissivities of the formation and the skin, respectively.

In practice, we cannot estimate separately the radius of the skin zone and its transmissivity. Therefore, S_w is generally treated as a lumped parameter.

Equation (13) can be rearranged to read:

$$S_w = \left(\frac{T}{T_s} - 1\right)\ ln\left\{\frac{r_s}{r_w}\right\} \tag{14}$$

This definition is presented as Eq. 2.10 in the classic petroleum engineering text of Earlougher (1977). In this form it is clear why petroleum engineers use the terminology “positive skin” to denote the effect of a reduced transmissivity of the skin, and “negative skin” to denote the effect of an increased transmissivity of the skin relative to the formation.

6.3 Representation of the additional head losses due to partial penetration

Additional head losses occur when a pumping well does not penetrate the full thickness of an aquifer (Figure 16).

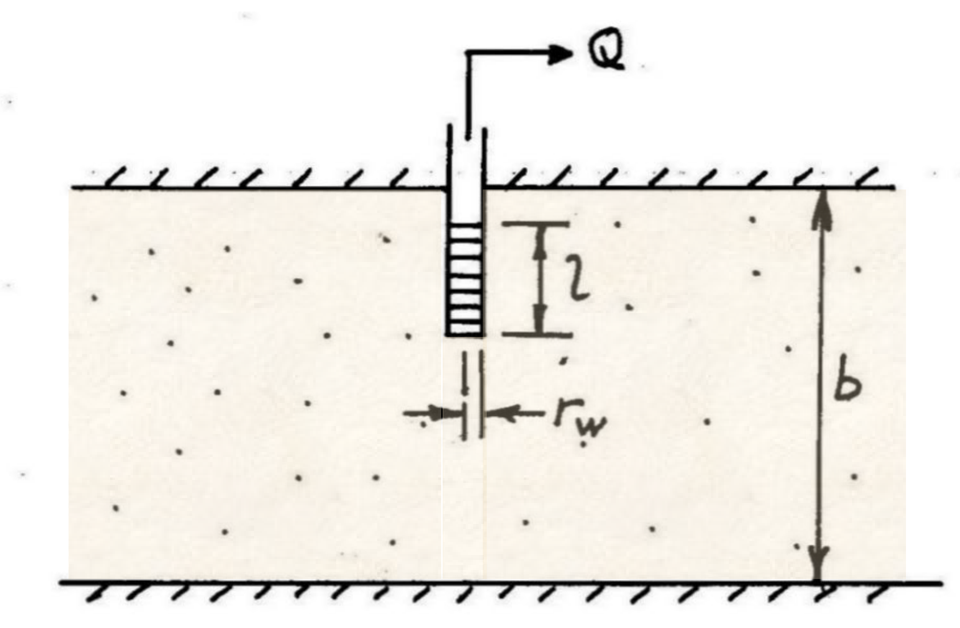

Figure 16. Conceptual model for a partially penetrating well

Analyses of flow to partially penetrating pumping wells suggest that the additional head losses caused by partial penetration are established relatively quickly and are directly proportional to the pumping rate (Hantush, 1961; Konikow et al., 2009). Therefore, they have the same general form as skin losses. The losses due to partial penetration are written in terms of a *pseudo-skin coefficient, S_{pp}*:

$$\Delta s_{\mathrm{pp}} = \frac{Q}{4\pi T} 2S_{\mathrm{pp}} \qquad (15)$$

Several approaches have been developed to estimate the additional head losses due to partial penetration. Brons and Marting (1961) developed a simple approach that in our experience closely approximates results obtained with more elaborate calculations:

$$S_{\mathrm{pp}} = \left(\frac{b-l}{l}\right)\left[ln\left\{\frac{b}{r_{\mathrm{w}}}\right\} - G\left(\frac{l}{b}\right)\right] \qquad (16)$$

Here b is the aquifer thickness, l is the length of the well screen, and $G\left(\frac{l}{b}\right)$ is a function tabulated in Brons and Marting (1961). Bradbury and Rothschild (1985) used regression to develop the following functional form from the tabulated values of G:

$$G\left(\frac{l}{b}\right) \cong 2.948 - 7.363\left(\frac{l}{b}\right) + 11.447\left(\frac{l}{b}\right)^2 - 4.675\left(\frac{l}{b}\right)^3 \qquad (17)$$

The values tabulated by Brons and Marting (1961) are plotted along with the regression of Bradbury and Rothschild (1985) in Figure 17. As shown in the figure, the results obtained with the functional form of $G(l/b)$ match closely the values in Brons and Marting (1961).

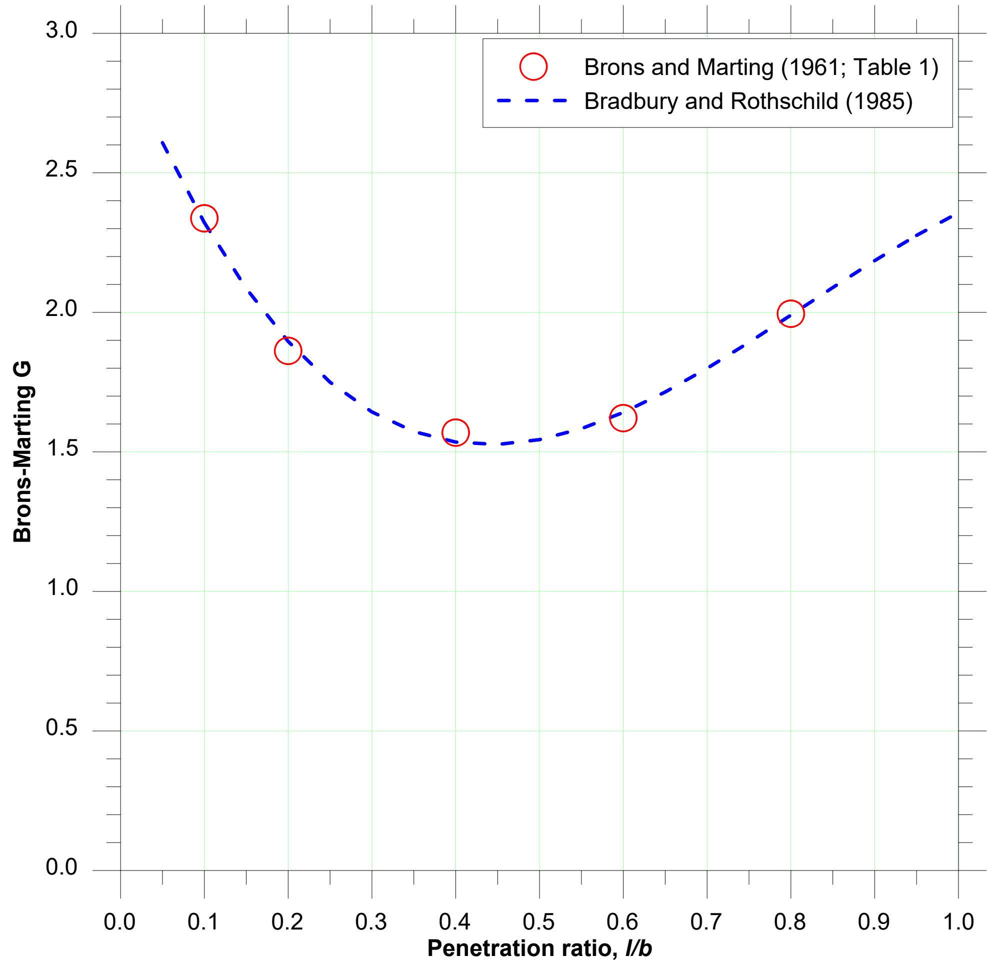

Figure 17. Values of the Brons-Marting function *G* for partially penetrating wells

6.4 Representation of the additional head losses due to turbulent flow near or within the well

The flow rate within the well casing itself and around the appurtenances may be turbulent. In the case of thin, transmissive aquifers the groundwater velocity of water in the immediate vicinity of the well may also be sufficiently high that flow is turbulent. Jacob (1946) proposed a simple phenomenological approach for estimating the head losses due to turbulent flow. There are two key aspects of the Jacob model of turbulent losses:

- Turbulent losses are established relatively quickly after pumping starts; and
- Turbulent losses are proportional to the pumping rate squared.

The Jacob model is expressed as:

$$\Delta s_{\text{turbulence}} = CQ^2 \tag{18}$$

The parameter C is designated the *well loss coefficient*. Rorabaugh (1953) suggested the following generalization:

$$\Delta s_{\text{turbulence}} = CQ^P \tag{19}$$

The parameter P is the *well loss exponent*. Rorabaugh reported exponents that were not too different from 2.0, and we recommend using Jacob's model except where there is compelling evidence that P should not be 2.0. The well loss coefficient C has the units of [drawdown]/[Pumping rate]^P. If the pumping rate is reported in m^3/day, the units of drawdown are m, and it is assumed that $P = 2$, then C has units of $m/(m^3/day)^2$, which is equivalent to day^2/m^5.

As discussed in a later section of the notes, the most reliable estimates of C are derived from the results of step tests. In the absence of site-specific data, the general guidance provided by Walton (1962; p. 27) is summarized below. Particularly close attention must be paid to the units.

Condition of well	***C*** **(sec^2/ft^5)**	***C*** **(day^2/ft^5)**	***C*** **(sec^2/m^5)**
Properly designed and developed	< 5	$< 6.7\times10^{-10}$	< 1900
Mild deterioration	< 10	$< 6.7\times10^{-9}$	< 3800

6.5 The specific capacity of a well with additional well losses

Including additional well losses, the expression for the specific capacity, Equation (1) is expanded as:

$$SC = \frac{Q}{s_{\text{formation}} + \Delta s_{\text{skin}} + \Delta s_{\text{nonlinear}}} \tag{20}$$

Substituting for the components of the drawdown in the pumping well, the specific capacity is given by:

$$SC = \frac{Q}{s_{\text{w}}} = \frac{Q}{\frac{Q}{2\pi T} ln\left\{\frac{R}{r_{\text{w}}}\right\} + \frac{Q}{4\pi T} 2S_{\text{w}} + CQ^2}$$

Simplifying:

$$SC = \frac{1}{\frac{1}{2\pi T}\left(ln\left\{\frac{R}{\text{r}_{\text{w}}}\right\} + S_{\text{w}}\right) + CQ} \tag{21}$$

If we only have only one value of the specific capacity we can only know the combined effects of the formation losses and the additional well losses.

Case study: Guelph municipal production well PW6/63

As part of a city-wide aquifer performance investigation, well performance tests were conducted in 1996-1998 on municipal supply wells in Guelph, Ontario (Jagger Hims Ltd., 1998). The record from the test conducted on bedrock well PW6/63 is reproduced in Figure 18. The drawdowns appear to approach stabile levels by the end of each pumping step. The stabilized drawdowns at the end of each pumping step are summarized below.

Step	Pumping rate, Q (L/s)	Drawdown, s_w (m)
1	11.5	0.87
2	18.6	1.53
3	25.3	2.46
4	32.0	3.60

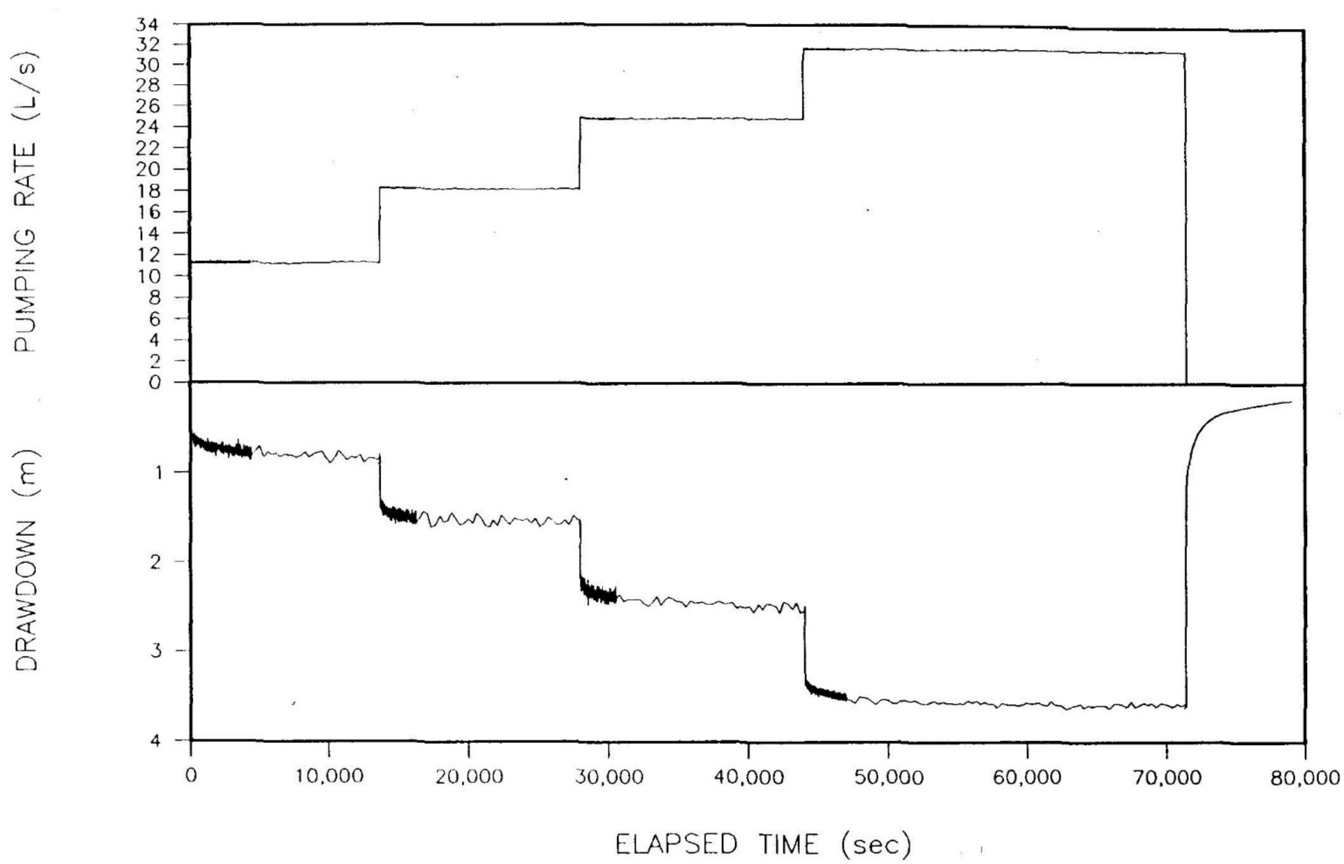

Figure 18. Step results for PW6/63

The pumping rates and drawdowns recorded at the end of each pumping step are plotted in Figure 19. The data do not approximate a straight line. Interpreting the specific capacity as the slope of the relation between the pumping rate and the drawdown, we see that the specific capacity for this test declines as the drawdown increases. A reduction of the specific capacity for increasing pumping rates is a direct indication that the pumping well drawdowns include nonlinear head losses.

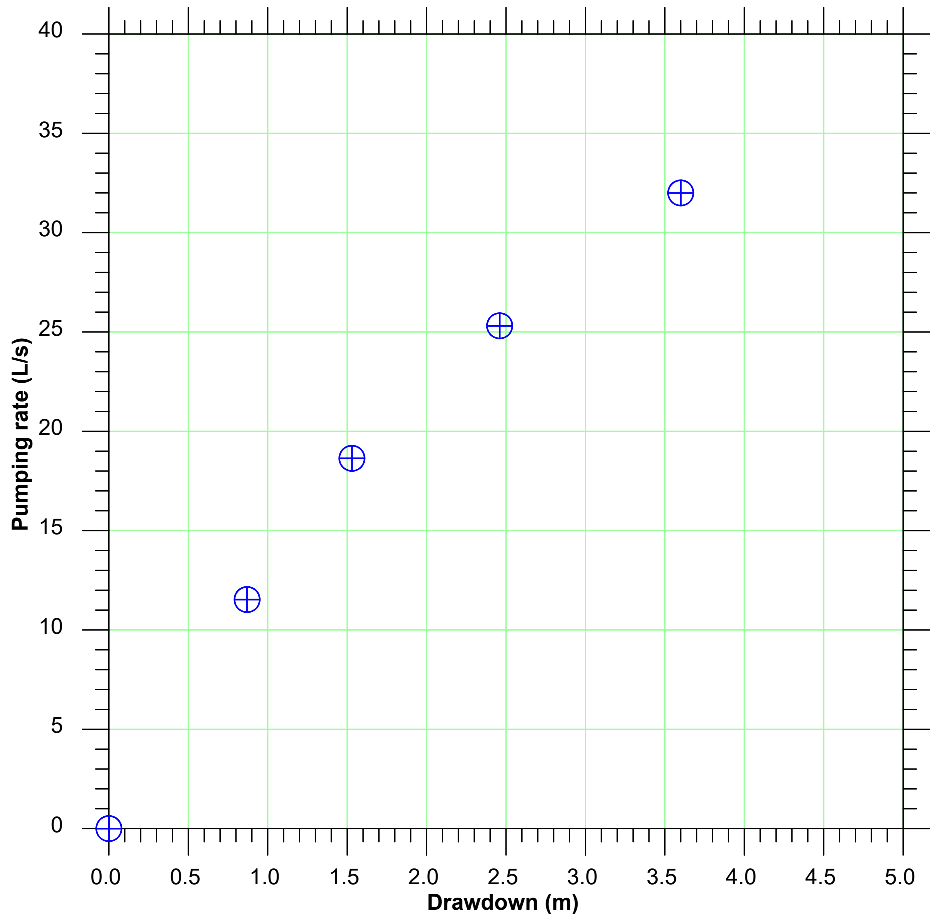

Figure 19. Reduced data from the PW6/63 step test

For tests during which stable conditions are approached but the response is nonlinear, a simple technique is available to distinguish between the linear and nonlinear well losses. For stabilized conditions, Jacob (1947) suggested that the drawdowns in a pumping well could be approximated as:

$$s_w = BQ + CQ^2 \quad (22)$$

Here B is the linear well loss coefficient and C is the nonlinear well loss coefficient. Dividing both sides by the pumping rate yields:

$$\frac{s_w}{Q} = B + CQ \quad (23)$$

The quantity s_w/Q is referred to as the *specific drawdown*, the reciprocal of the specific capacity. A plot of the specific drawdown against the pumping rate is referred to as a *Hantush-Bierschenk plot* (Hantush, 1964; Bierschenk, 1964). As shown in the Hantush-Bierschenk plot for PW6/63 (Figure 20), the relation between the specific drawdown and the pumping rate is nearly linear, suggesting that the Jacob (1947) model is appropriate.

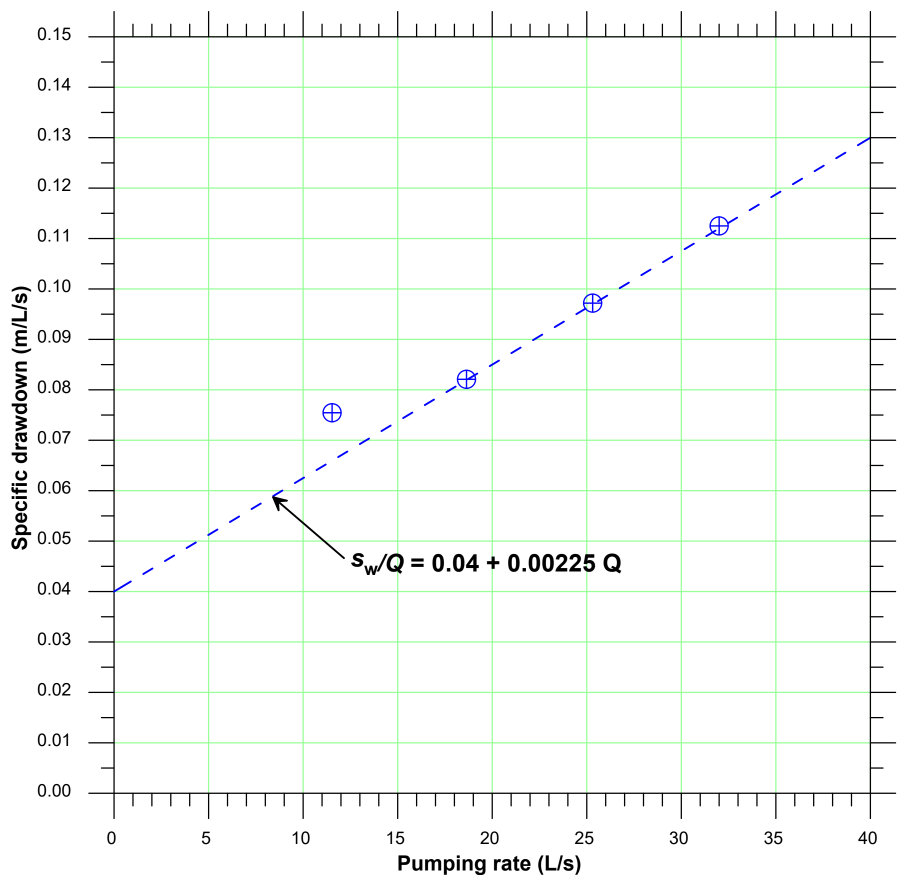

Figure 20. Hantush-Bierschenk plot for the PW6/63 step test

The parameters estimated with a linear regression are:

- $B = 0.04$ m/(L/s); and
- $C = 2.25\times10^{-3}$ m/(L/s)^2.

As shown in Figure 21, these parameter values suggest that the nonlinear losses are an important component of the total drawdown in the well.

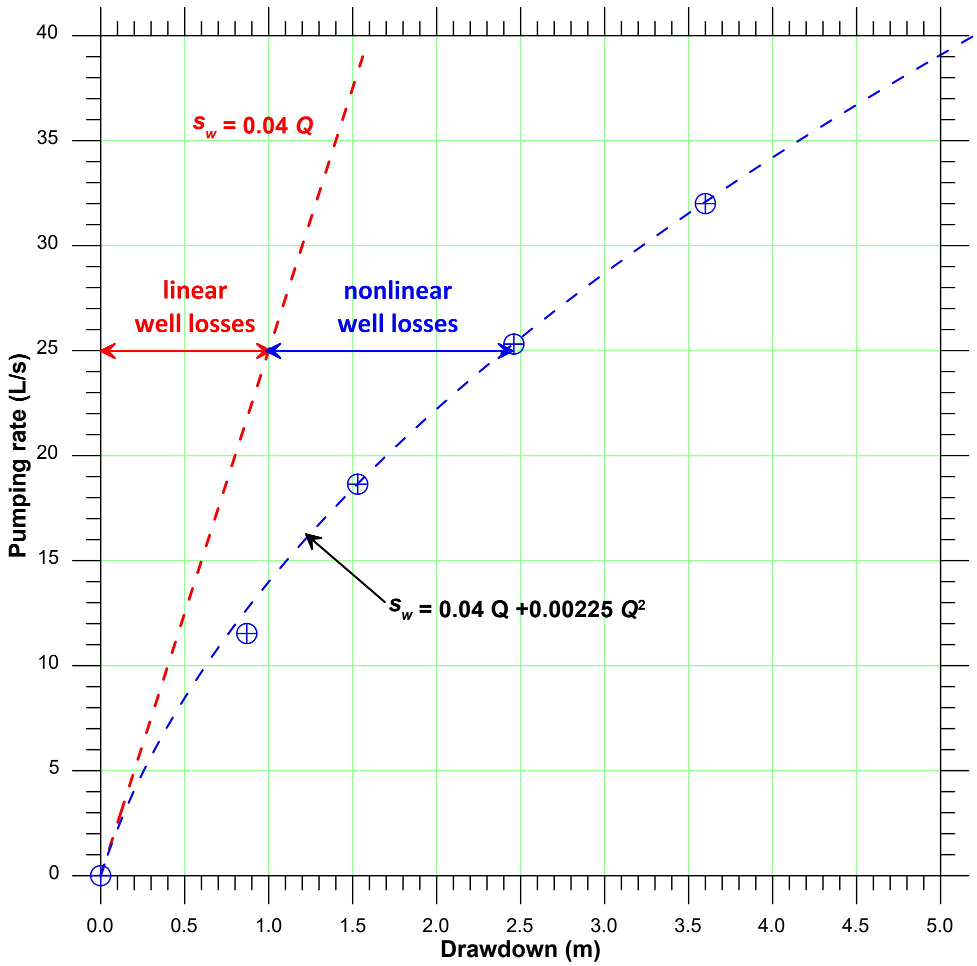

Figure 21. Separation of linear and nonlinear well losses with the Hantush-Bierschenk analysis

As shown in Figure 22, if there are nonlinear well losses, the specific capacity will decline as the pumping rate increases:

$$SC = \frac{1}{B + CQ} = \frac{1}{0.04\ \mathrm{m/(L/s)}\ + 2.25 \times 10^{-3}\ \mathrm{m/(L/s)^2}\ Q}$$

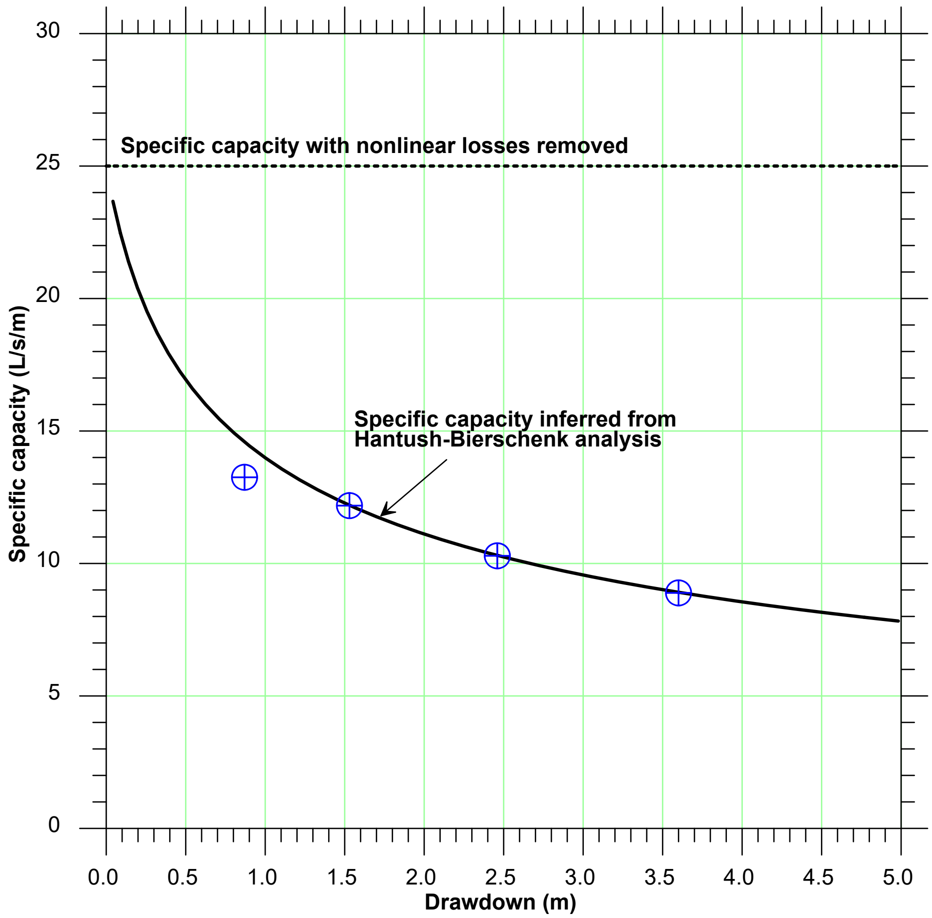

Figure 22. Specific capacity with inferred relation from the Hantush-Bierschenk plot

7. Extension to transient conditions: Ideal wells

Thus far we have assumed that conditions in the pumping well are stable (i.e., steady-state conditions are attained). In many situations the drawdowns do not stabilize, and we must take time into account when characterizing well performance and estimating the capacity of a well.

The Theis (1935) solution is invoked frequently to represent the component of the total drawdown due to head losses in the formation is given by:

$$s_{\text{formation}}(r_{\text{w}}, t) = \frac{Q}{4\pi T} W(\frac{r_{\text{w}}^2 S}{4Tt}) \qquad (24)$$

Here T denotes the transmissivity of the formation, S the storativity (confined storage coefficient) and t is the elapsed time. The term W denotes the Theis well function (the exponential integral). The drawdown due to laminar head losses in the formation are evaluated at the effective radius of the well, r_{w}. Application of the Theis solution assumes that the aquifer is extensive, uniform, isotropic, perfectly confined and pumped by a fully penetrating well.

Transmissivity data are frequently limited in regional groundwater studies. Controlled pumping tests with observation wells are often available at only a few locations. However, the records for private water wells often contain information that can supplement the available data. In particular, these records include pumping data that can be used to calculate specific capacities for the wells, and these specific capacities can be correlated to transmissivity with simple models. These correlations yield reconnaissance-level estimates of transmissivity. Where more detailed data are available, specific capacity values can also serve to provide simple check on the interpretations. Here we describe a simple approach for estimating the transmissivity from specific capacity data. The crucial assumption of the analysis is that the drawdowns in the pumping well are due primarily to head losses in the formation.

Re-arranging Equation (24), the specific capacity for an ideal well is:

$$SC = \frac{Q}{s_w} = \frac{4\pi T}{W\left(\frac{r_w^2 S}{4Tt}\right)} \qquad (25)$$

The transmissivity can be back-calculated from the reported value of the specific capacity with known or assumed values for the well radius and storage coefficient:

$$T = \frac{1}{4\pi} W\left(\frac{r_w^2 S}{4Tt}\right) \times SC \qquad (26)$$

Equation (26) is an implicit function of the transmissivity T. Although it is possible to estimate T using a root-finding algorithm, a simpler approach is described here. For a particular well size and duration of pumping, it is possible to use Equation (26) directly to plot the relation between the SC and T.

The relation between specific capacity and transmissivity for typical conditions reported in water well records in Ontario is shown in Figure 23. The relationship is shown for a typical range of storage coefficients for confined conditions ($S = 1\times10^{-5}$ to 1×10^{-3}). The results plotted in Figure 23 demonstrate that the specific capacity is relatively insensitive to the assumed value of the storage coefficient.

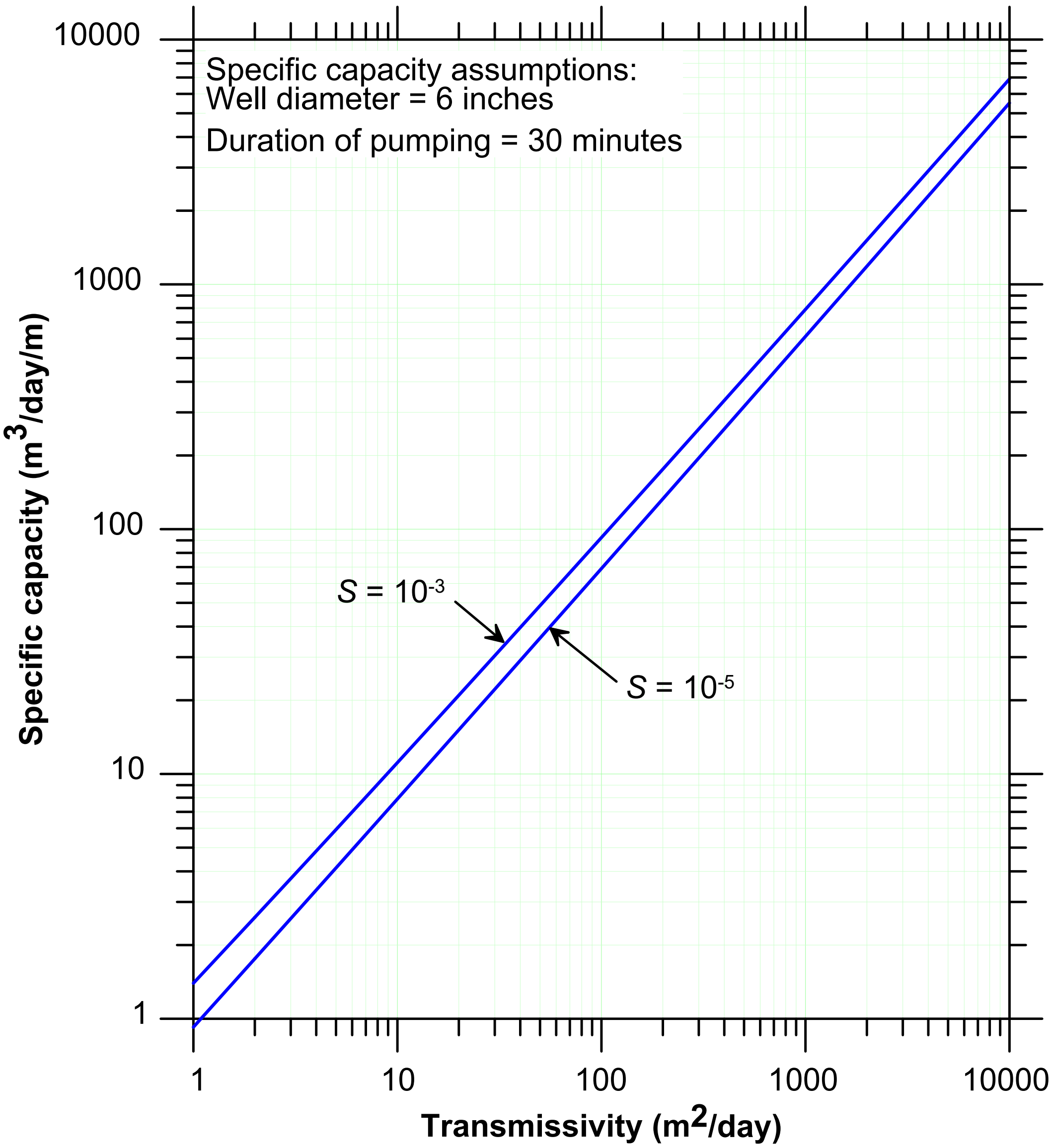

Figure 23. Specific capacity as a function of transmissivity

The results shown in Figure 23 suggest that over the range of 1 to 10,000 m^2/day, the log of the specific capacity is nearly a linear function of the log of the transmissivity. Over this range the exact results are matched relatively closely with the simple relation (assuming consistent units):

$$T \approx 1.3 \times \ SC \tag{27}$$

The simplified relation is superimposed on the exact results in Figure 24. Equation (27) may be applied to developing reconnaissance-level estimates of transmissivity, or to estimate the specific capacity if an estimate of the transmissivity is available.

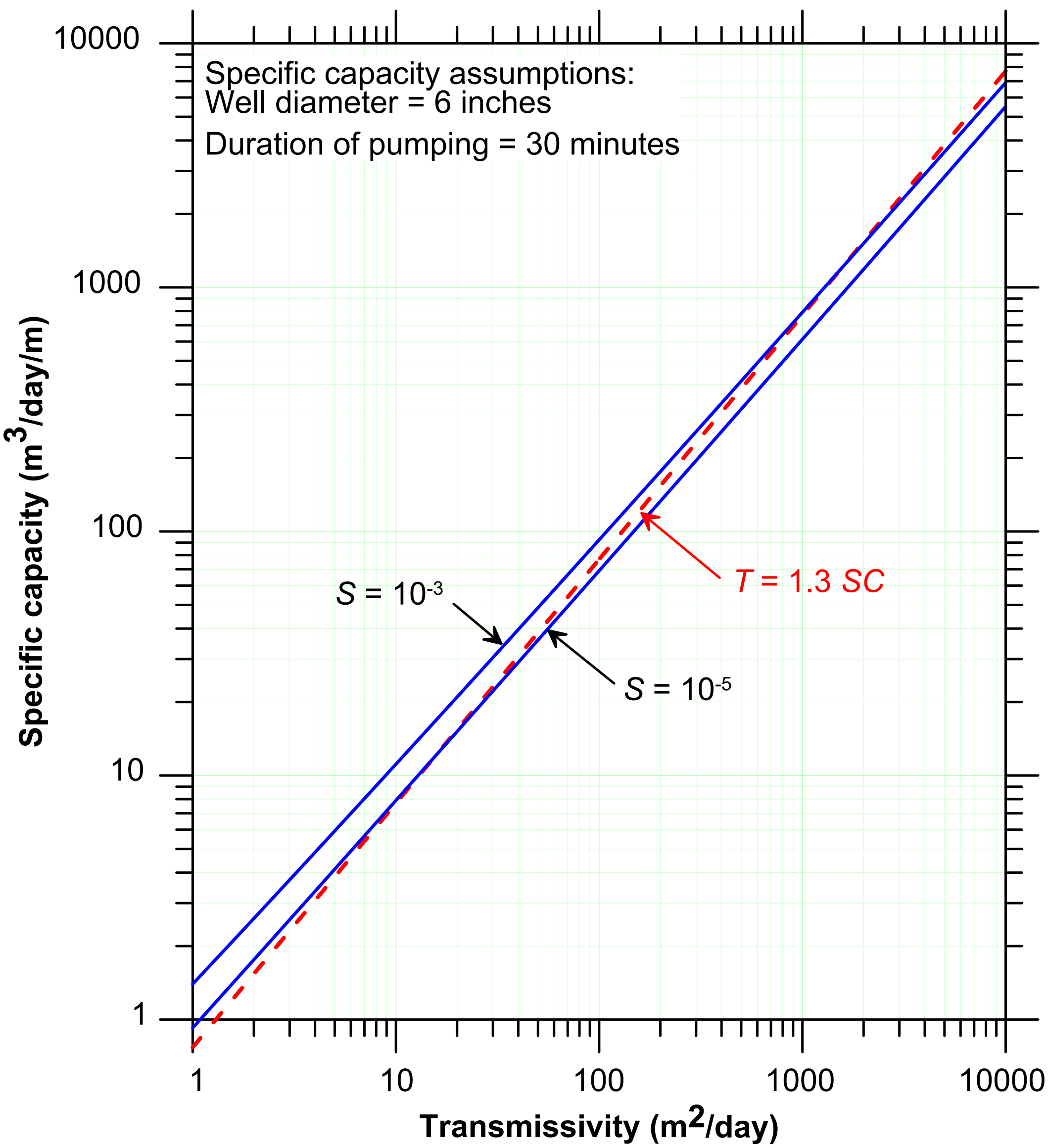

Figure 24. Specific capacity-transmissivity relation, with suggested correlation

Case study: Rosemont, Ontario well PW3

The first-cut estimation of transmissivity from the specific capacity is also useful for conducting a quick check on more complete analyses. The data from a pumping test conducted at Rosemont, Ontario is used to illustrate the approach. Well PW3 was pumped for three days at an average rate of 0.6 L/s (51.84 m^3/d). The complete record of drawdowns is shown in Figure 25. The drawdown at the end of 60 minutes of pumping was 5.94 m. Therefore, the specific capacity after 60 minutes is:

$$SC = \frac{(51.84\ \mathrm{m^3/d})}{(5.94\ \mathrm{m})} = 8.73\ \mathrm{m^3/d/m}$$

The transmissivity estimated from specific capacity is:

$$T \approx 1.30 \times (8.73\ \mathrm{m^3/d/m}) = \mathbf{11.3\ m^2/d}$$

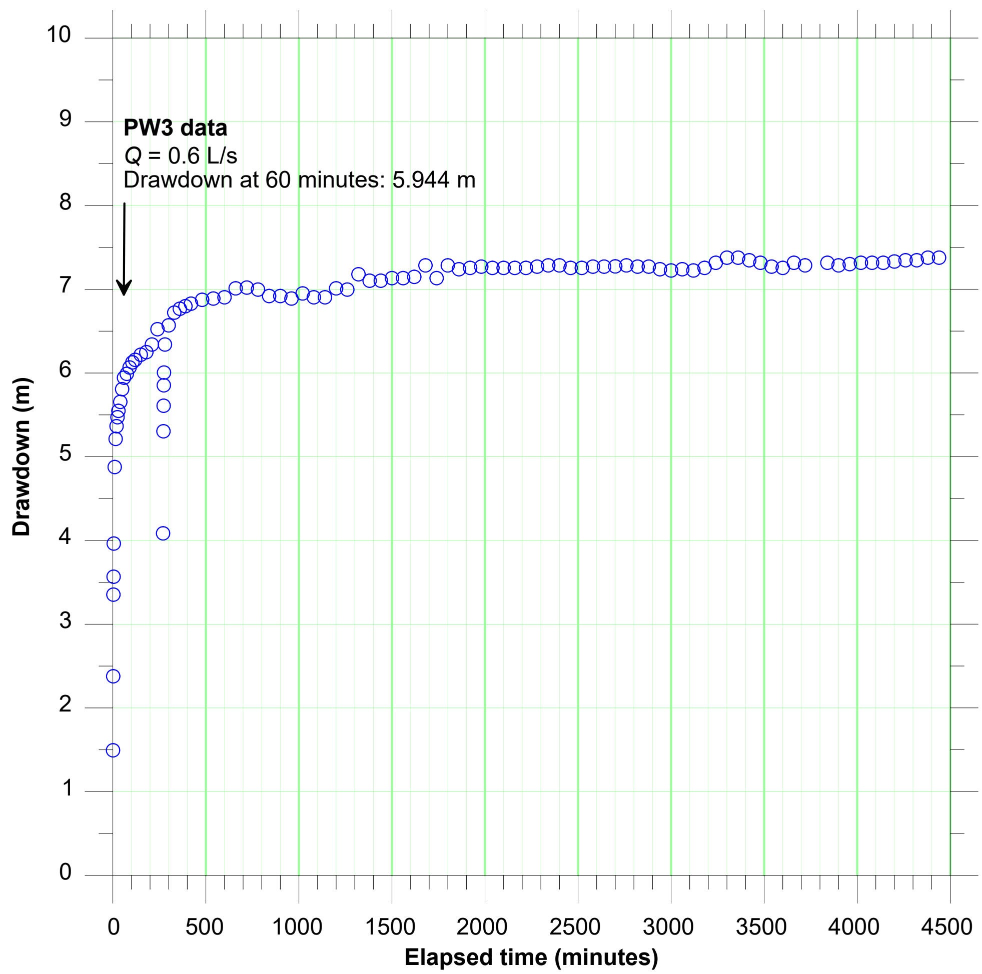

Figure 25. Drawdown record for the PW3 pumping test

The results of more rigorous analyses are shown in Figure 26. The transmissivity is estimated with the Cooper-Jacob analysis and by matching the complete drawdown record with the Papadopulos and Cooper (1967) solution. A transmissivity of about **11 m²/day** is estimated from both analyses. The close agreement between the two analyses suggests that well losses do not have a significant influence on the estimation of transmissivity for this test.

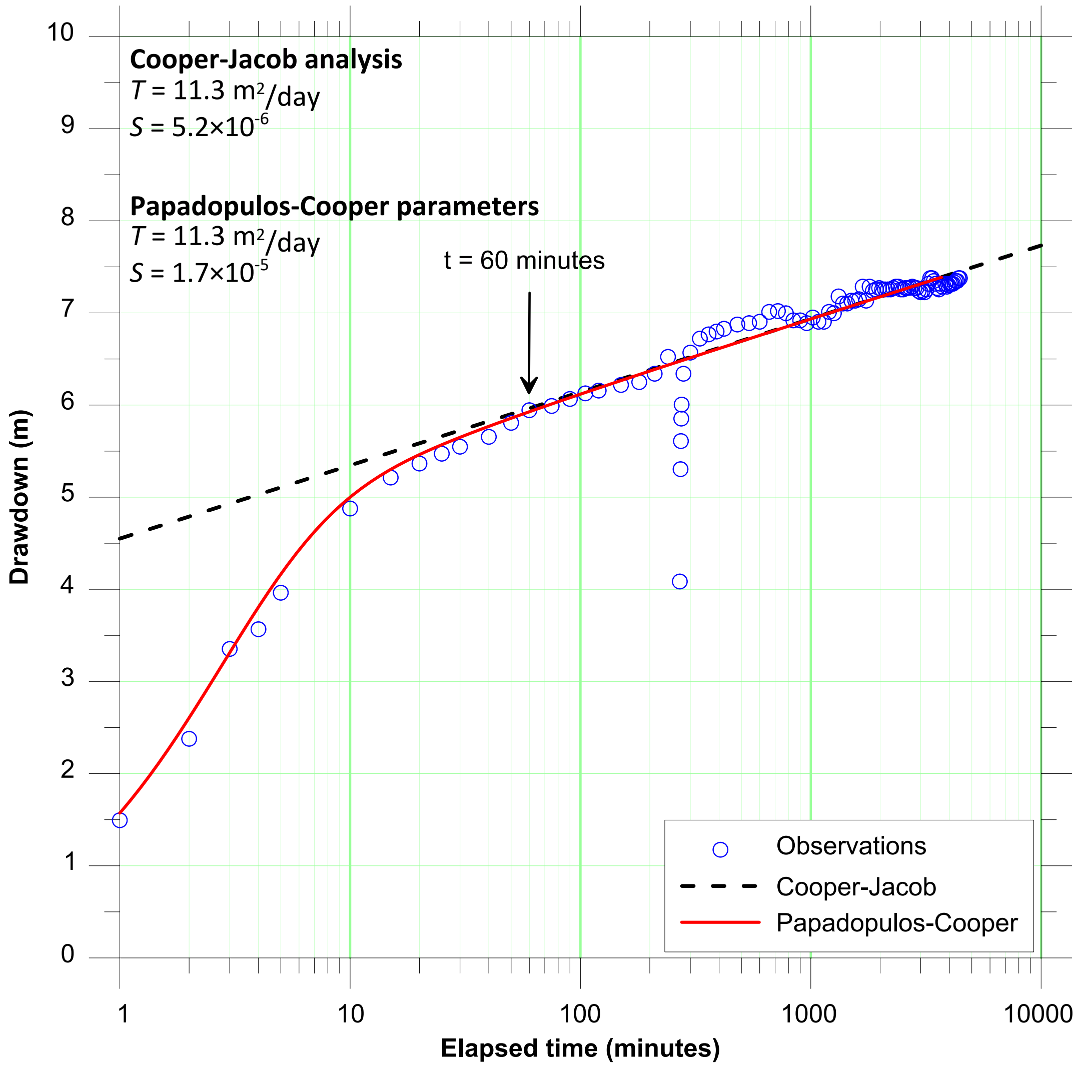

Figure 26. Rigorous analyses of the PW3 pumping test

The transmissivity estimated from the specific capacity for the Roseville well is close to the estimates developed from the more rigorous analyses of the complete drawdown record. This is not simply fortuitous. The availability of a complete drawdown record allows us the opportunity to confirm the following *in this case*.

- The time corresponding to the drawdown specified in the calculation of the specific capacity was sufficiently long for the effects of wellbore to dissipate. Referring to Figure 26, after about 60 minutes of pumping the differences between the Papadopulos and Cooper (1967) solution and the Cooper-Jacob straight line approximation are relatively small. This suggests that the effects of wellbore storage are almost completely dissipated within about 60 minutes so that the drawdown measured at 60 minutes provides a representative impression of the response of the formation.

- The early-time drawdowns are relatively small, which suggests that additional well losses are not significant. Therefore, the observed drawdowns in the pumping well provide a reliable impression of the head losses in the formation in the vicinity of the pumping well.

- The storage coefficients estimated from the Papadopulos-Cooper and Cooper-Jacob analyses are within the range of realistic storage coefficients for a confined aquifer that is relatively thin. This is consistent with the inference that the primary component of the observed drawdowns is head losses within the formation.

8. Transient conditions with additional well losses

Drawdown data from constant-rate pumping tests generally confirm that the additional drawdowns due to skin effects and in-well losses are established relatively soon after pumping starts, compared with the head losses in the formation. When evaluated at small values of the radial distance *r*, the Cooper-Jacob approximation is appropriate for all but the earliest values of time. Supplementing Equation 24) with the expressions introduced previously for Δs_{skin} and $\Delta s_{\text{turbulence}}$ yields the following expression for the evolution of the total drawdown in a pumping well:

$$s_w(t) = \frac{Q}{4\pi T}\, 2.303 \log\left\{2.246\, \frac{Tt}{r_w^2 S}\right\} + \frac{Q}{4\pi T}\, 2S_w + CQ^2 \qquad (28)$$

Expanding the log term:

$$s_w(t) = \frac{Q}{4\pi T}\, 2.303 \left(\log\left\{2.246\, \frac{T}{r_w^2 S}\right\} + \log\{t\}\right) + \frac{Q}{4\pi T}\, 2S_w + CQ^2$$

Re-arranging:

$$s_w(t) = \frac{Q}{4\pi T}\, 2.303\ \log\{t\} + \frac{Q}{4\pi T}\, 2.303 \log\left\{2.246\, \frac{T}{r_w^2 S}\right\} + \frac{Q}{4\pi T}\, 2S_w + CQ^2 \qquad (29)$$

The first term is a function of time, but the other three terms are constant. In other words, the time rate of change of drawdown is <u>not</u> affected by the processes that cause additional drawdown in the pumping well. Since the Cooper-Jacob analysis is based on the rate of change of drawdown rather than the absolute magnitude of the drawdown, it is possible to obtain a reliable estimate of the transmissivity from a Cooper-Jacob straight-line analysis, regardless of the magnitudes of the skin losses and turbulent well losses.

Example calculations:

Let us consider an ideal aquifer that is homogeneous, horizontal, perfectly confined, infinite in extent, and pumped by a fully penetrating well. The aquifer is assumed to have a transmissivity of 8.64 m^2/day and a storativity of 1.0×10^{-4}. These properties are typical of an aquifer consisting of medium sand that is 10 m thick. The pumping well has a radius of 0.05 m. The aquifer is pumped at a constant rate of 104.54 m^3/day. Let us further assume that the additional well losses are characterized by the following parameter values:

- $S_w = 0.5193$; and
- $C = 1.340 \times 10^{-4}$ $m^{-5}d^2$.

These values have been specified only for illustrative purposes – under no circumstances would we report estimates from a real test with so many significant figures. The total drawdowns in the pumping well are plotted in Figure 27.

The slope of the line plotted through the drawdown data is approximately 2.2 m. Therefore, the transmissivity is estimated as:

$$T = 2.303 \frac{Q}{4\pi} \frac{1}{SLOPE}$$

$$= 2.303 \frac{(104.54 \text{ m}^3/\text{d})}{4\pi} \frac{1}{(2.2 \text{ m})} = \mathbf{8.7\ m^2/d}$$

The estimated transmissivity is close to the specified value of 8.64 m^2/d.

The transmissivity with the Cooper-Jacob analysis is estimated from the semilog slope of the drawdowns and *not* the magnitudes of the drawdowns. Therefore, for a constant-rate pumping test the transmissivity estimate is not affected by the constant offsets of the additional well losses.

The storage coefficient is estimated with the Cooper-Jacob analysis according to:

$$S = 2.2459 \frac{T t_0}{r_w^2}$$

Here t_0 is the intercept of the straight-line approximation, which is about 4×10^{-10} days. Therefore, the fitted storage coefficient is estimated as:

$$S = 2.2459 \frac{(8.64 \text{ m}^2/\text{d})(4 \times 10^{-10} \text{ days})}{(0.1 \text{ m})^2} = \mathbf{7.7 \times 10^{-7}}$$

The "fitted" storage coefficient is more than a factor 100 less than the specified value and is well outside of the range of typical values of the storage coefficient for confined sand and gravel aquifers, from about 10^{-5} to 10^{-4}. The storage coefficient is estimated from the intercept of the plot; therefore, in contrast to the estimation of the transmissivity, the inferred magnitude of the storage coefficient *does* depend on the magnitudes of the drawdowns. When we use the Cooper-Jacob straight-line analysis, we effectively estimate a storativity that accounts in a "lumped" sense for the effects of storage and additional well losses. Although we do not obtain a true estimate of the storage coefficient, its estimation still has useful diagnostic value. Estimation of an unrealistic value of the storage coefficient suggests there are additional sources of drawdown beyond head losses in the formation.

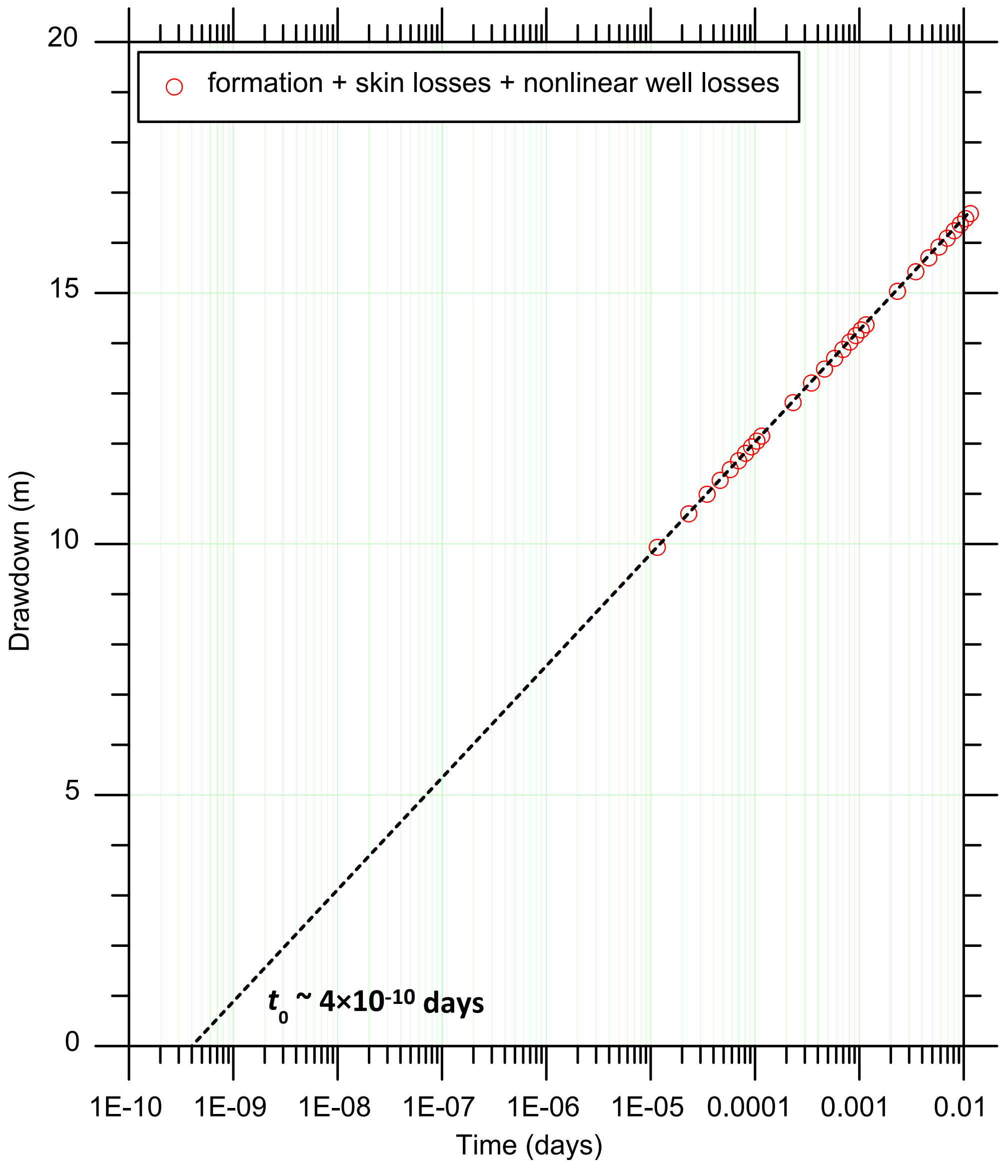

Figure 27. Drawdowns at the pumping well, with expanded time axis

9. The interpretation of step tests

If all we have are the data from the pumping well when it is pumped at a constant rate, then we must accept the fact that we cannot obtain reliable estimates of the storativity and the well loss parameters. If we want to obtain reliable estimates of the transmissivity, storativity, and the well loss characteristics, we must monitor the level in the well as it is pumped at different rates. Each interval of pumping is referred to as a step, and this testing sequence is referred to as a *step test* (Jacob, 1946).

The dataset for a step test conducted on a proposed municipal supply well in southern Cambodia is shown in Figure 28.

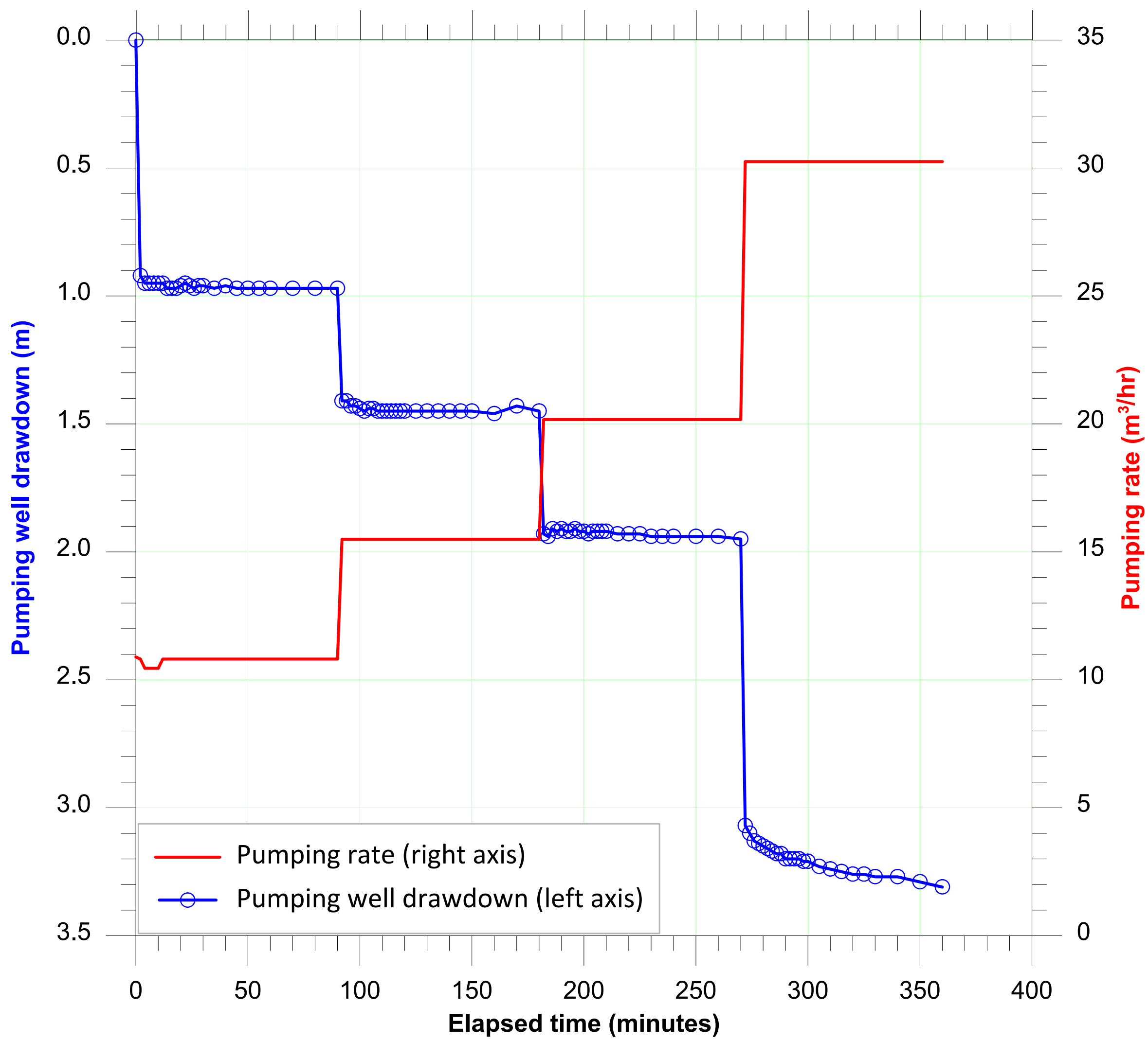

Figure 28. Example step test data

If a complete time history of drawdown is available during a step test, we can try to make use of all of the data in a transient analysis. The transient data are interpreted using the expanded form of the Theis solution. The generalization for a test in which the pumping rate varies is derived using the principle of superposition (Figure 29):

$$s_w(t) = \frac{2.303}{4\pi T}\sum_{i=1}^{NP(t)} \Delta Q_i \; W\left(\frac{r_w^2 S}{4T(t-ts_i)}\right) + \frac{Q_t}{4\pi T} 2S_w + CQ_t^2 \tag{30}$$

Here ts_i denotes the starting time of the i^{th} pumping step, ΔQ_i represents the change in the pumping rate at the start of this step, $NP(t)$ represents the number of steps that have occurred up to the current time t, and Q_t is the current pumping rate. The current pumping rate is related to the steps according to:

$$Q_t = \sum_{i=1}^{NP(t)} \Delta Q_i \tag{31}$$

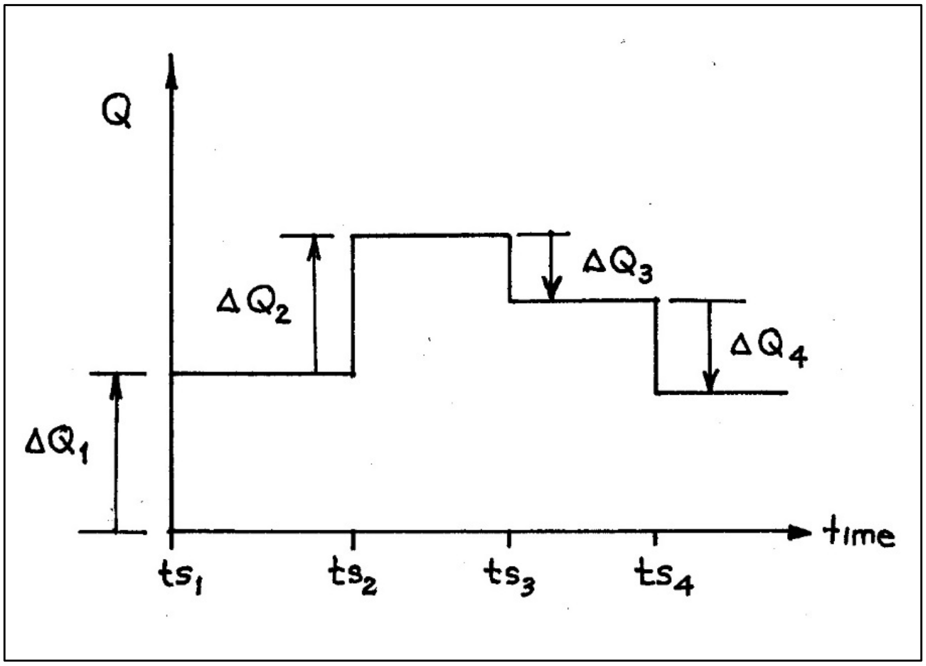

Figure 29. Schematic representation of time-varying pumping

In practice, the data collected during a step test are matched with Equation (31) by applying a fitting routine, such as that incorporated in packages like AQTESOLV. The application of the transient analyses will be demonstrated with a case study but first we consider a simple example to introduce a note of caution regarding the analyses.

Example calculations:

In Section 8 we considered an example of a pumping well that penetrated the full thickness of an ideal aquifer. The following parameters were specified for the example:

- Transmissivity, $T = 8.64$ m^2/d;
- Storativity, $S = 10^{-4}$;
- Dimensionless skin factor, $S_w = 0.5193$; and
- Nonlinear well loss coefficient, $C = 1.340\times10^{-4}$ m^{-5}d^2.

In the previous calculation, we assumed that the well was pumped at a constant rate. This time, let us assume that the well is pumped for three even steps according to the following schedule:

Elapsed time	**Pumping rate, m^3/day**
0 to 60 minutes	34.848
60-120 minutes	69.696
120-180 minutes	104.544

The drawdowns at the pumping are plotted in Figure 30.

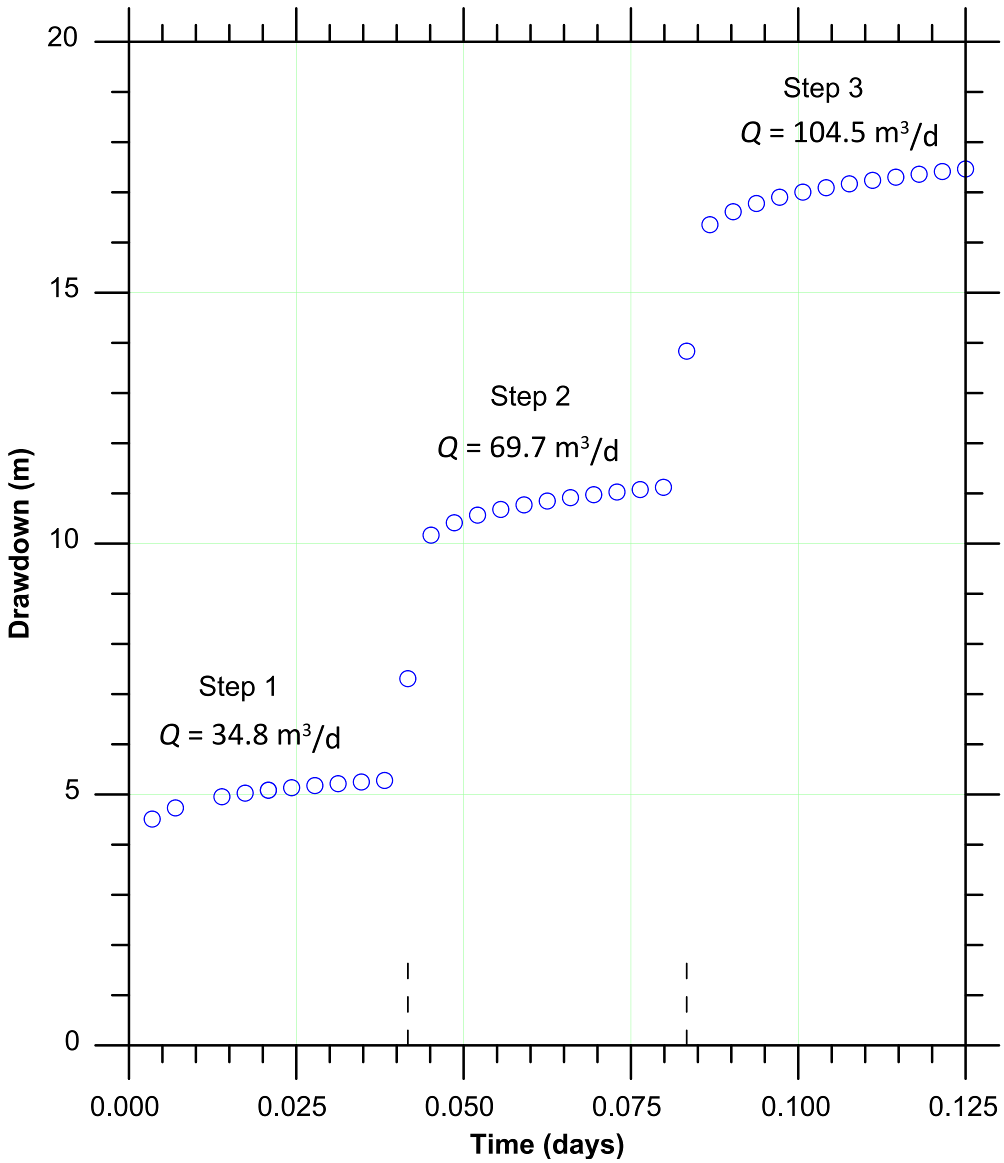

Figure 30. Pumping well drawdowns for a hypothetical step test

The analysis package AQTESOLV is used to fit the full transient record with Equation (31). How well does AQTESOLV do when it is asked to estimate simultaneously the transmissivity and storativity, T and S, *and* the well loss parameters C and S_w? The results of the automatic fit are shown in Figure 31. As shown in the figure, the drawdowns are matched very closely.

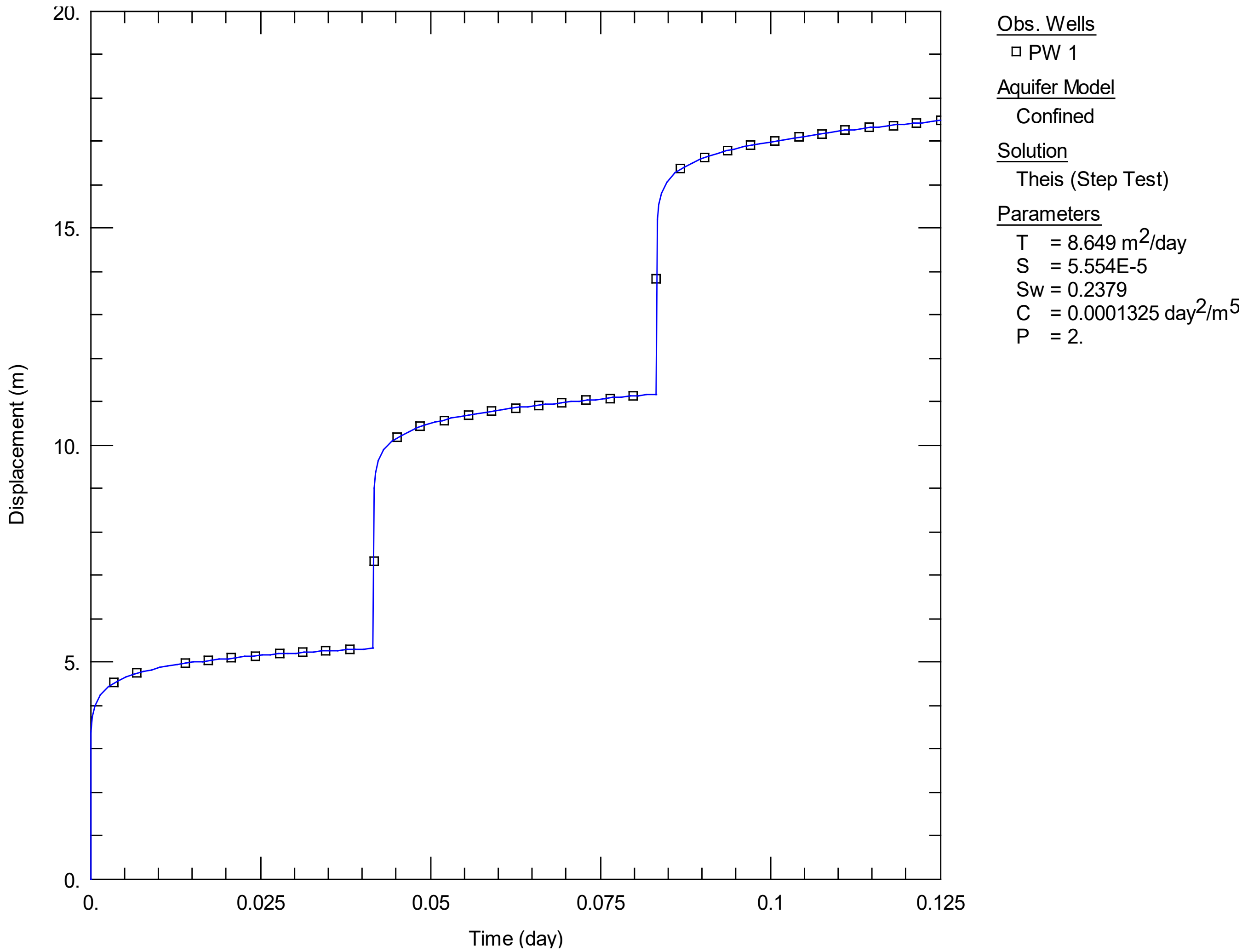

Figure 31. AQTESOLV match to hypothetical step test results

The specified and fitted parameter values are listed below.

Parameter	Specified value	Fitted value
T	8.64 m^2/d	8.65 m^2/d
S	1.0×10^{-4}	5.55×10^{-5}
S_w	0.5193	0.2379
C	1.34×10^{-4} d^2/m^5	1.32×10^{-4} d^2/m^5
P	2.0 (fixed)	2.0 (fixed)

The fitted values of the transmissivity, T, and the nonlinear well loss coefficient, C, are very close to the values that were specified to simulate the drawdowns. By pumping the well at more than one pumping rate, we increase our chances of obtaining unique estimates for these parameters. However, the storativity, S, and the skin loss coefficient, S_w, are significantly different from the specified values.

Why do we obtain an essentially perfect match to the drawdowns but with very different parameter values? Is it possible that the parameters estimated through the "objective" nonlinear least-squares fitting are not unique?

To assess whether the parameter values estimated for a particular analysis are unique, it is necessary to examine whether any of the fitted parameters are correlated. With the AQTESOLV software it is possible to examine parameter correlation, under the window labeled **diagnostics** (Figure 32). Reviewing the reported "Parameter Correlations", we see that the storage coefficient and the skin loss coefficient have Parameter Correlation values of 1.00.

Diagnostic Statistics

Estimation complete! Parameter change criterion (ETOL) reached.

Aquifer Model: Confined
Solution Method: Theis (Step Test)

Estimated Parameters

Parameter	Estimate	Std. Error	Approx. C.I.	t-Ratio	
T	8.649	0.004118	+/- 0.008397	2100.2	m^2/day
S	5.554E-5	4.83E-5	+/- 9.848E-5	1.15	
Sw	0.2379	0.4298	+/- 0.8763	0.5536	
C	0.0001325	1.319E-7	+/- 2.689E-7	1004.7	day^2/m^5
P	2.	not estimated			

C.I. is approximate 95% confidence interval for parameter
t-ratio = estimate/std. error
No estimation window

K = T/b = 0.8649 m/day (0.001001 cm/sec)
Ss = S/b = 5.554E-6 1/m

Parameter Correlations

	T	S	Sw	C
T	1.00	-0.85	-0.85	0.31
S	-0.85	1.00	1.00	-0.21
Sw	-0.85	1.00	1.00	-0.21
C	0.31	-0.21	-0.21	1.00

Residual Statistics

for weighted residuals

Sum of Squares .... 4.392E-5 m^2
Variance .... 1.417E-6 m^2
Std. Deviation....... 0.00119 m
Mean ....-0.0001331 m
No. of Residuals 35
No. of Estimates 4

Figure 32. Diagnostic reports for the step test example

What does a Parameter Correlation value of 1.00 mean? In this case, it means that the storativity S and the dimensionless skin factor S_w are perfectly correlated. From the perspective of model fitting, it means that the values of S and S_w *cannot* be estimated independently; that is, it is impossible to obtain unique estimates of S and S_w. As shown in Figure 33, if we fix S at two widely different values we obtain equally good matches to the observations with two very different values of S_w.

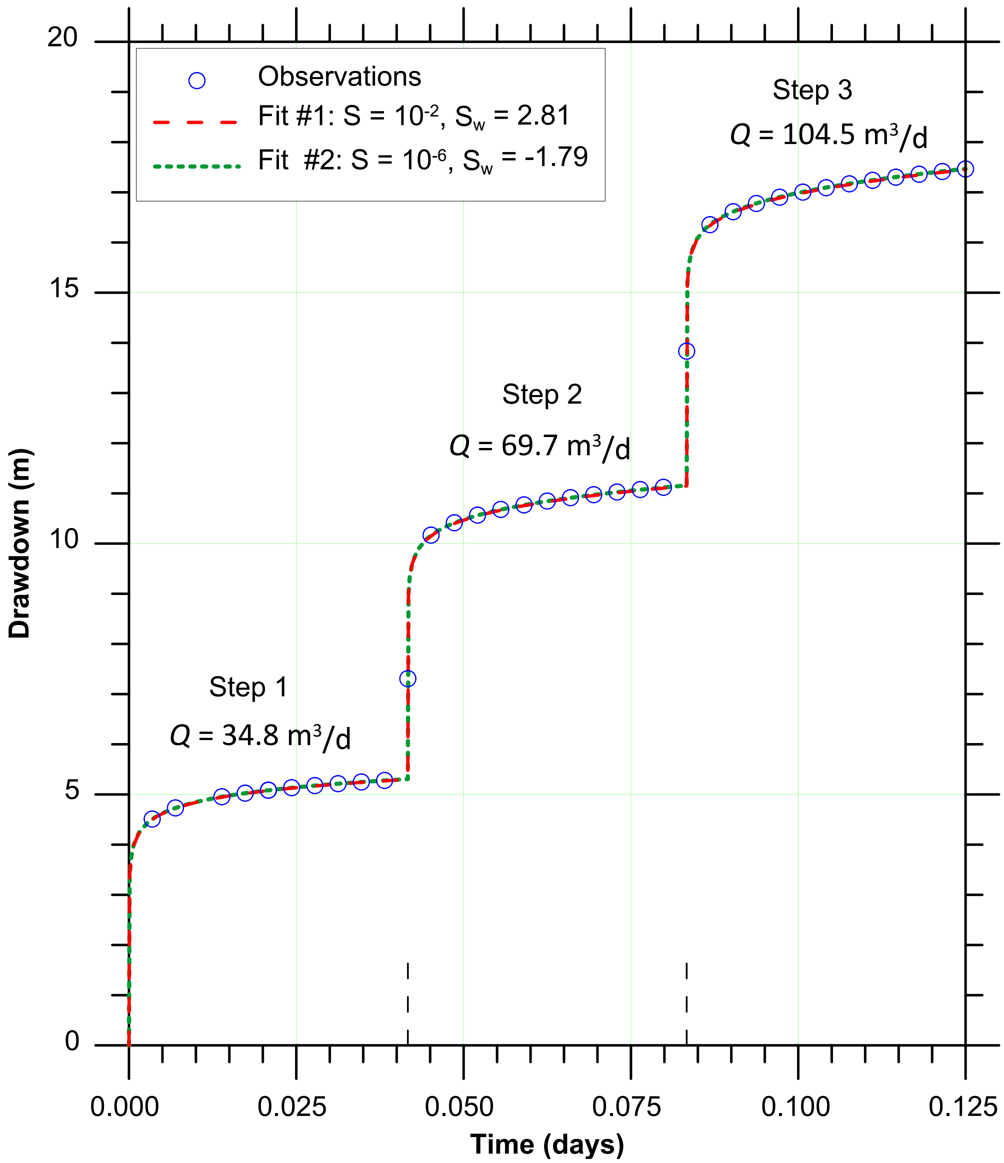

Figure 33. Alternative AQTESOLV matches to hypothetical step test results

Case study: Guelph municipal production well PW6/63 revisited

The processed data from the PW6/63 step test are shown in Figure 34. The data are of sufficient quality to support a more rigorous transient analysis beyond the steady-state approach applied previously. The case study is used to illustrate a preferred approach for interpreting the data from step tests.

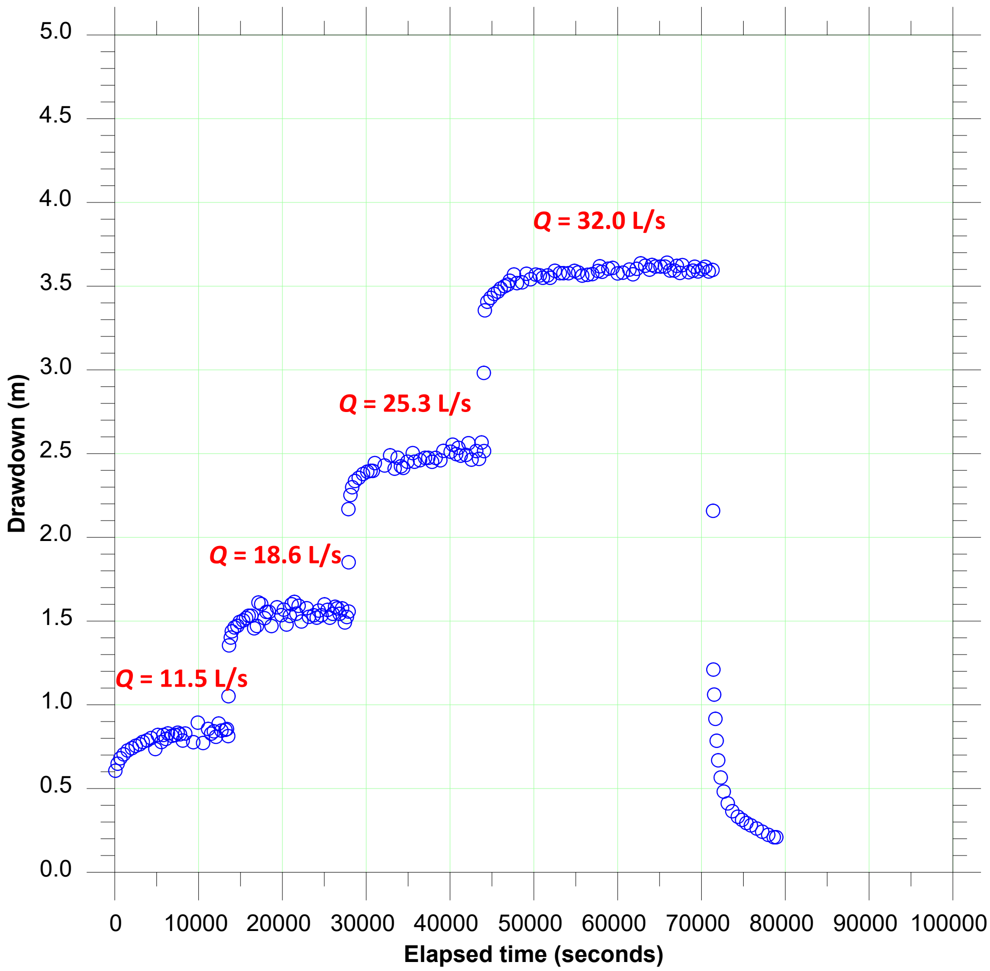

Figure 34. PW6/63 transient drawdown record

A computer-assisted analysis package is used to match the Theis solution to the drawdowns. The following decisions are made to constrain the analysis and avoid the non-uniqueness arising from parameter correlation:

- The storage coefficient is fixed at a "physically realistic" value, $S = 1.0 \times 10^{-5}$; and
- The value of the nonlinear well loss coefficient, C, is fixed based on the results from the Hantush-Bierschenk plot.

$$C = 0.00225 \frac{\text{m}}{(\text{L/s})^2} \left| \frac{1000 \text{ L}}{\text{m}^3} \right|^2 = 2{,}250 \frac{\text{m}}{(\text{m}^2/\text{s})^2}$$

The results of the computer-assisted analysis are shown in Figure 35. As shown in the figure, it is possible to match closely the entire time-drawdown record with a transmissivity of about **3,400 m²/d**.

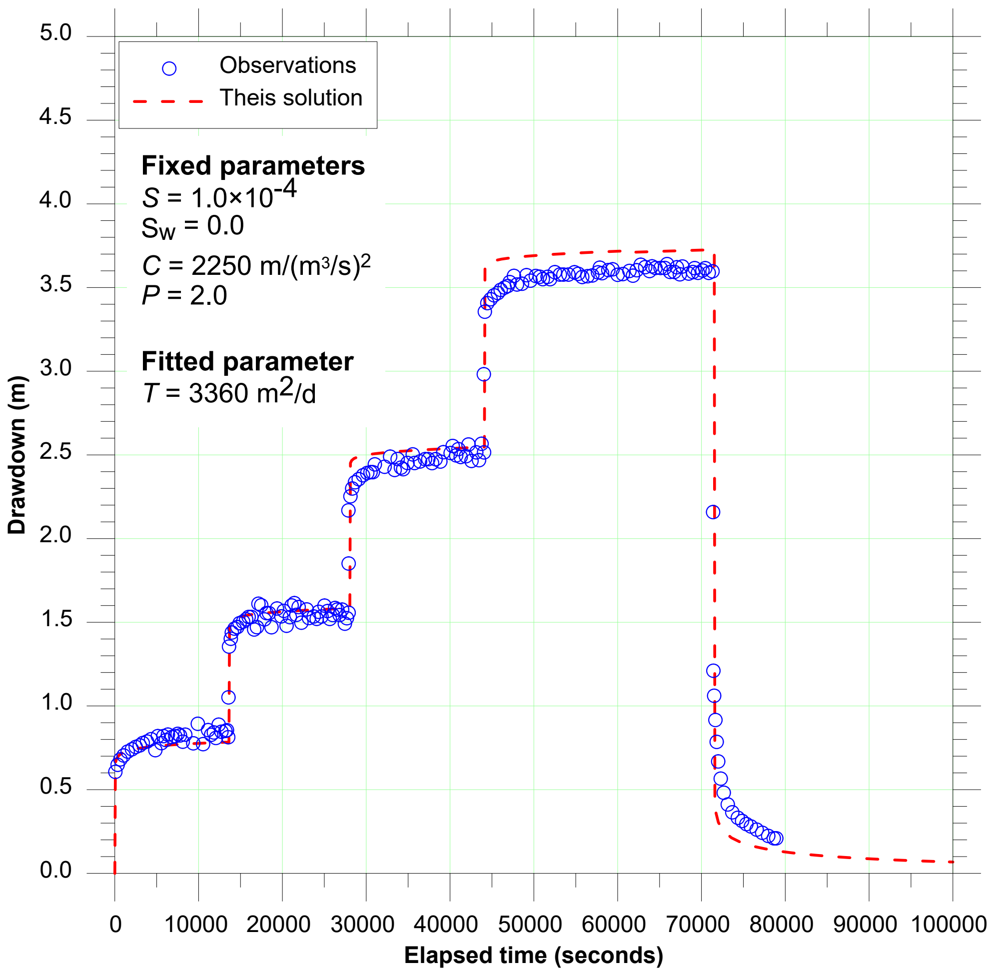

Figure 35. Match to the full transient drawdown record

As a simple check on our analysis, we can apply our "reconnaissance-level" estimator for the transmissivity, Equation (27):

$$T \approx 1.3 \times \ SC$$

However, Equation (27) was developed with the assumption that the drawdowns in the pumping well are due entirely to head losses in the formation. We should therefore use the value of the specific capacity with the nonlinear well losses removed. Referring to Figure 20, this is given by the reciprocal of the linear well loss coefficient *B*:

$$SC_{\mathrm{corr}} = \frac{1}{B} = \frac{1}{0.04\ \mathrm{m/L/s}} = 25\ \frac{\mathrm{L/s}}{\mathrm{m}}$$

The "reconnaissance-level" estimate of the transmissivity is therefore:

$$T \approx 1.3 \times \left(\frac{25\ \mathrm{L/s}}{\mathrm{m}}\right)\left|\frac{\mathrm{m}^3}{1000\ \mathrm{L}}\right|\left|\frac{86400\ \mathrm{seconds}}{\mathrm{day}}\right| = \mathbf{2800\ \ m^2/day}$$

The advantage of estimating the transmissivity with the corrected specific capacity is that it is simple to do. The transmissivity estimate obtained with the corrected specific capacity, **2,800 $\mathbf{m^2}$/d**, is relatively close to the estimate developed from the rigorous analysis, **3,400 $\mathbf{m^2}$/d**. It is certainly consistent with our expectations regarding a "reconnaissance-level" estimate. The preliminary estimate of the transmissivity derived with the estimate of the specific capacity with the nonlinear losses removed provides a useful check on our more rigorous analysis.

The results of the analyses highlight the importance of accounting for well losses in this case. The "raw" specific capacities range from 13.2 to 8.9 L/s/m. These are significantly smaller than the value estimated after the nonlinear well losses are removed, 25 L/s/m.

Armed with the results of the more rigorous analysis of a step test, the observations can be extended to predict the evolution of the drawdown for extended pumping. In Figure 36, the match to the observations of the City of Guelph PW6-63 testing is extended to about 3 years. Beyond the end of the step test, the well is assumed to be pumped continuously at the final rate of the step test, 32 L/s. The analysis could be supplemented with additional results for different rates, to estimate a pumping rate for which the projected drawdown remains less than the maximum allowable drawdown. However, we recommend that the approach be limited to the rates at which the well was pumped during the step test.

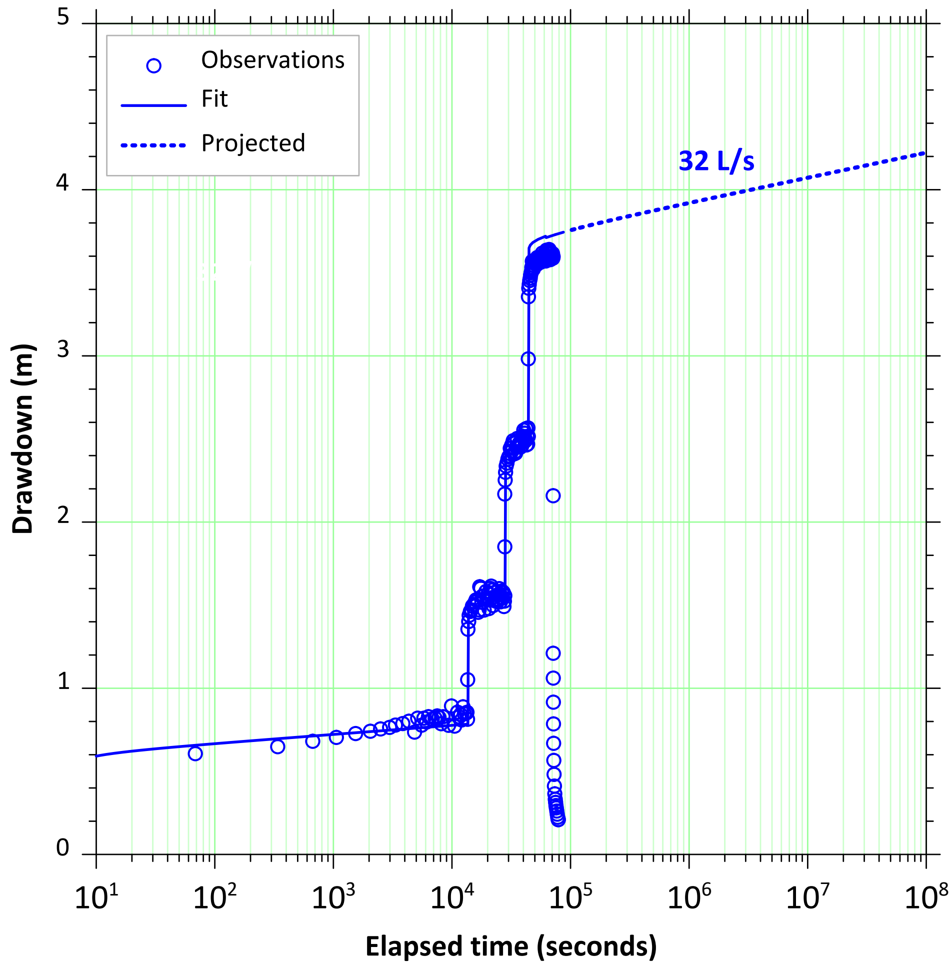

Figure 36. Extension of the analysis of PW6-63

10. Estimation of the long-term capacity of a pumping well

If the water level in the well does not stabilize during test, we also need to account for the planned duration of pumping. The duration of pumping might be days, months, or years, depending on the purpose of the well.

10.1. "Straight-line" projection

The simplest possible approach to estimating the long-term capacity of a well is shown schematically in Figure 37. The calculation involves only two steps: (1) projection of the drawdowns observed during testing to the target duration of pumping; and (2) scaling the long-term drawdown with respect to the pumping rate maintained during testing.

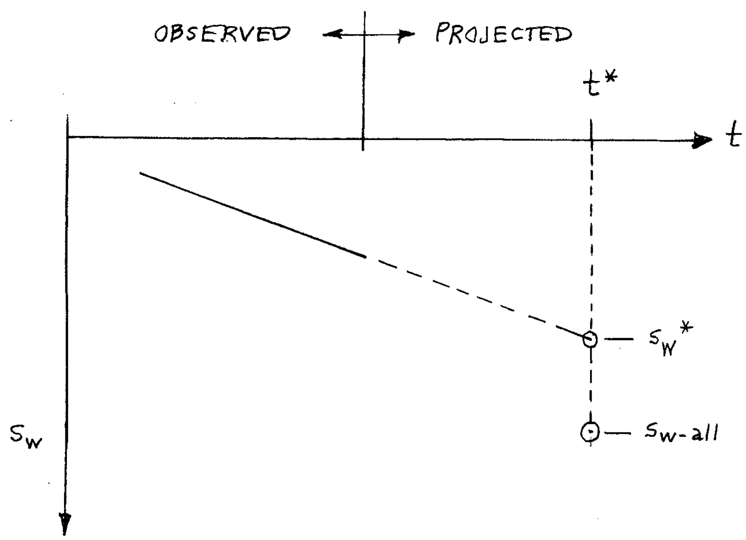

Figure 37. Illustration of the "straight-line" project approach

If we denote the test pumping rate as Q_{test}, the target duration of pumping as t*, and s_w* as the drawdown projected to t*, and the maximum allowable drawdown as $s_{w\text{-}all}$, the maximum allowable pumping rate is simply:

$$Q_{max} = Q_{test} \frac{s_{w-all}}{s_w^*(t^*)} \tag{32}$$

This is a straightforward calculation, but it is based on two important assumptions:

- The drawdowns can be reliably extrapolated from the available observations; and
- The pumping well drawdown is directly proportional to the pumping rate.

Case study: Conestogo well C3

Well C3 (TW 1-89) was constructed in 1989. The "as-constructed" drawing of the well is reproduced in Figure 38. The well is screened from a depth of 29 to 32.2 m below ground in a sand and gravel aquifer between 24.5 m and 32.2 m below ground surface. The pre-pumping depth to water was 5.56 m below ground surface, We are charged with estimating the long-term capacity of Well C3 for a time of interest of 10,000 days (about 27 years).

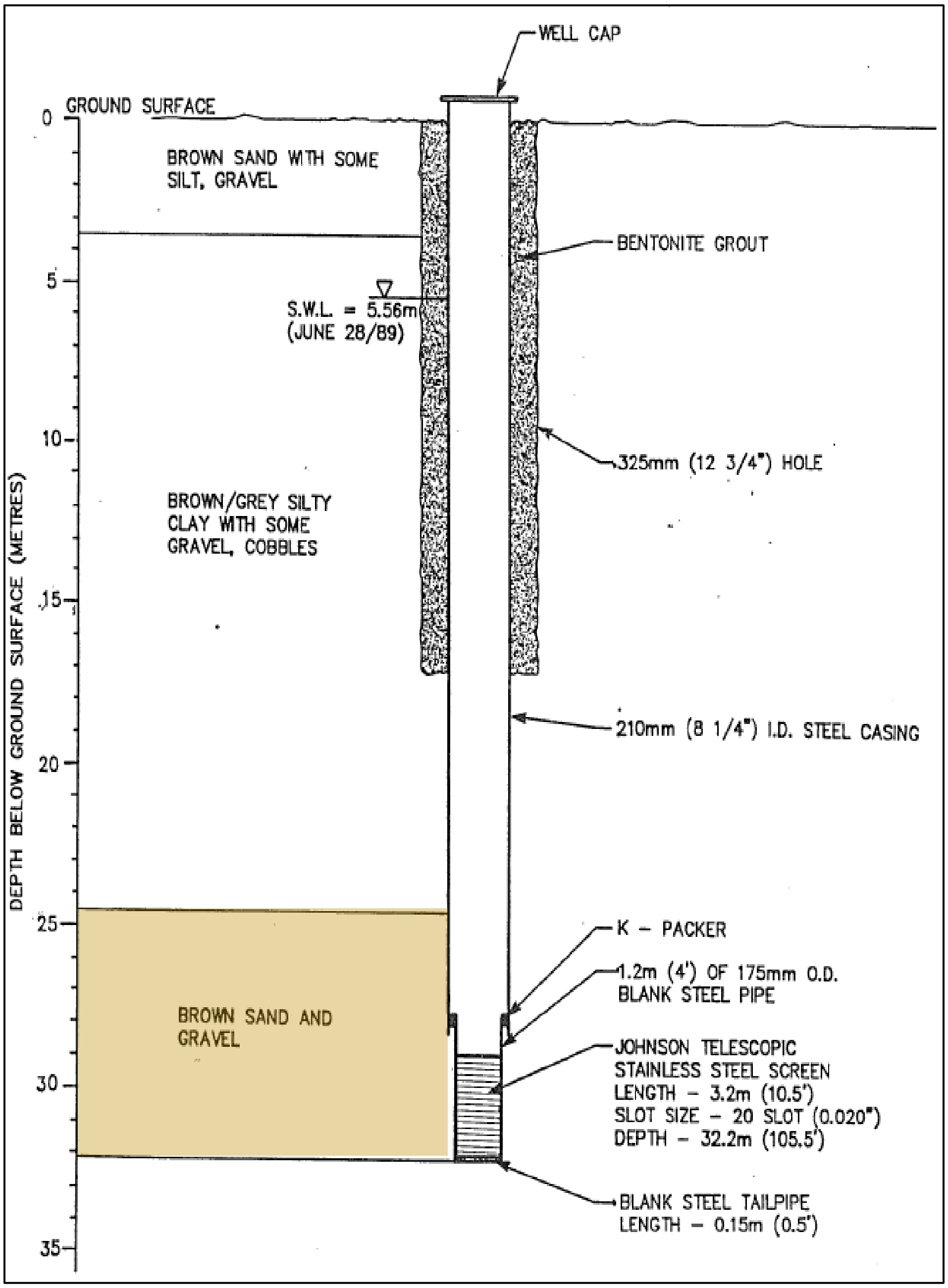

Figure 38. C3 "as-built" well diagram

At the time of construction, a 24-hour constant-rate pumping test was conducted at a rate of 7.6 L/s. The water levels in the pumping well during the constant-rate test are shown in Figure 39.

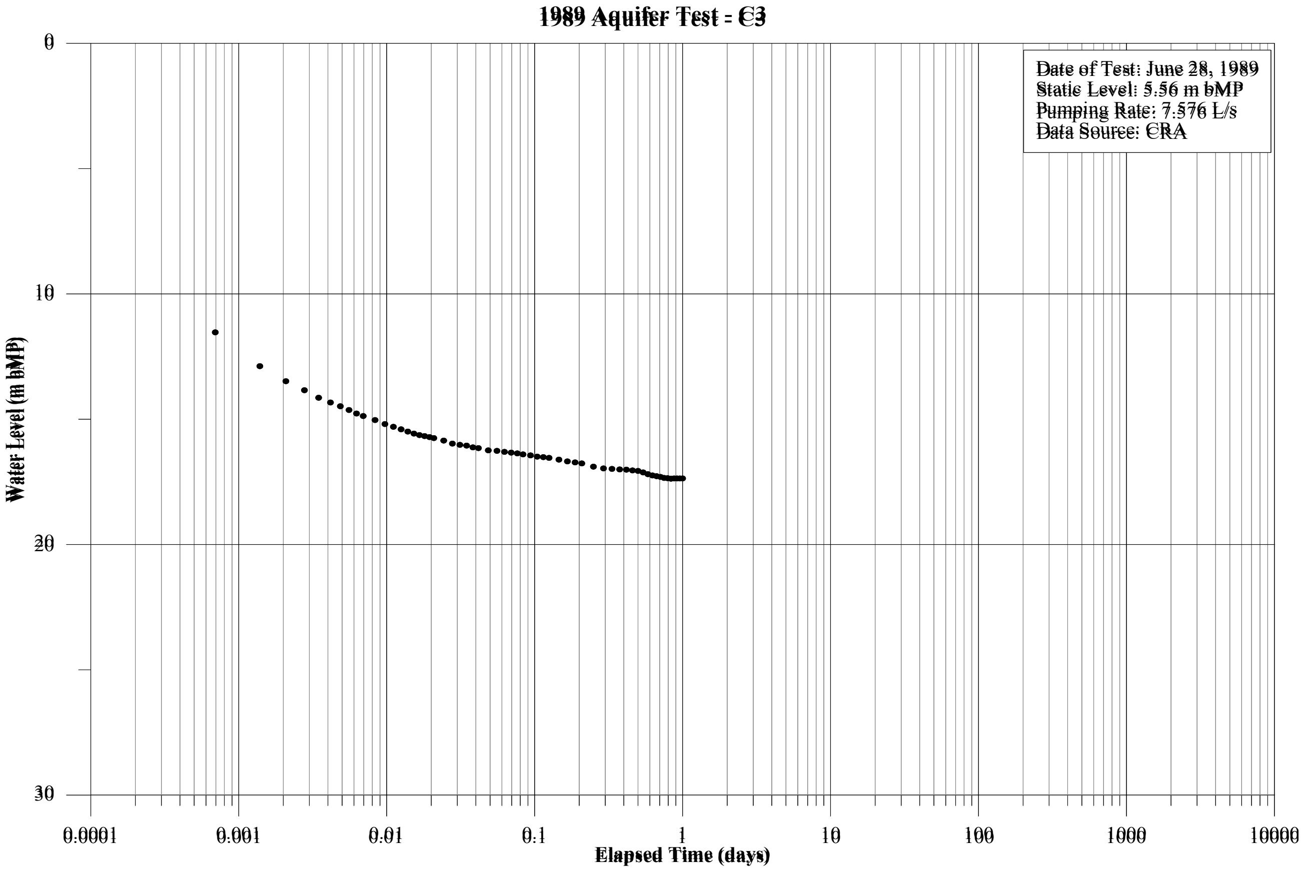

Figure 39. C3 drawdowns during the constant-rate pumping test

The straight-line projection shown in Figure 40 suggests that after 10,000 days of continuous pumping at 7.6 L/s, the depth to water in the well would be about 21 m. Assuming a static water level of 5.56 m below ground surface, the projected drawdown is about **15.4 m**.

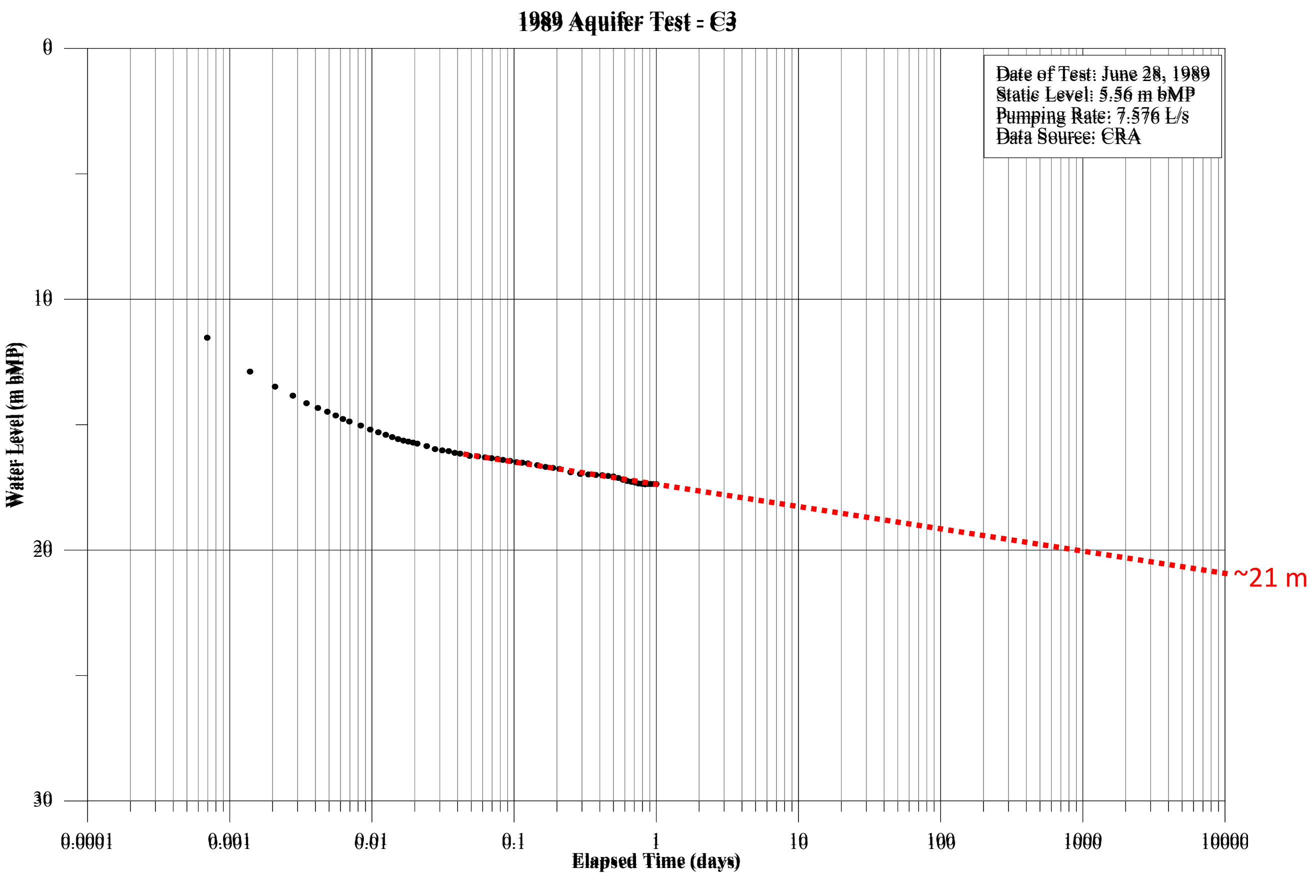

Figure 40. C3 projection of drawdowns from the constant-rate pumping test

Three criteria for the maximum allowable drawdown are considered:

- Drawdown to the top of the aquifer;
- Drawdown to the top of the well screen; and
- Drawdown to the pump intake.

The depths to water corresponding to each criterion are listed below.

Criterion	Depth (m below ground surface)
Top of the aquifer	24.5
Top of the well screen	29.0
Pump intake	28.3

Let us choose the elevation of the pump intake as the criterion for the maximum available drawdown (depth = 28.3 m). Noting a static water level of 5.56 m below ground surface and incorporating a margin of safety of 1.5 m we estimate:

$$s_{\mathrm{w-all}} = (28.3\text{ m} - 5.56\text{ m}) - 1.5\text{ m} = 21.2\text{ m}$$

The maximum allowable pumping rate is therefore estimated as:

$$Q_{\max} = (7.6\text{ L/s})\,\frac{(21.2\text{ m})}{(15.4\text{ m})} = \mathbf{10.5\ L/s}$$

If we decided to be more conservative and set the minimum pumping level as the top of the aquifer, we would obtain:

$$s_{\mathrm{w-all}} = (24.5\text{ m} - 5.56\text{ m}) - 1.5\text{ m} = 17.4\text{ m}$$

$$Q_{\max} = (7.6\text{ L/s})\,\frac{(17.4\text{ m})}{(15.4\text{ m})} = \mathbf{8.6\ L/s}$$

Based on the results of the aquifer test, a long-term safe yield of 9.1 L/s. was recommended and in 1991 a Permit to Take Water was issued allowing a maximum average daily taking at this rate.

10.2. The Q_{20} method

An approach that has been applied widely in Canada to estimate the long-term safe yield of a well is the Q_{20} method (Farvolden, 1959). For a confined aquifer, the theoretical safe yield, Q_{20}, represents the pumping rate that may be supported for 20 years without exceeding the available drawdown, H_A.

The safe yield calculated with the Q_{20} method is given by:

$$Q_{20} = 0.7 \times 0.68\, T\, H_{\mathrm{A}} \tag{33}$$

Here T is the transmissivity of the aquifer in the vicinity of the pumping well.

Farvolden (1959) does not include any details on the development of Equation (26). To assess the Q_{20} method, it is first necessary to understand its foundations.

The Q_{20} method is a direct application of the Cooper and Jacob (1946) approximation of the Theis solution. The drawdown in the pumping well, $s(r_w,t)$, predicted with the Cooper-Jacob approximation is:

$$s(r_{\mathrm{w}}, t) = \frac{Q}{4\pi T} 2.303 \log\left(\frac{2.25Tt}{r_{\mathrm{w}}^2 S}\right) \tag{34}$$

Here Q is the pumping rate, r_w is the radius of the pumping well, t is the elapsed duration of pumping, T is the aquifer transmissivity and S is the storage coefficient (storativity).

We consider two points along the Cooper-Jacob straight line.

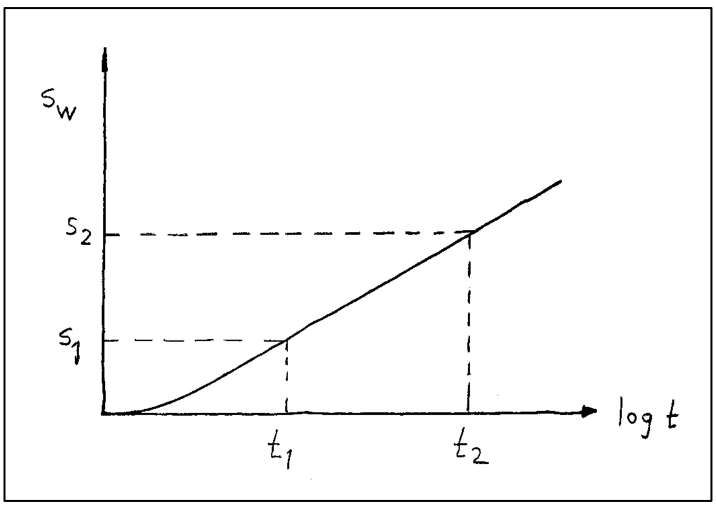

Figure 41. Cooper-Jacob straight line

The drawdowns at times t_1 and t_2 are given by:

$$s(r_{\mathrm{w}}, t_1) = \frac{Q}{4\pi T} 2.303 \log\left(\frac{2.25 T t_1}{r_{\mathrm{w}}^2 S}\right)$$

$$s(r_{\mathrm{w}}, t_2) = \frac{Q}{4\pi T} 2.303 \log\left(\frac{2.25 T t_2}{r_{\mathrm{w}}^2 S}\right)$$

The difference between the drawdowns at times t_1 and t_2, is given by:

$$s(r_w, t_2) - s(r_w, t_1) = \frac{Q}{4\pi T} 2.303 \log\left(\frac{t_2}{t_1}\right) \tag{35}$$

If t_2 is taken as 20 years (roughly 10^8 seconds) and it is assumed that the drawdown is relatively small before an elapsed time t_1 of 10 seconds, the ratio in the log term is about 10^8. Therefore, Equation (35) reduces to:

$$s(r_w, 20\text{ years}) - 0 \approx \frac{Q}{4\pi T} 2.303\ (8) \tag{36}$$

Fixing the drawdown after 20 years as the allowable drawdown H_A, incorporating a "factor of safety" of 0.7, and solving for Q yields:

$$Q_{20} = 0.7 \frac{1}{2.303\ (8)} 4\pi T\ H_{\mathrm{A}}$$

Simplifying yields Equation (33):

$$Q_{20} = 0.7 \times 0.68\ T\ H_A$$

Example calculations:

As shown in Figure 39, for the C3 well a transmissivity of about 130 m^2/day is estimated from the 24-hour pumping test:

$$T = 2.303 \frac{Q}{4\pi}\frac{1}{\Delta s}$$

$$= 2.303 \frac{\left(7.576 \text{ L/s} \left|\frac{86.4 \text{ m}^3/\text{day}}{\text{L/s}}\right|\right)}{4\pi} \frac{1}{(0.91 \text{ m})} = 132 \text{ m}^2/\text{day}$$

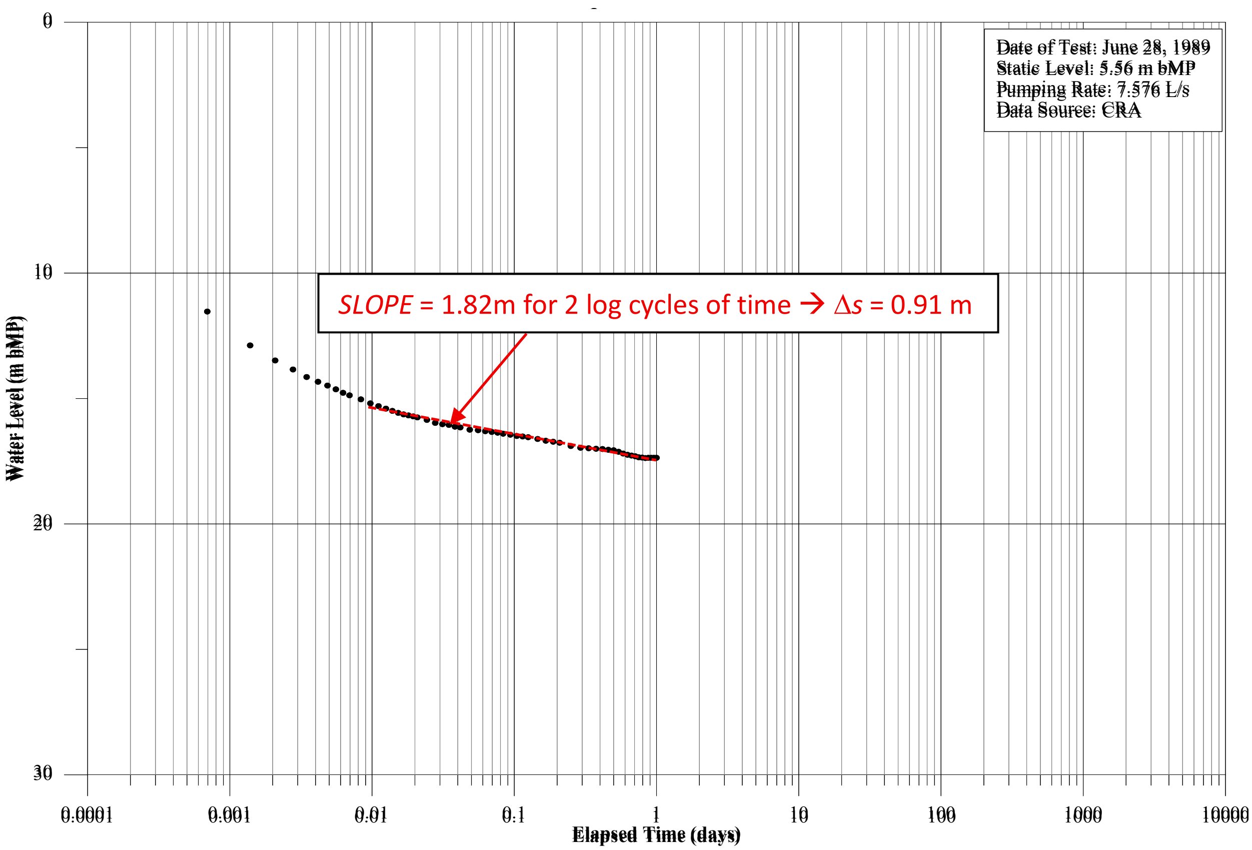

Figure 42. C3 Cooper-Jacob analysis of constant-rate pumping test

With the elevation of the pump intake set as the criterion for the maximum available drawdown:

$$s_{\mathrm{w-all}} = (28.3\ \mathrm{m} - 5.56\ \mathrm{m}) - 1.5\ \mathrm{m} = 21.2\ \mathrm{m}$$

The maximum allowable pumping rate is:

$$Q_{20} = 0.7 \times 0.68\ (132\ \mathrm{m}^2/\mathrm{day})\ (21.2\ \mathrm{m}) = 1300\ \mathrm{m}^3/\mathrm{day}, \text{or } \mathbf{15.5\ L/s}$$

With the elevation of the top of the aquifer set as criterion for the maximum available drawdown:

$$s_{\mathrm{w-all}} = (24.5\ \mathrm{m} - 5.56\ \mathrm{m}) - 1.5\ \mathrm{m} = 17.4\ \mathrm{m}$$

$$Q_{20} = 0.7 \times 0.68\ (132\ \mathrm{m}^2/\mathrm{day})\ (17.4\ \mathrm{m}) = 1100\ \mathrm{m}^3/\mathrm{day}, \text{or } \mathbf{12.7\ L/s}$$

These estimates are somewhat larger than the estimates of 10.5 L/s and 8.6 L/s that were developed from the straight-line projection on the semilog plot.

10.3. Critique of the "straight-line" projection and Q_{20} methods

When applied on a semilog plot, the "straight-line" projection approach is similar to the Q_{20} method. Both approaches are based on the Cooper-Jacob approximation of the Theis (1935) solution. The Theis model is based on a highly idealized representation of the aquifer. Key assumptions of the conceptual model include:

- The aquifer is homogeneous;
- The aquifer is of infinite areal extent;
- The aquifer is confined between completely impermeable strata; and
- The water level remains above the top of the aquifer at all times.

These assumptions imply that the only source of water for the pumped well is confined storage. The drawdown cone must therefore expand indefinitely in space and time. A conceptual model of the aquifer that assumes that confined storage is the only source of water may be reasonable for a relatively brief test in which the effects of pumping have not propagated far beyond the pumping well. However, this conceptual model is not realistic when considering long-term conditions. In the long-term, the supplies for a production well do not come from confined storage. Long-term sources of supply include leakage from overlying aquifers across confining units, capture of water from surface water sources, and capture of recharge at the water table (Theis, 1940). None of these sources are considered in the simplified calculations. These long-term projections require the extrapolation of the observations made during pumping into periods during which the assumptions of the underlying conceptual model will almost certainly be violated.

Also implicit in these methods is the assumption that the additional well losses are negligible. The assumption of a perfectly efficient well is not realistic. Additional well losses will arise for several reasons. First, installation of the well will generally result in some alteration of the properties of the formation surrounding the well. Additional losses will occur if the well screen does not penetrate the full thickness of the aquifer. Head losses will also arise as water flows through the well screen; these losses will increase through time unless the well screen is maintained in pristine condition over its life. Finally, there are usually turbulent losses within the well itself.

It is impossible to generalize whether the straight-line projection and the Q_{20} method will always overestimate or underestimate the safe yield of a well. The direction of the deviations between the predictions and the long-term responses will depend on the characteristics of each particular site.

10.4. The Modified Moell method

Maathuis and van der Kamp (2006) have proposed an alternative to the Q_{20} method, the Modified Moell method. According to the Modified Moell method, the safe yield for 20 years of pumping is given by:

$$Q_{20} = 0.7 \times \frac{Q\, H_A}{s_{100\text{ min}} + (s_{20\text{ yrs}} - s_{100\text{ min}})_{\text{theo}}} \tag{37}$$

Here:

- Q_{20} denotes the safe yield for 20 years of pumping;
- Q denotes the actual discharge rate during the pumping test;
- H_A denotes the available drawdown;
- $s_{100\text{ min}}$ denotes the drawdown observed after 100 minutes of pumping;
- $s_{100\text{ min-theo}}$ denotes the calculated theoretical drawdown after 100 minutes of pumping; and
- $s_{20\text{ yrs-theo}}$ denotes the calculated theoretical drawdown after 20 years of pumping.

The Modified Moell method is founded firmly in both observations made during the pumping test and on a more general strategy for extrapolation beyond the duration of the test. Equation (37) is straightforward to interpret. The Modified Moell method can be expressed in general form as:

$$Q_{20\text{ years}} = FS \times SC \times H_{\text{A}} \tag{38}$$

The factor of safety, *FS*, corresponds to the leading coefficient of 0.7. This is the same value as was adopted for the Q_{20} calculation. The term *SC* corresponds to the long-term specific capacity of the well:

$$SC = \frac{Q}{s_{100\text{ min}} + (s_{20\ yrs} - s_{100\text{ min}})_{\text{theo}}} \tag{39}$$

As noted previously, the additional sources of drawdown in the pumping well are established quickly and remain constant through time (see for example, Walton, 1970; Herbert and Barker, 1995). Therefore, an appropriate proxy for the additional wells losses is the observed drawdown after 100 minutes of pumping, $s_{100\text{ min}}$. The quantity $(s_{20\text{ years}} - s_{100\text{ min}})_{\text{theo}}$ represents the drawdown that would occur in the formation beyond 100 minutes of pumping. In contrast to the Q_{20} method, no specific conceptual model is assumed. The choice of the appropriate conceptual model is left to the analyst.

Case study: Kandieng Reay well BHKR-1

The results of a pumping test conducted on a municipal supply well for the town of Kandieng Reay in southern Cambodia are used to illustrate the interpretation of the Modified Moell method (CCEC, 2005). The geologic log and well construction details are reproduced in Figure 43.

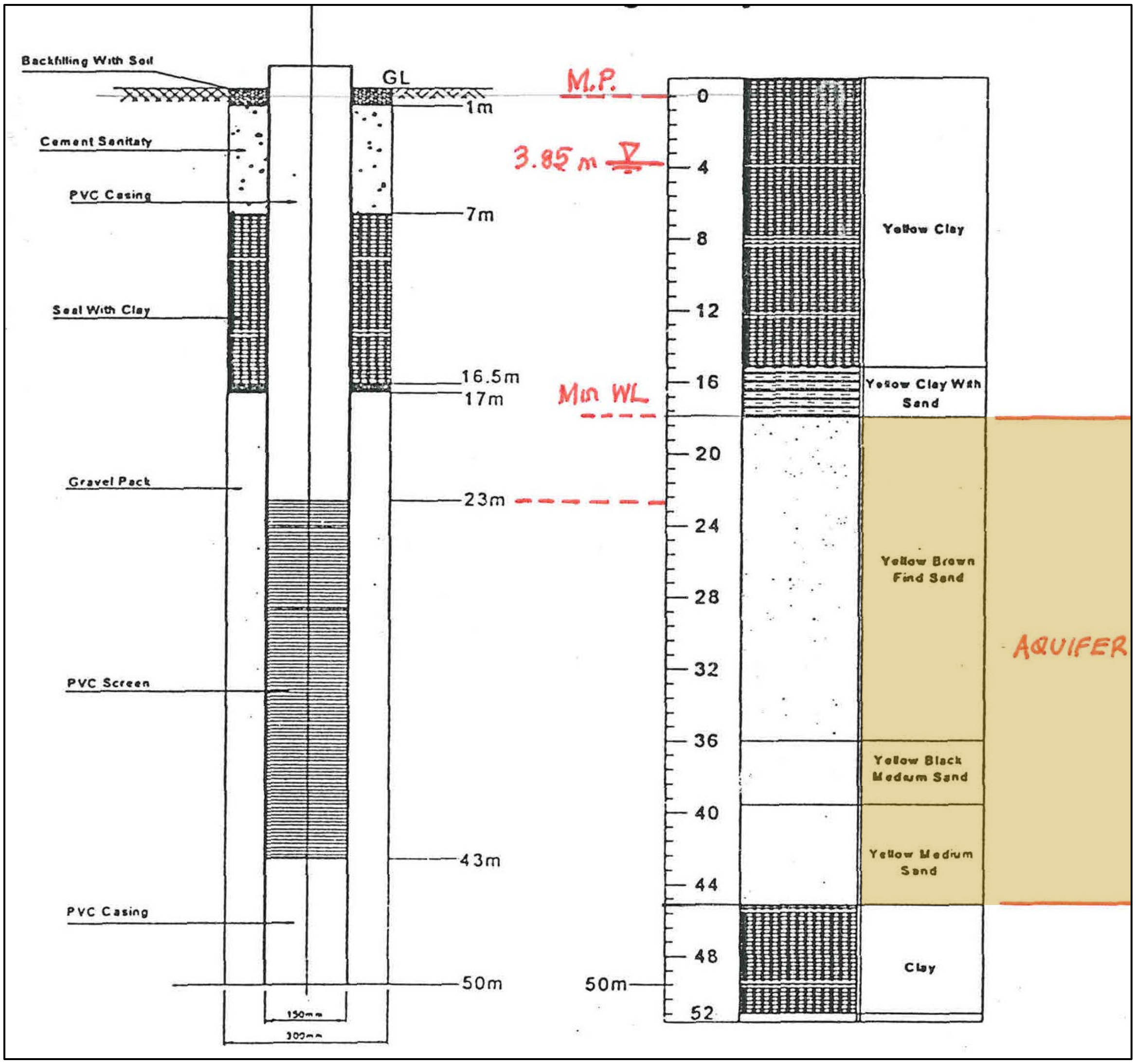

Figure 43. Construction details for BHKR-1 well, Kandieng Reay, Cambodia

The pumping well drawdowns during a 48-hour constant-rate pumping test are plotted in Figure 44. The average pumping rate was 25.2 m^3/hr (604.8 m^3/day). As shown in the figure, most of the drawdown occurs within the first few minutes of pumping. The drawdown after 2 minutes is about 2.35 m, compared with a drawdown at the end of the test of 2.75 m.

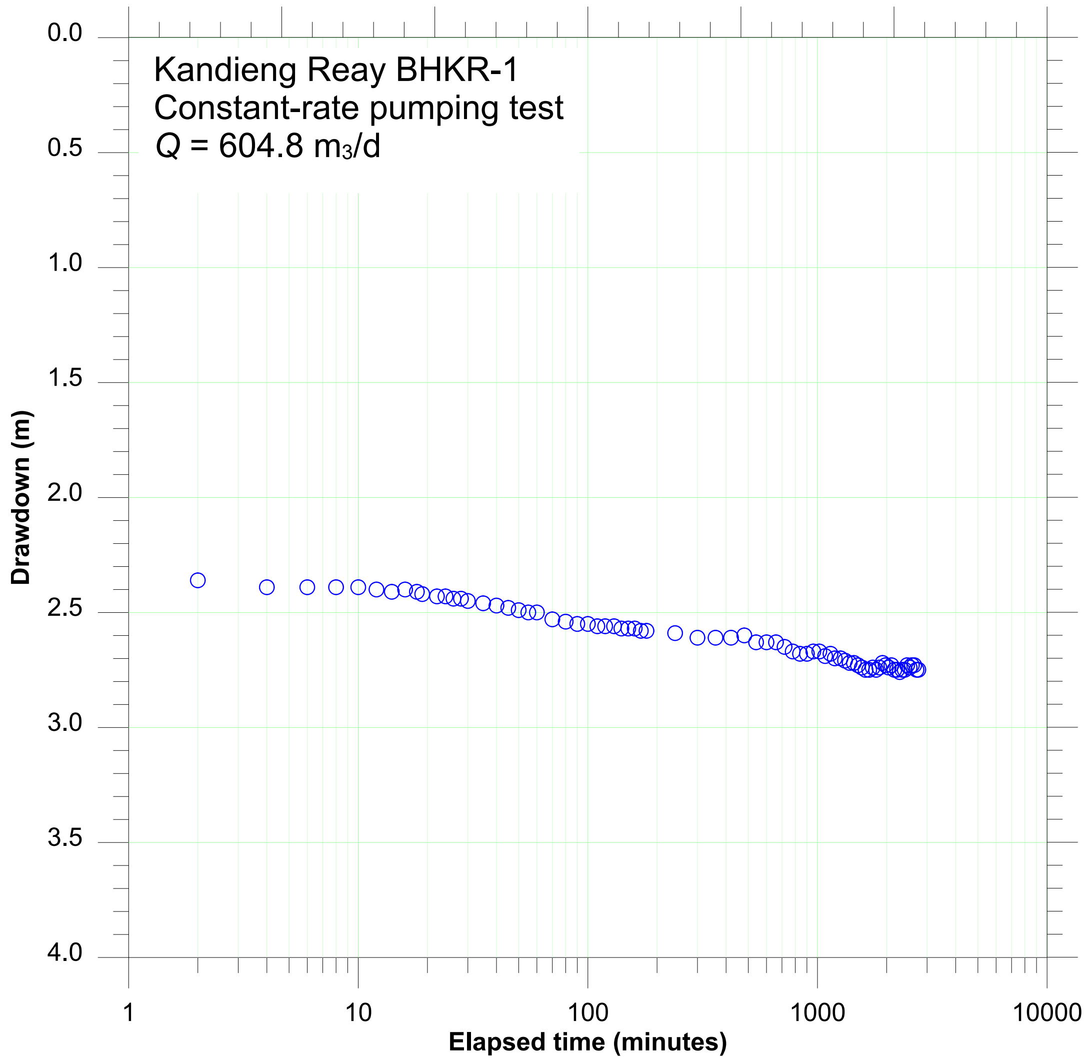

Figure 44. Pumping well drawdowns observed during the 48-hour pumping test

The data from the constant-rate test demonstrate that the head losses in the formation represent a relatively small fraction of the observed drawdown. To estimate the drawdown after 20 years, a simple conceptual model is adopted that is consistent with the limited available data:

$$s_w(t) = \frac{Q}{4\pi T} W\left(\frac{r_w^2 S}{4Tt}\right) + \frac{Q}{4\pi T} 2S_w + CQ^2 \tag{40}$$

The first quantity represents head losses in the formation, with the aquifer modeled as an ideal confined aquifer with the Theis (1935) solution. The second term represents the additional nonlinear well losses. The third term represents the additional losses across a skin zone.

Some of the parameters in Equation (34) can be estimated from the constant-rate drawdowns, but others cannot. A transmissivity of 770 m^2/day is estimated from a Cooper-Jacob analysis. For a single pumping rate it is not possible to distinguish between the additional skin losses and nonlinear well losses. When we are faced with such a situation we look for other sources of data that may help to constrain the parameter estimates. For the BHKR-1 well, we can take advantage of the availability of data from a step test conducted prior to the constant-rate test. When both data sets are available, we seek a single set of parameter values that yields an acceptable match to both data sets with the same aquifer-test model.

The step test data are shown in Figure 45. The results of the analysis of the step test data and the constant-rate data are shown in Figure 46, Figure 47 and Figure 47. The analyses proceeded with an iterative approach until a common set of parameter values was obtained from both tests.

The well was drilled with a mud rotary rig, and it is reasonable to assume that the invasion of drilling mud into the formation resulted in a localized reduction of the hydraulic conductivity of the aquifer. The skin loss is characterized by the dimensionless skin loss coefficient, S_w (Ramey, 1982). A value of S_w of 9.18 is estimated from the analyses of both tests. The skin losses during the constant-rate test are therefore estimated as:

$$\frac{Q}{4\pi T} 2\, S_w = \frac{\left(604.8\ \frac{\text{m}^3}{\text{d}}\right)}{4\pi\left(770\,\frac{\text{m}^2}{\text{d}}\right)} 2\ (9.18) = 1.15\ \text{m}$$

As shown in Figure 45, the drawdowns were nearly stable by the end of each step. Therefore, a Hantush-Bierschenk analysis is appropriate. Referring to Figure 46, the value of the nonlinear well coefficient, C, estimated from the step test is 9.95×10^{-4} m/(m^3/hr)^2 (3.58 m/(m^3/min)^2. The nonlinear losses during the constant-rate test are therefore estimated as:

$$CQ^2 = 9.95 \times 10^{-4}\ \frac{\text{m}}{(\text{m}^3/\text{hr})^2}\left(25.2\ \frac{\text{m}^3}{\text{hr}}\right)^2 = 0.63\ \text{m}$$

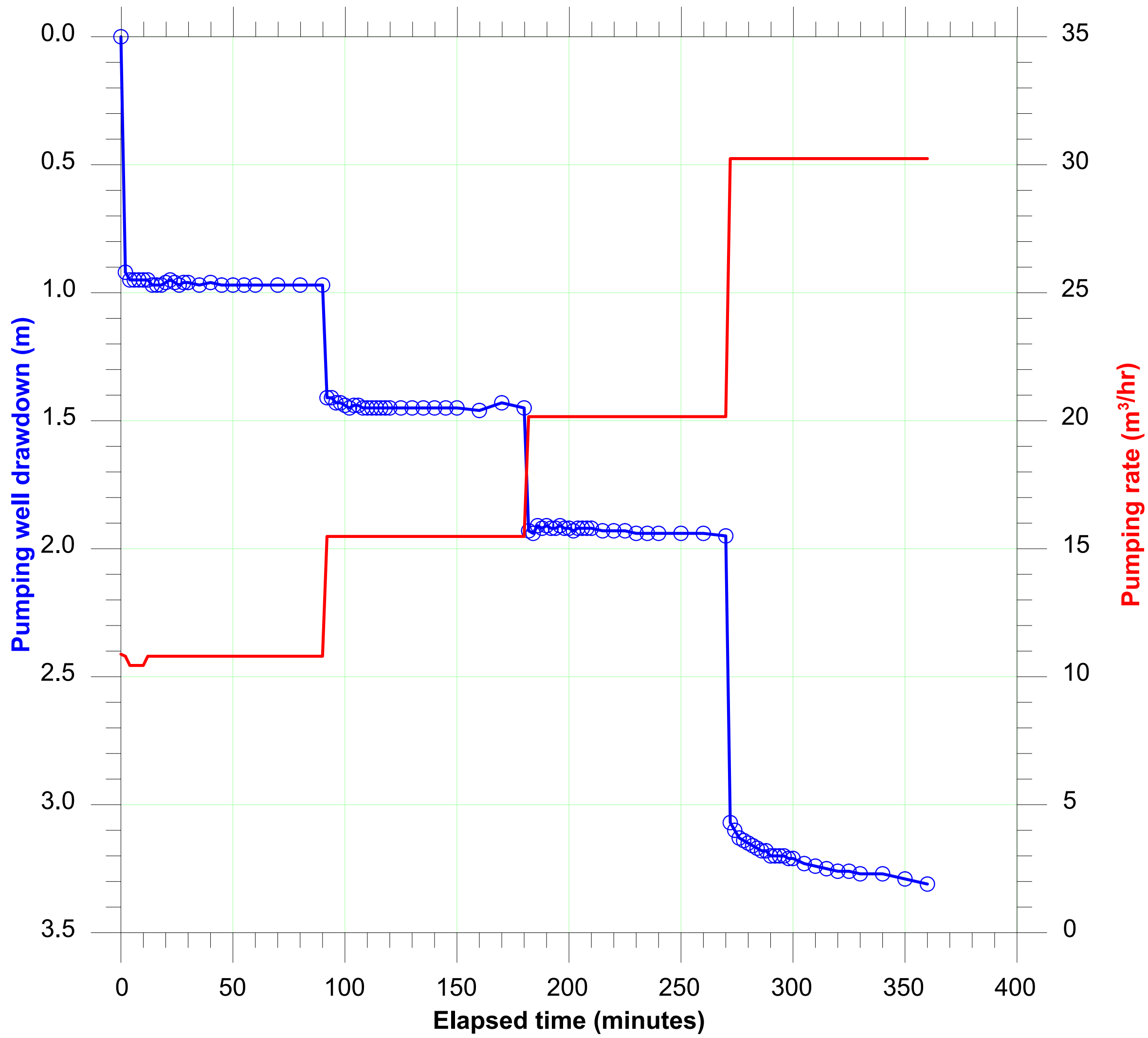

Figure 45. BHKR-1 step test data

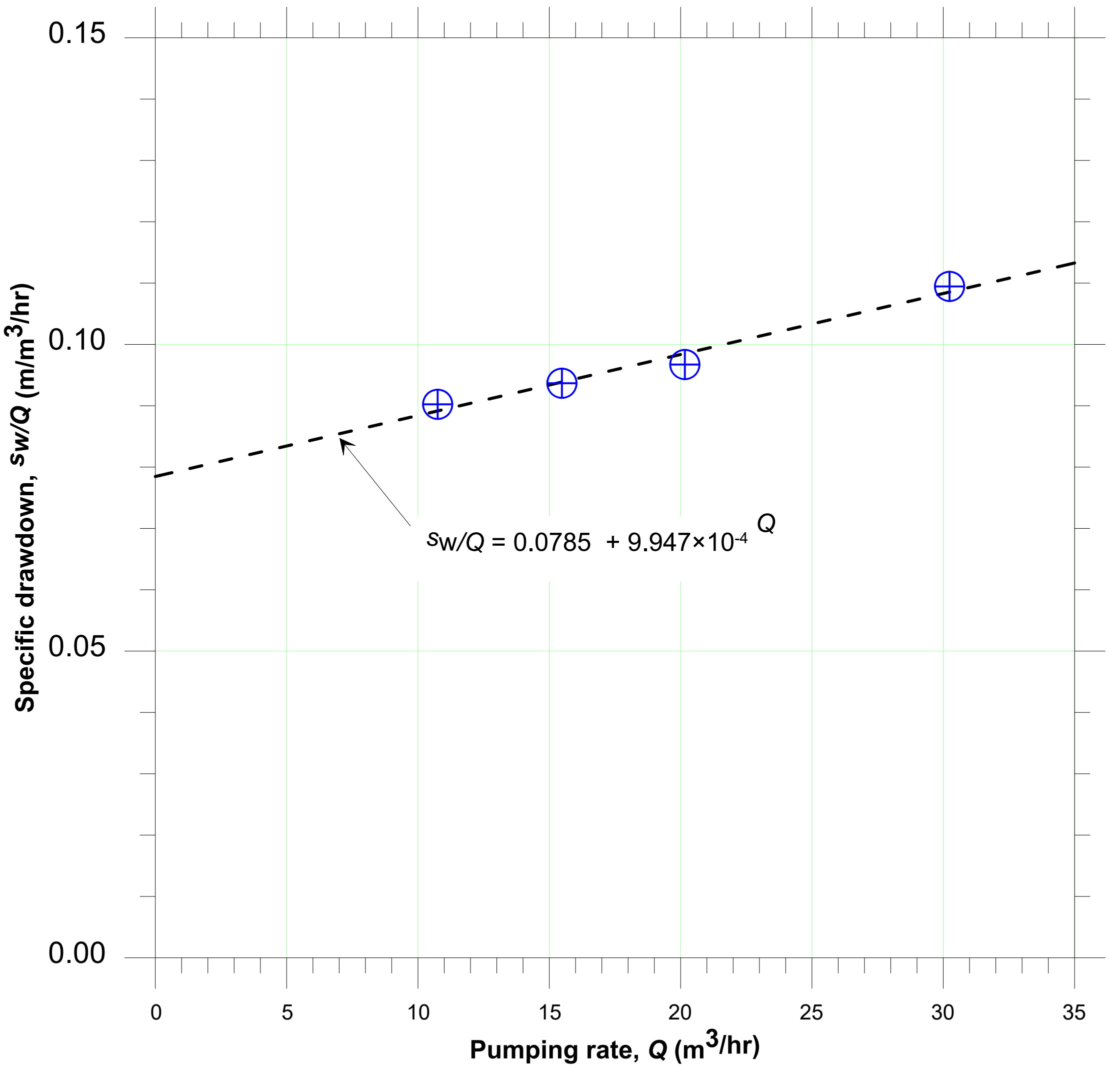

Figure 46. Hantush-Bierschenk analysis for the BHKR-1 step test

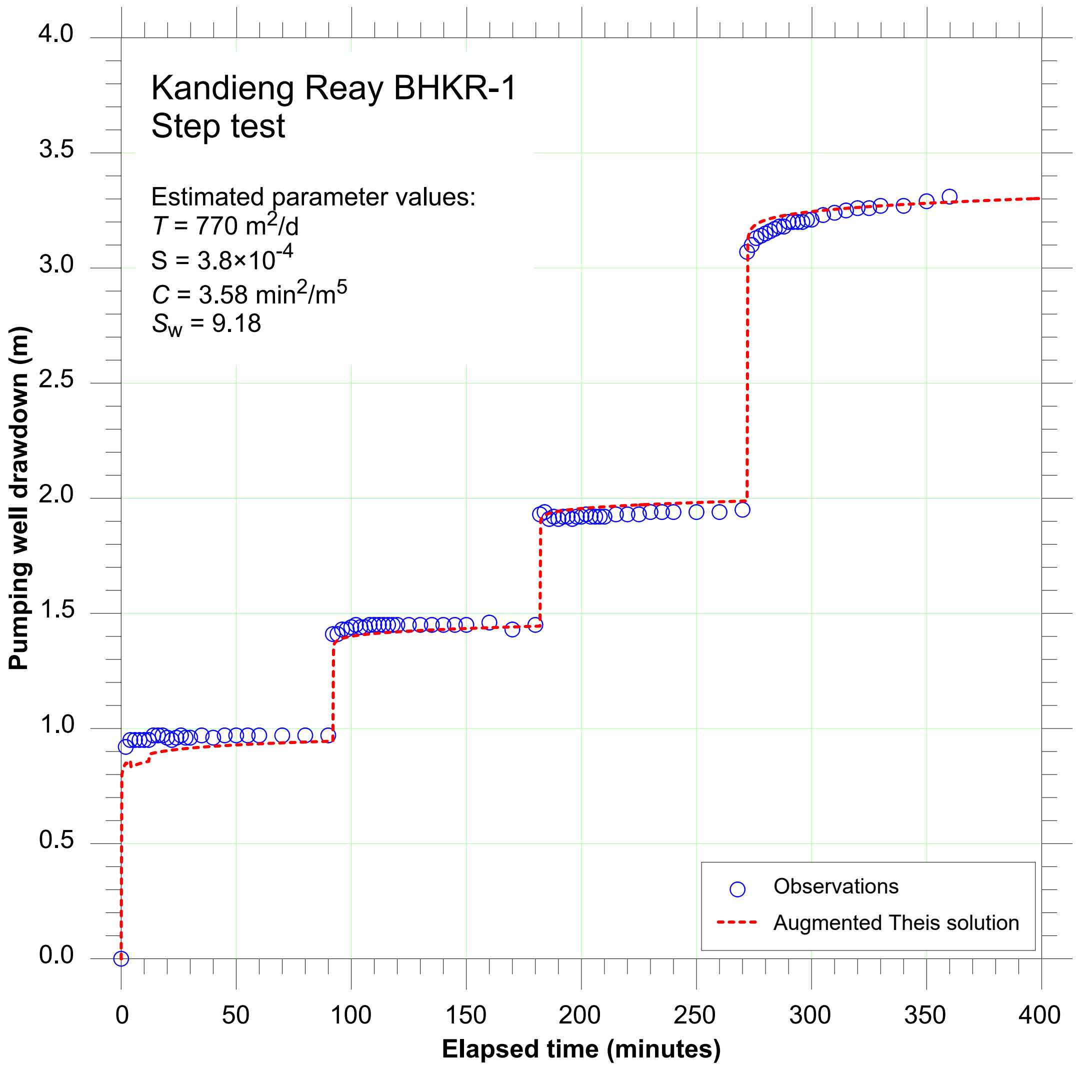

Figure 47. Match to the observed drawdowns during the step test

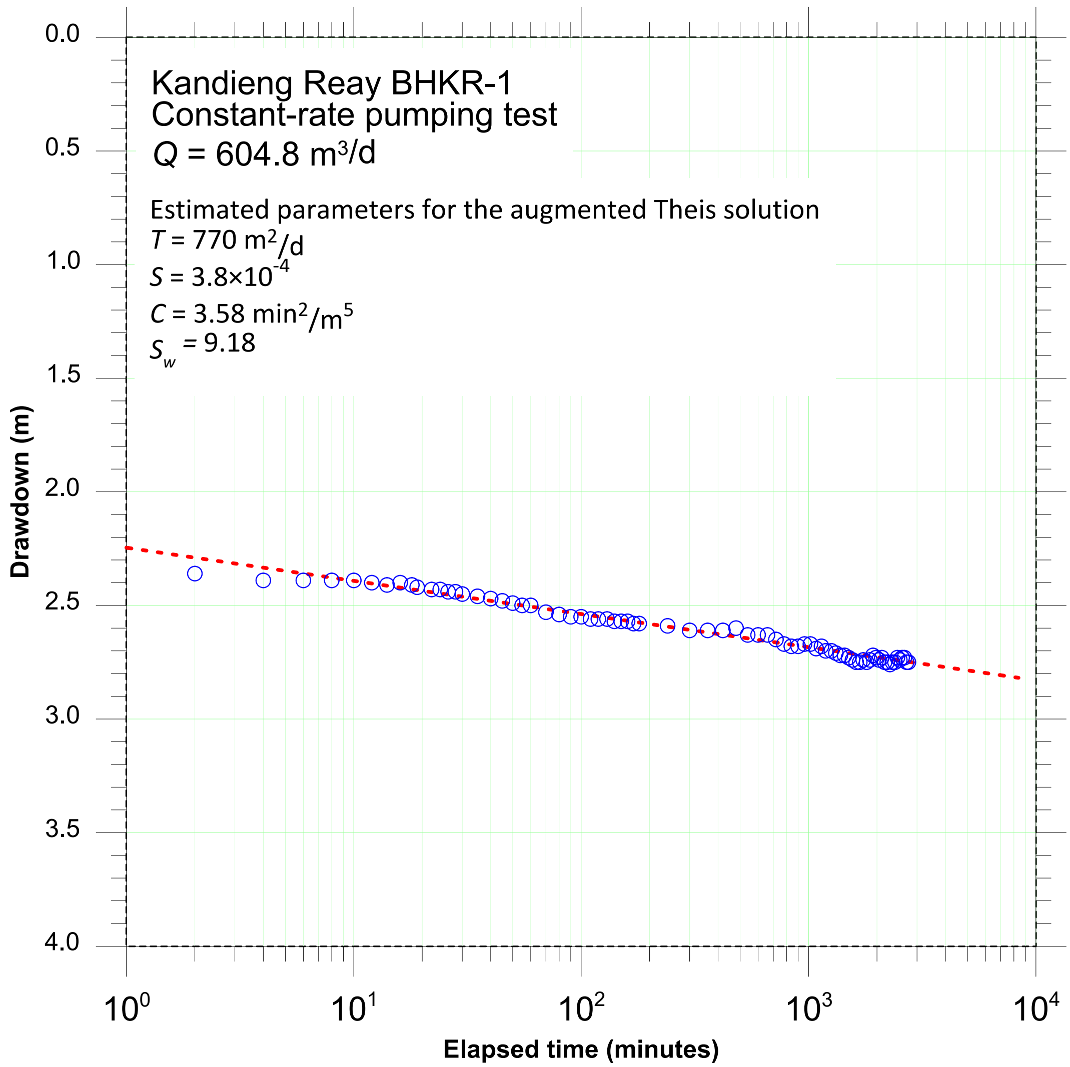

Figure 48. Match to observed drawdowns during the constant-rate pumping test

The projection of the match to the constant-rate drawdowns to 20 years of pumping is shown in Figure 49. Results at selected times are tabulated below.

Time	Nonlinear losses (m)	Skin losses (m)	Aquifer losses (m)	Total drawdown (m)
100 min	0.63	1.15	0.85	2.63
20 years	0.63	1.15	1.57	3.35

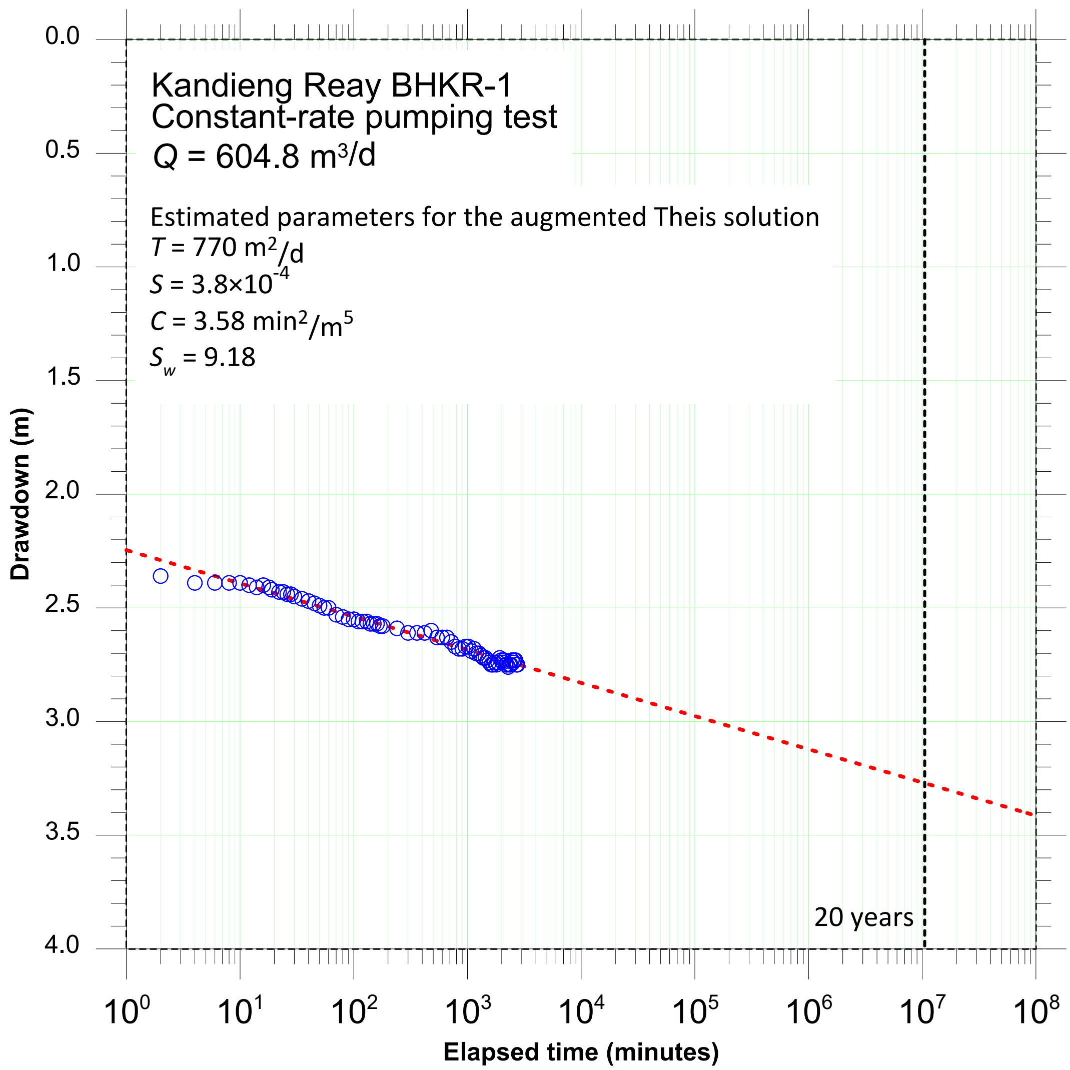

Figure 49. Extrapolation of the drawdowns to 20 years of pumping

The pre-pumping level in the well was 3.85 m below the measuring point.

The uppermost slot of the well screen is 23.5 m below the measuring point. If the pumping is not allowed to draw the water level in the well to a depth within 1.5 m of the well screen, the maximum allowable drawdown is (23.5 m -1.5 m) - 3.85 m = 18.15 m.

The top of the confined aquifer is 17.9 m below the measuring point. If the pumping is not allowed to draw the water level below the top of the aquifer, the maximum allowable drawdown is 17.9 m - 3.85 m = 14.05 m.

- The maximum allowable drawdown is taken as the more stringent of these two criteria: **14.05 m**.
- The observed drawdown after 100 minutes, $s_{100\ min}$, was **2.55 m**.
- The theoretical drawdown after 100 minutes of pumping is **2.63 m**
- The theoretical drawdown after 20 years of pumping is 3.27 m.

Substituting into Equation (11):

$$Q_{20} = 0.7 \times \frac{\left(604.8\ \frac{\mathrm{m}^3}{\mathrm{d}}\right)(14.05\ \mathrm{m})}{(2.55\ \mathrm{m}) + \left((3.27\ \mathrm{m}) - (2.63\ \mathrm{m})\right)}$$

$$= \mathbf{1,800\ m^3/d}$$

<u>A final note of caution</u>

It is important to note that the estimated long-term yield of the well is about three times larger than the rate at which the well was pumped during the constant-rate test. Since this is a theoretical result, and an extrapolation at that, it is *always* advisable to confirm that the well can actually be pumped at this rate.

11. Case study: Estevan, Saskatchewan

Approaches for estimating the long-term capacity of a well are illustrated with the detailed analyses of a pumping test conducted in a buried-valley aquifer near the town of Estevan, southern Saskatchewan. Buried-valley aquifers are a major element of the hydrogeology of the Western Glaciated Plains (Lennox and others, 1988; Cummings and others, 2011). The Estevan test has been selected because it is well-documented and because the aquifer in which it was conducted has been the focus of ongoing studies that extend over a fifty-year period (Walton, 1970, Maathuis and van der Kamp, 2003; van der Kamp and Maathuis, 2002, 2012). The results of the analyses and discussion reveal that the estimation of the sustainable yield of a well is a subtle task, and that a wide range of results may be obtained.

The documentation of the case study is divided into six main sections.

1. The hydrogeologic setting
2. Analysis of the step test
3. Initial analysis of the constant-rate pumping test
4. Buried valley aquifer analysis
5. Estimation of the long-term capacity of the Estevan production well
6. Assessment of the estimates of the long-term capacity of the Estevan well

11.1. The hydrogeologic setting

In March 1965, the Saskatchewan Research Council conducted a constant-rate pumping test about 13 miles northwest of Estevan, Saskatchewan. The test was conducted in a long, sinuous paleochannel infilled with permeable sand and gravel. The channel is part of a complex network of buried valley aquifers across the Canadian Prairies of Western Canada. A recent interpretation of this network is reproduced in Figure 50.

Descriptions of the hydrogeology of the Estevan area and the responses to pumping are presented in van der Kamp and Maathuis (2002), Maathuis and van der Kamp (2003) and van der Kamp and Maathuis (2012). The current interpretation of the buried channel aquifer network in the Estevan area is shown in Figure 51. Similar large–scale networks have been mapped throughout Alberta (Farvolden, 1963; Evans and Campbell, 1995; Andriashek and Atkins, 2007; Rayner and Rosenthal, 2008; and Atkinson and Slattery, 2011). A geologic log for the production well is reproduced in Figure 52. The buried valley aquifer is overlain by about 150 m of low-permeability glacial till.

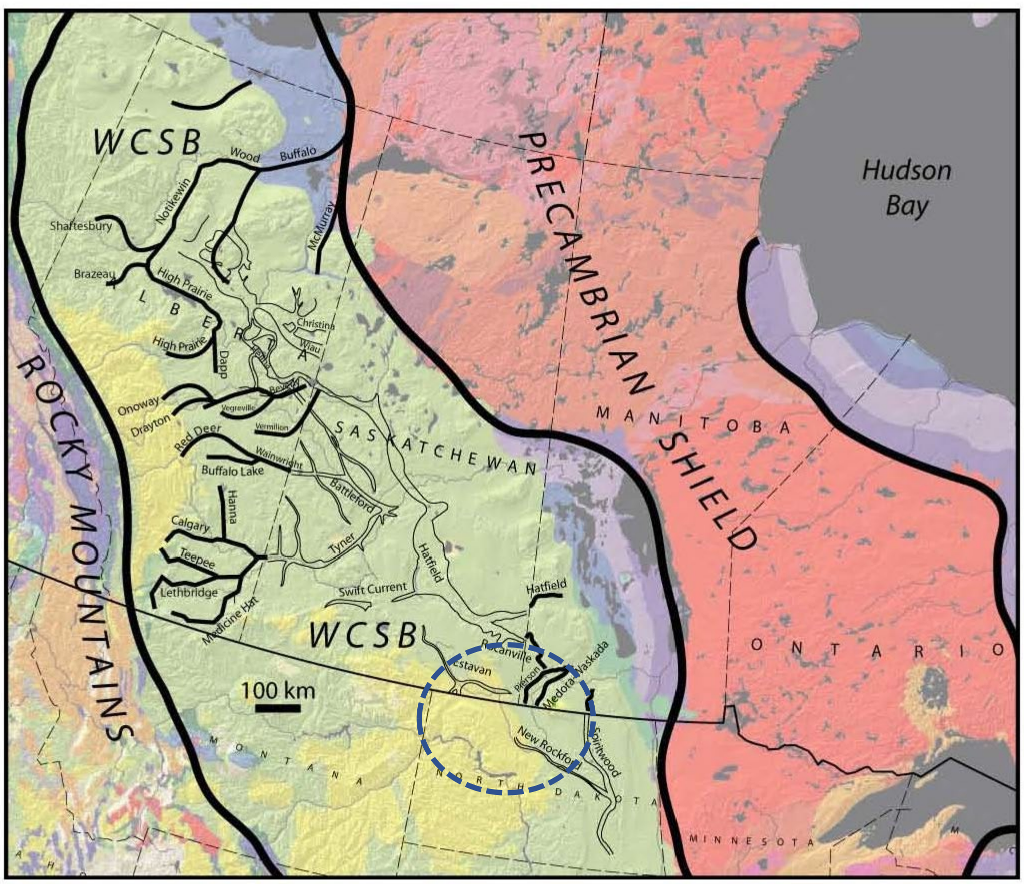

Figure 50. Buried channel aquifers in Western Canada
Reproduced from Cummings and others (2011)

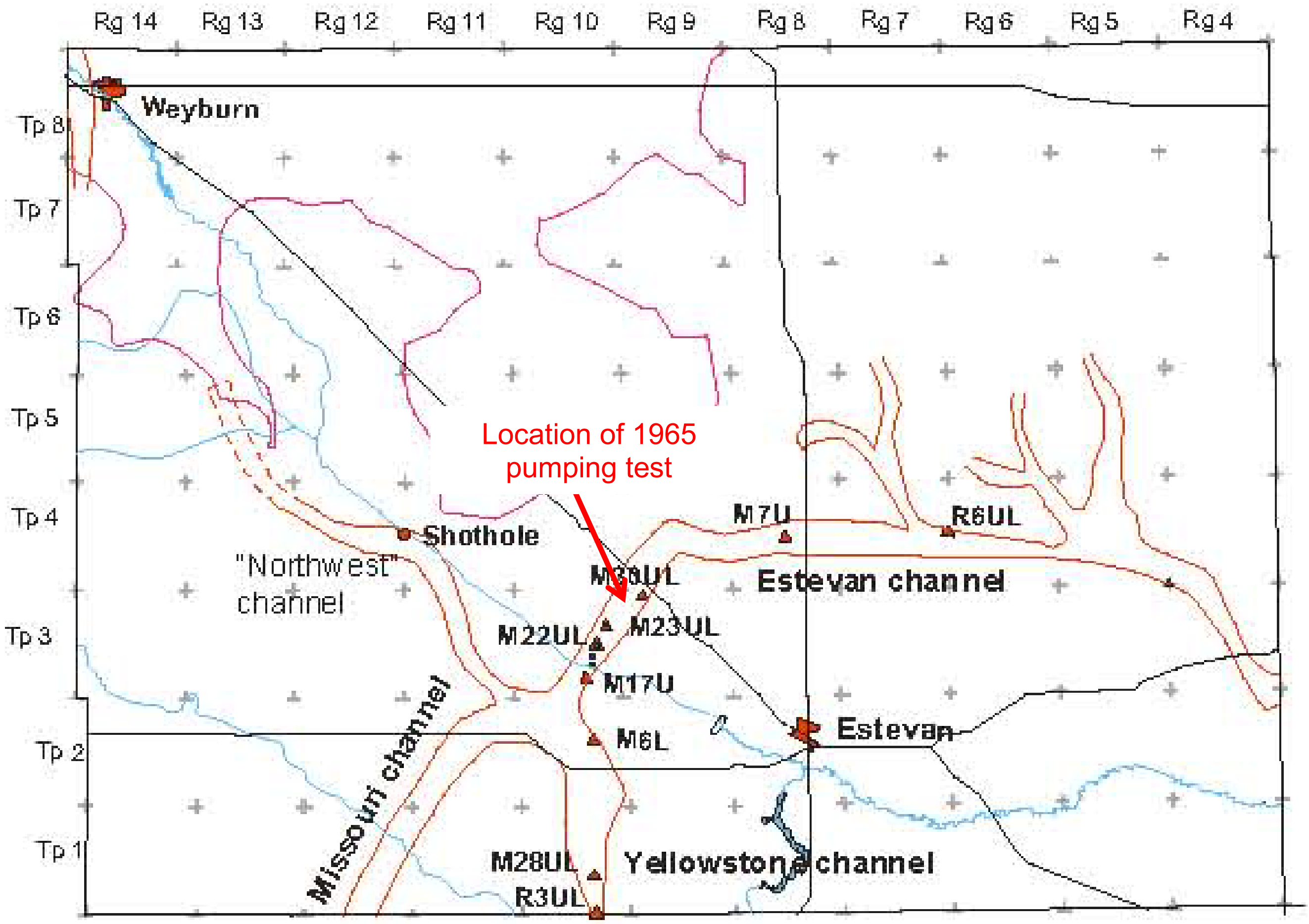

Figure 51. Buried valley aquifer system in southern Saskatchewan
Reproduced from Maathuis and van der Kamp (2003)

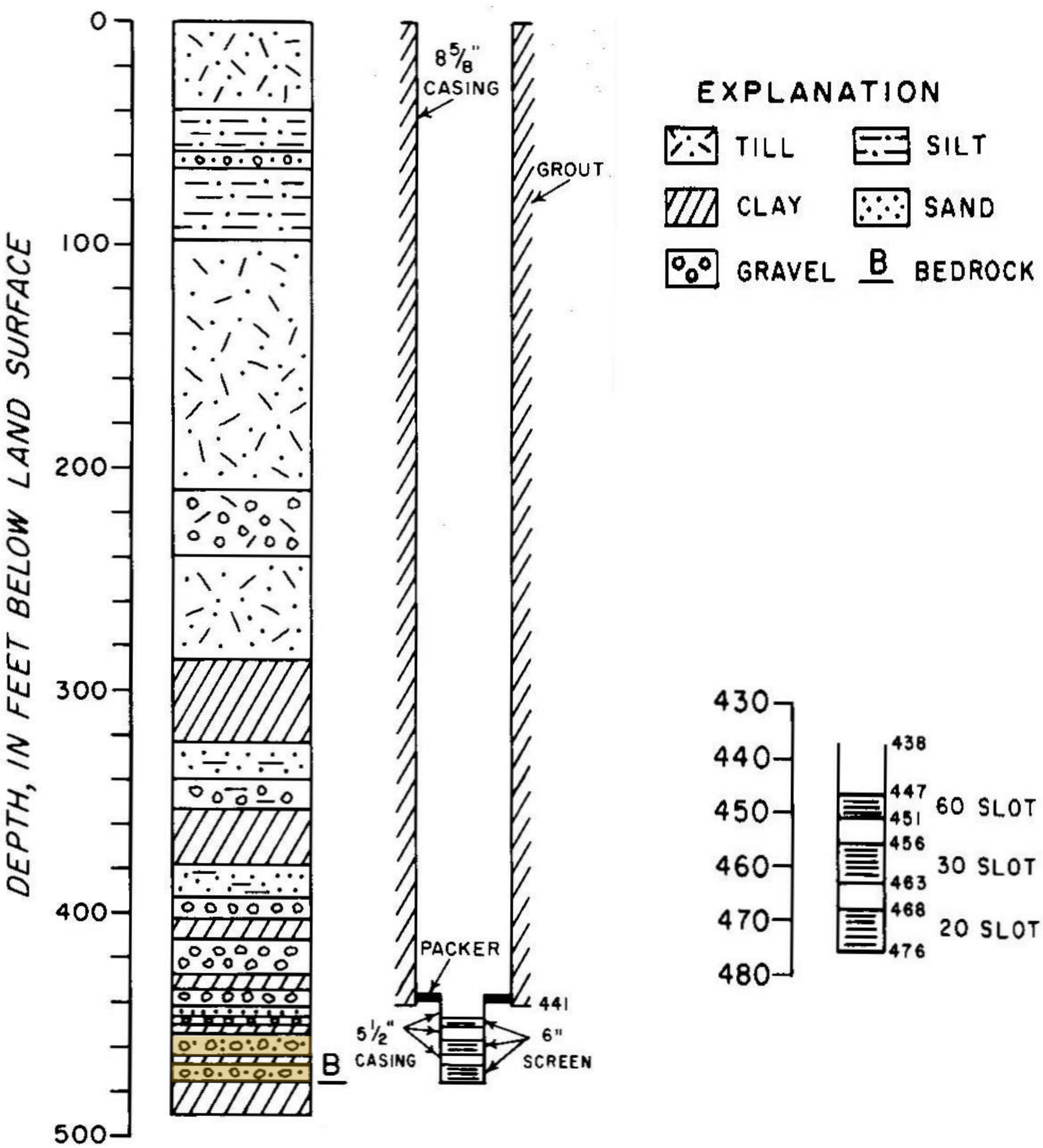

Figure 2. Geologic log and production well construction details
Adapted from Walton (1970)

11.2. Analysis of the step test data

A step test was conducted in anticipation of the constant-rate pumping test. The results of the step test are provided in the original report of the test (Walton, 1965). The drawdowns observed during the three steps of the Estevan step test are plotted in Figure 53.

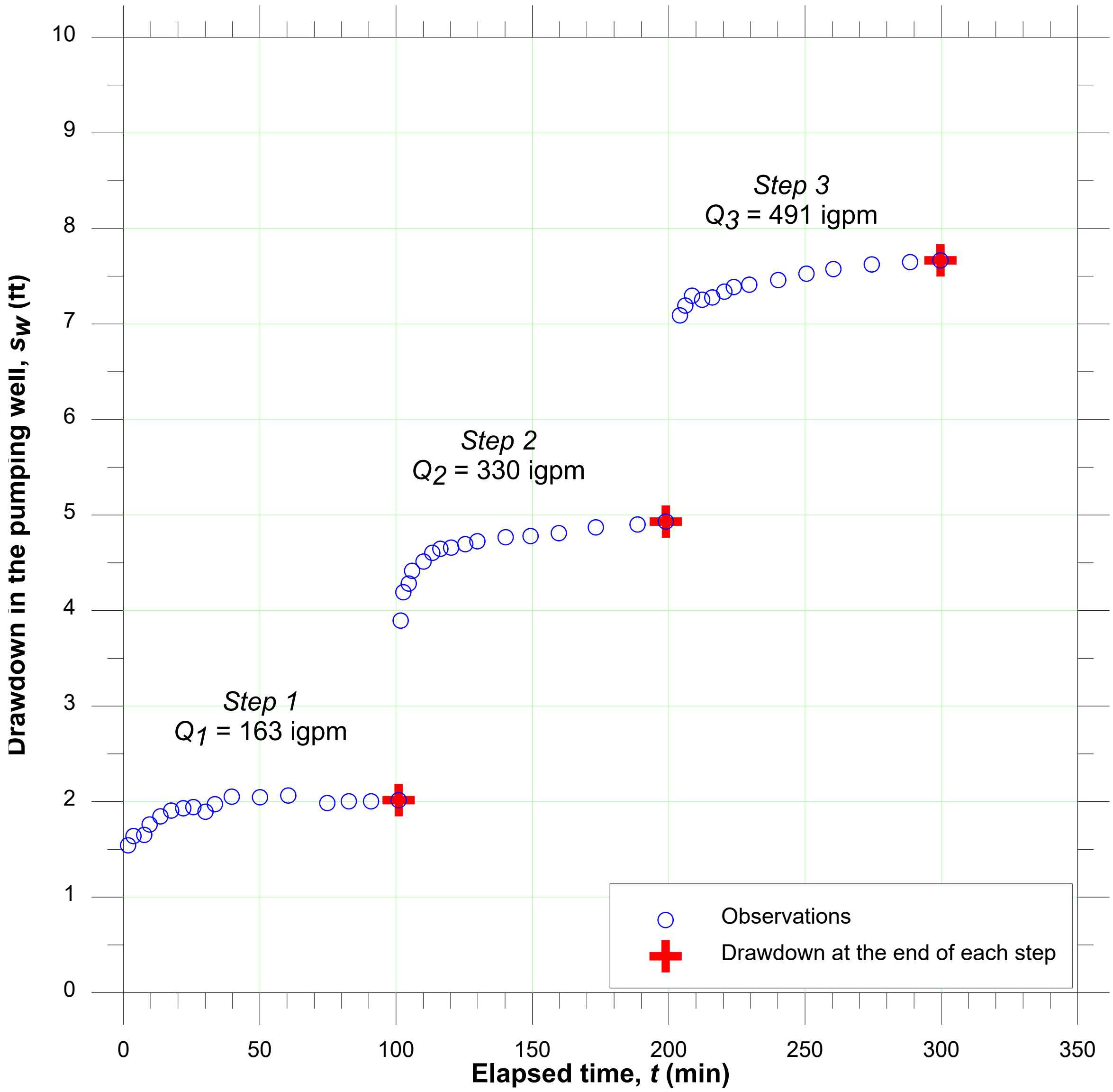

Figure 53. Estevan step test data

Values of the specific drawdown, s_w/Q, at the end of each step are plotted in Figure 54. As shown in the figure, the specific drawdown does not vary significantly with the pumping rate. This suggests that nonlinear well losses are not significant during this test. The drawdowns at the ends of the last two steps are approximated closely with the relation:

$$\frac{s_w}{Q} = 0.015 \text{ ft/igpm}$$

Here s_w are specified in feet and the pumping rate Q is specified in Imperial gallons per minute (igpm).

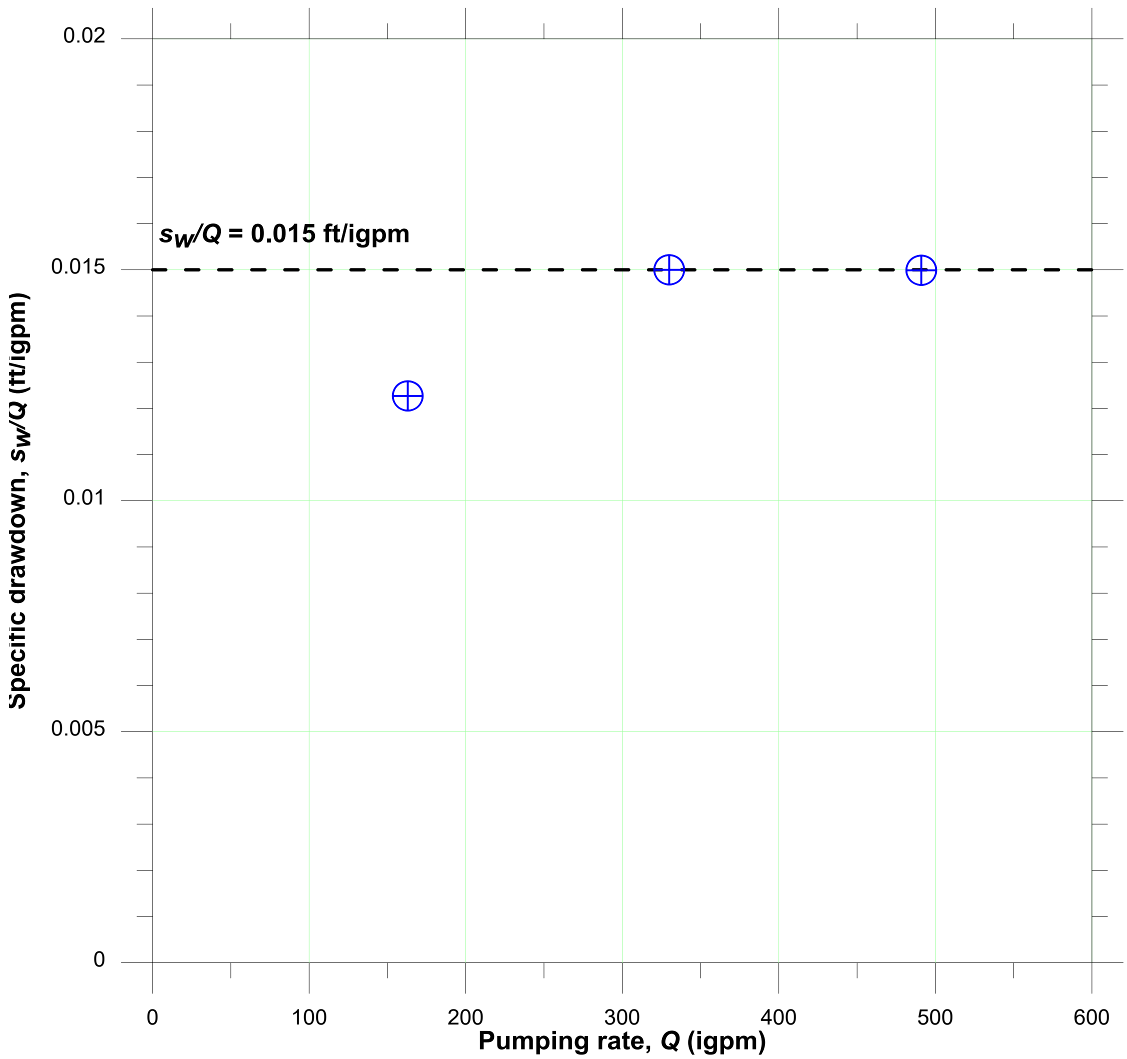

Figure 54. Estevan step test, Hantush-Bierschenk plot

As a check on the Hantush-Bierschenk analysis, in Figure 54 the pumping rate is plotted against the drawdown at the end of each. The data approximate closely a linear relation, confirming that the nonlinear well losses are likely not significant.

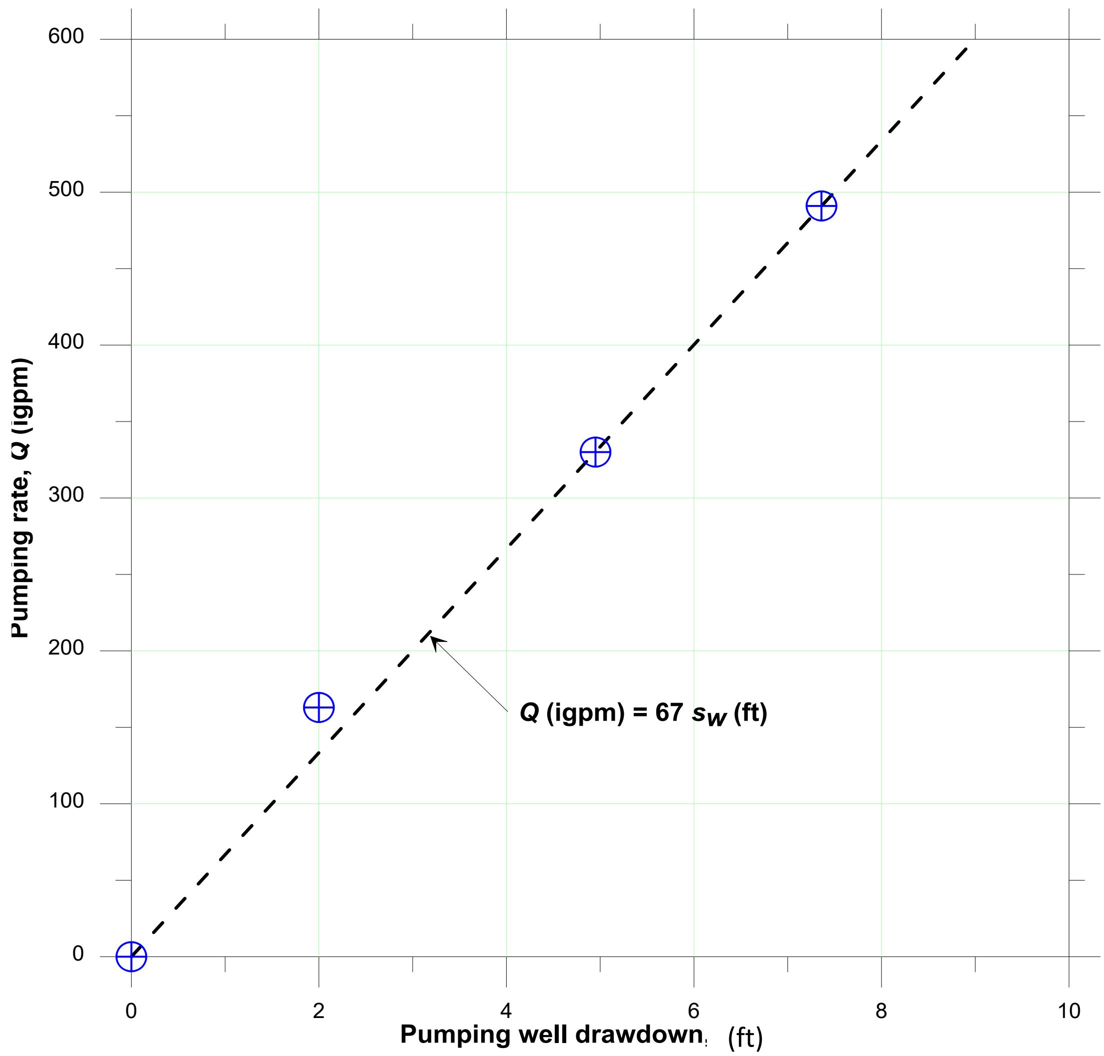

Figure 55. Specific capacity plot of Estevan step test

Using this value and the approach of Driscoll (1986), a first-cut transmissivity estimate is calculated as:

$$T \approx 1.3 \times SC$$
$$= 1.3 \left| 67\ \frac{\text{igpm}}{\text{ft}} \right| \left| \frac{\text{ft}^3}{6.229\ \text{igal}} \right| \left| \frac{1440\ \text{min}}{\text{day}} \right| = 20{,}100\ \text{ft}^3/\text{d}$$

A more refined, but still preliminary, estimate of the transmissivity can be developed by matching the complete record of drawdowns during the step test with the Theis solution generalized for time-varying pumping:

$$s_w(t) = \sum_{i=1}^{NS} \frac{\Delta Q_i}{4\pi T} W\left(\frac{r_w^2 S}{4T(t - ts_i)}\right)$$

Here NS denotes the number of steps in the test, ΔQ_i denotes the pumping increment, t is the total elapsed time since the start of pumping, ts_i is the starting time for each step, r_w is the radius of the well, and T and S denote the transmissivity and storage coefficient, respectively.

The results of the analysis are shown in Figure 56. A relatively close match to the observations is achieved with the following parameters:

$T = 23{,}300$ ft^2/day; and
$S = 2\times10^{-4}$.

This estimate of the transmissivity is close to the first-cut estimate derived from the estimated specific capacity.

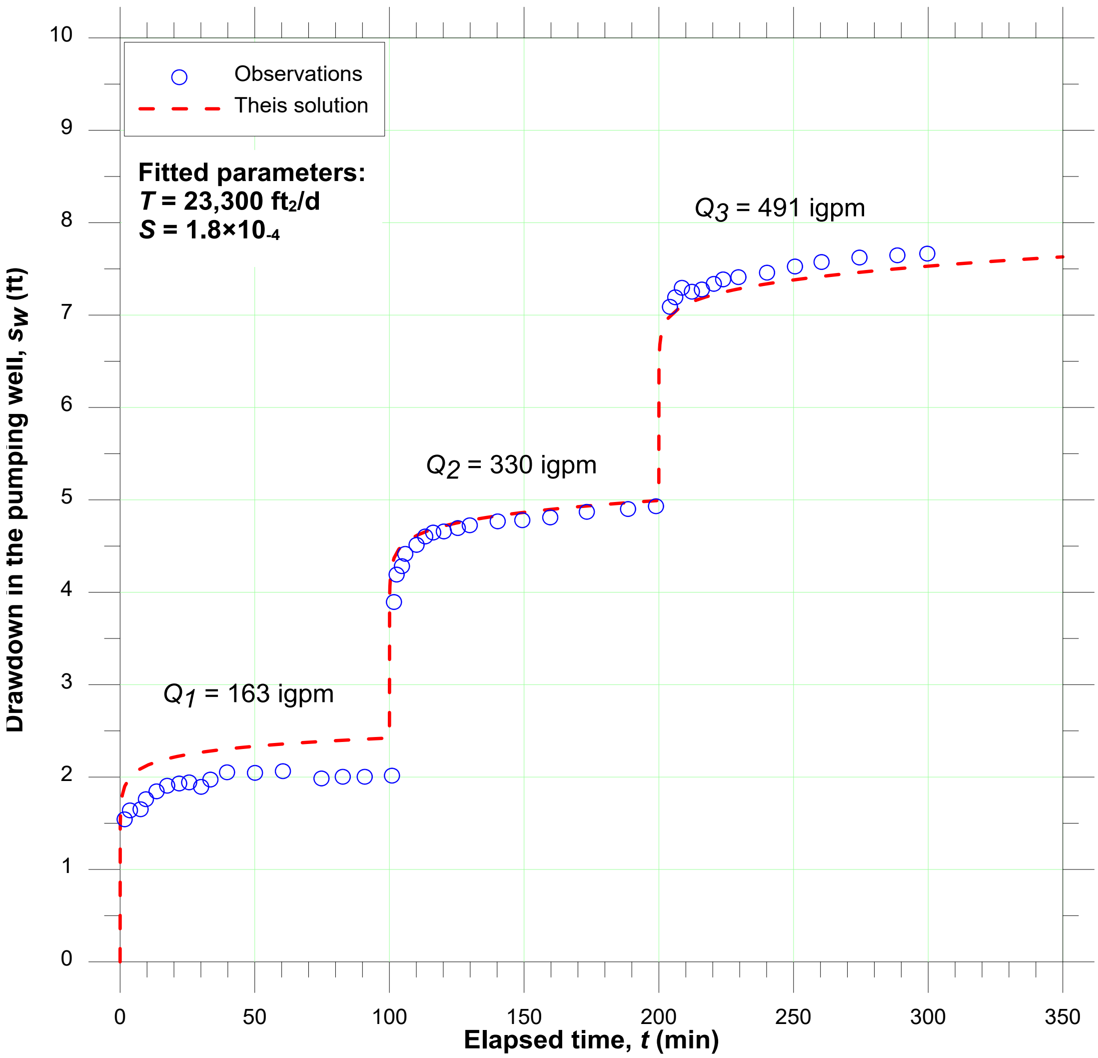

Figure 56. Match of the Estevan step test data

11.3. Initial analysis of the constant-rate pumping test

The pumping test started on March 4, 1965 at 3:00 PM and continued until March 12 at 2:00 PM. The duration of pumping was 11,520 minutes. The pumping rate was held nearly constant by means of a gate valve installed in the discharge pipe. A circular orifice and a manometer tube installed in the end of the discharge pipe were used to measure the pumping rate. The pumping rate varied between 457 igpm (imperial gallons per minute) and 464 igpm, with an average pumping rate of 460 igpm (106,340 ft^3/d).

Water levels were measured at the production well and at three observation wells. The locations of the wells are shown in Figure 57.

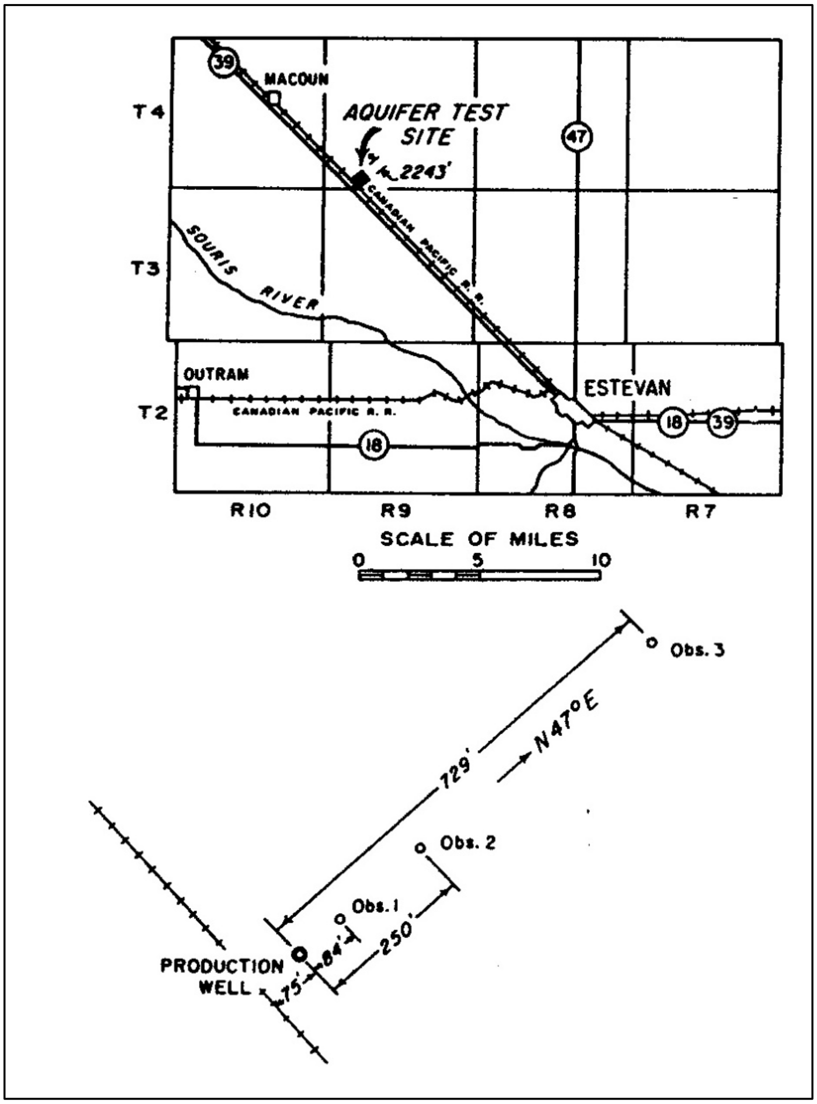

Figure 57. Locations of wells monitored during the Estevan pumping test
Adapted from Walton (1970)

The drawdown data from the pumping well and the observation wells are plotted in three formats to assist in inferring the appropriate conceptual model for the aquifer:

- Log-log time-drawdown plot;
- Semi-log Drawdown Derivative plot; and
- Semi-log composite plot.

The drawdowns for the pumping well and the three observation wells are plotted against time on log-log axes in Figure 58. As shown in the figure, the final portion of the drawdown record for each well approximates a straight line. This response is characteristic of a linear flow regime that is observed when a strip aquifer is pumped (see for example, Boonstra and Boehmer, 1986; Butler and Liu, 1991). This model is representative of a buried-valley aquifer for which the inflow across the valley walls and the leakage from the overlying confining unit are not significant over the duration of the pumping test.

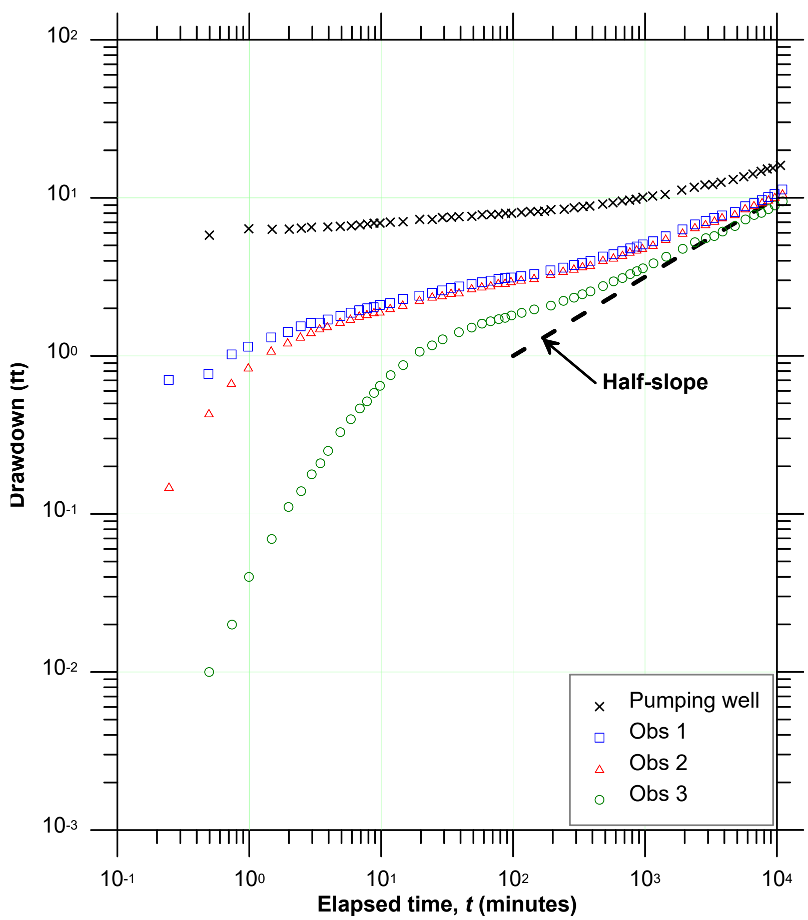

Figure 58. Log-log plot of drawdowns during the Estevan constant-rate pumping test

The Drawdown Derivatives for the pumping well and the three observation wells are plotted against time on semi-log axes in Figure 59. The Drawdown Derivatives are smoothed slightly with respect to the “raw” values calculated with the nearest-neighbor approach. Two distinct regimes are evident in the figure. Between about 10 and 50 minutes, the Drawdown Derivatives approach a plateau. This is designated as the period of Infinite-Acting-Radial-Flow (***IARF***). During this period, the drawdowns approximate the response that would be observed in an ideal confined aquifer of infinite extent. Beyond 50 minutes of pumping, the Drawdown Derivatives accelerate rapidly. This response is characteristic of an aquifer in which boundary effects are increasingly significant, which is again consistent with the conceptual model of a buried-valley aquifer.

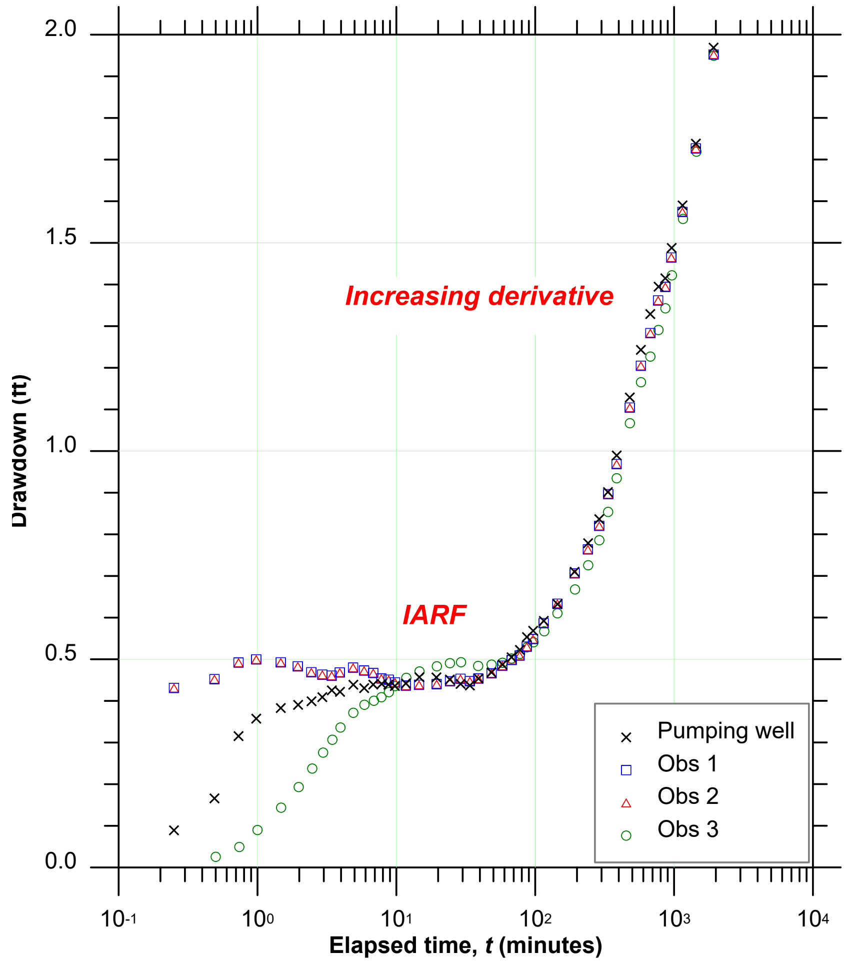

Figure 59. Semi-log plot of drawdown derivative

A third diagnostic plot is presented in Figure 60. The drawdowns for the pumping well and the three observation wells are plotted against t/r^2 on semi-log axes, where r is the distance between the pumping well and each observation well. Cooper and Jacob (1946) refer to this as a composite plot. Two distinct regimes are evident for each well. For relatively small values of t/r^2, the drawdowns approximate a common straight line. The interval of this response corresponds to the ***IARF*** period for each well. For larger values of t/r^2, the drawdowns for each well appear to deviate systematically from the common straight line. The onset of this deviation marks the time at which the influence of pumping propagates to the walls of the buried valley.

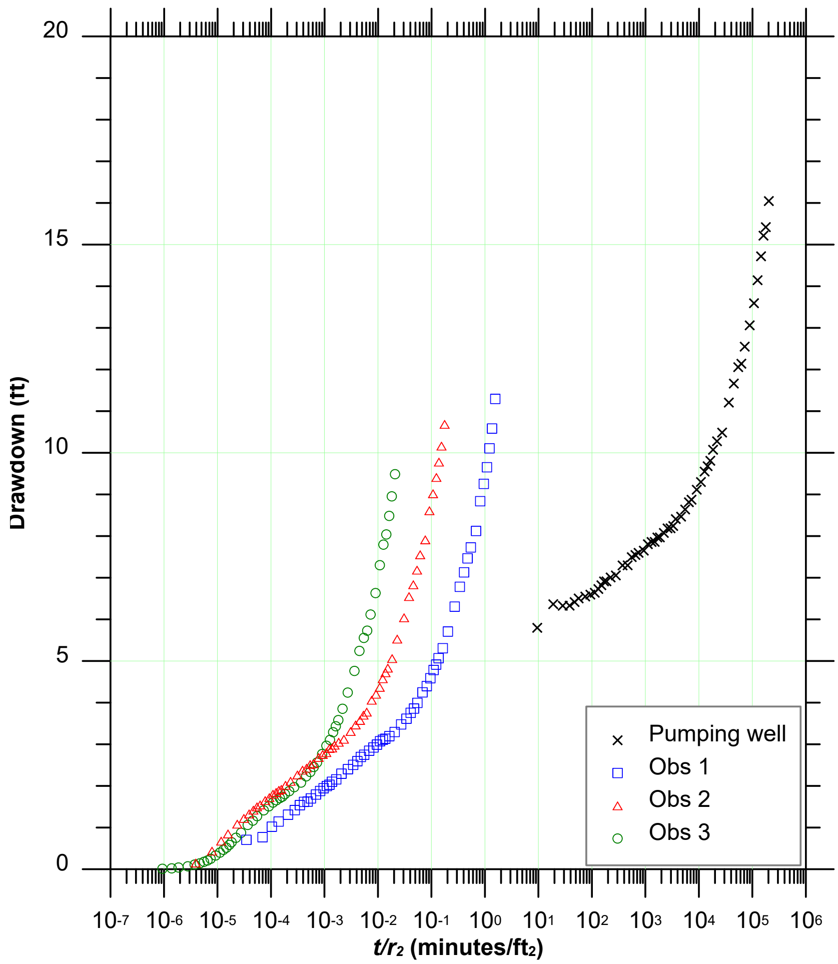

Figure 60. Semi-log composite plot of drawdowns

The results of a Cooper-Jacob straight-line analysis on the composite plot are shown in Figure 61. The drawdowns do not all fall on the same straight line, which suggest that the aquifer is heterogeneous. However, the early-time slopes of the linear portions of the drawdowns are consistent, including the drawdowns for the pumping well. The straight-line portions of the pumping well and observation well records yield a single, internally consistent estimate of the bulk-average transmissivity for all four wells. This consistency is a necessary condition for the reliability of the analysis, as the key assumption of the Cooper-Jacob model is that at the large scale, a bulk-average transmissivity can be inferred]

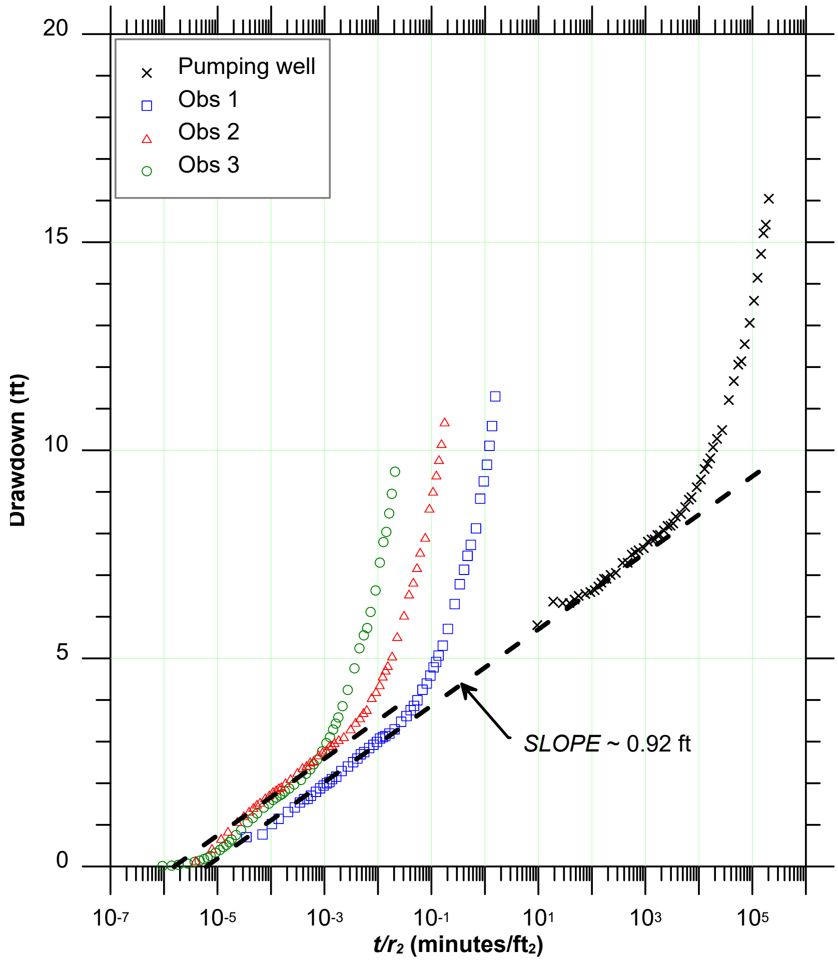

Figure 61. Cooper-Jacob straight-line analysis

The transmissivity is estimated from the Cooper-Jacob analysis according to:

$$T = 2.303\,\frac{Q}{4\pi}\,\frac{1}{\Delta s}$$

Here Q is the pumping rate, and Δs is the *s*lope of the straight-line portion of the drawdown. The common slope of the early-time response is about 0.92 ft per log cycle t/r^2. For a pumping rate of 460 igpm, the transmissivity is estimated as:

$$T = 2.303\,\frac{(460\text{ ipgm})}{4\pi}\,\frac{1}{(0.92\text{ ft})}\left|\frac{\text{ft}^3}{6.229\text{ gal}}\right|\left|\frac{1440\text{ min}}{\text{day}}\right| = 21{,}200\text{ ft}^2/\text{d}$$

The transmissivity estimate from the Cooper-Jacob analysis is consistent with estimate obtained from the analysis of the step test. This consistency does not prove that the analyses are correct, but it is a necessary condition of a reliable interpretation.

Using the straight line fit through the pumping well and Obs 1 drawdowns, a storage coefficient, *S*, of 2×10^{-4} is estimated. The storage coefficient is within the typical range for confined aquifers, 5×10^{-5} to 5×10^{-3} (Boonstra, 1989).

11.4. Buried-valley aquifer analysis

The drawdown data are interpreted with a buried valley aquifer analysis by retaining the conceptual model of an ideal confined aquifer, but with the added assumption that the pumping well and observation wells are located along the axis of a long rectangular aquifer, bounded by parallel impermeable surfaces that penetrate the full thickness of the aquifer. The analysis is conducted with an automated implementation of image theory. The image well model is illustrated in Figure 62. The black circle indicates the real well and the white circles indicate the image wells, all of which pump at the same rate as the real well.

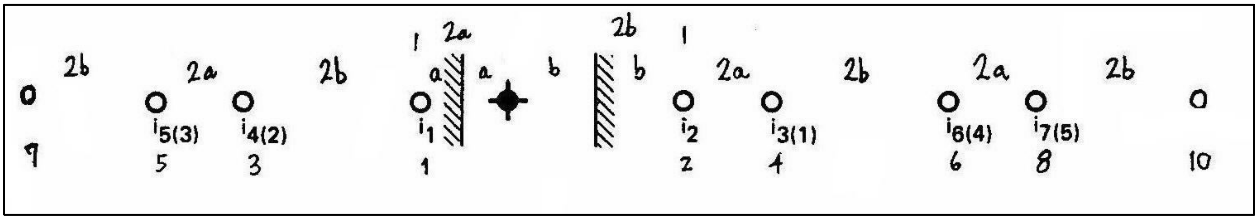

Figure 62. Image well model for a buried-valley aquifer

The solution for pumping between two linear impermeable boundaries is given by (Kruseman and de Ridder, 1990; p. 114):

$$s(r,t) = \frac{Q}{4\pi T}\left[W\left(\frac{r^2 S}{4Tt}\right) + \sum_{i=1}^{\infty} W\left(A_{ri}^2 \frac{r^2 S}{4Tt}\right)\right]$$

The right-hand term in brackets represent the contributions of the image wells. The quantity A_{ri} is defined as:

$$A_{ri} = \frac{r_i}{r}$$

Here r denotes the distance between the pumping well and each observation well, and r_i denotes the distance between the i^{th} image well and the observation well.

In theory, infinitely many image wells are required. In practice, the calculations frequently converge for a relatively small number of image wells. The number of image wells required depends on the location of the observation well and the elapsed time; a convergence analysis is generally required, in which the number of image wells is increased until the addition of another image well has negligible effect on the calculated drawdowns.

The results of a match to the drawdowns are shown in Figure 63. The solid lines in the figure are calculated with a transmissivity of 19,800 ft^2/d, storage coefficient of 2.8×10^{-4}, and a valley width of 8,000 ft (2,430 m). The valley width is estimated through trial-and-error. As shown in the figure, it is possible to obtain a close match to the complete drawdown records from the pumping well *and* all three observation wells, with a consistent set of aquifer properties. The parameters are close to those estimated with the Cooper-Jacob straight-line analysis ($T = 21{,}200$ ft^2/d, $S = 2.8\times10^{-4}$). As a further check on the analysis, in Figure 64 the drawdown derivatives for the analytical model are superimposed on the values calculated from the observations.

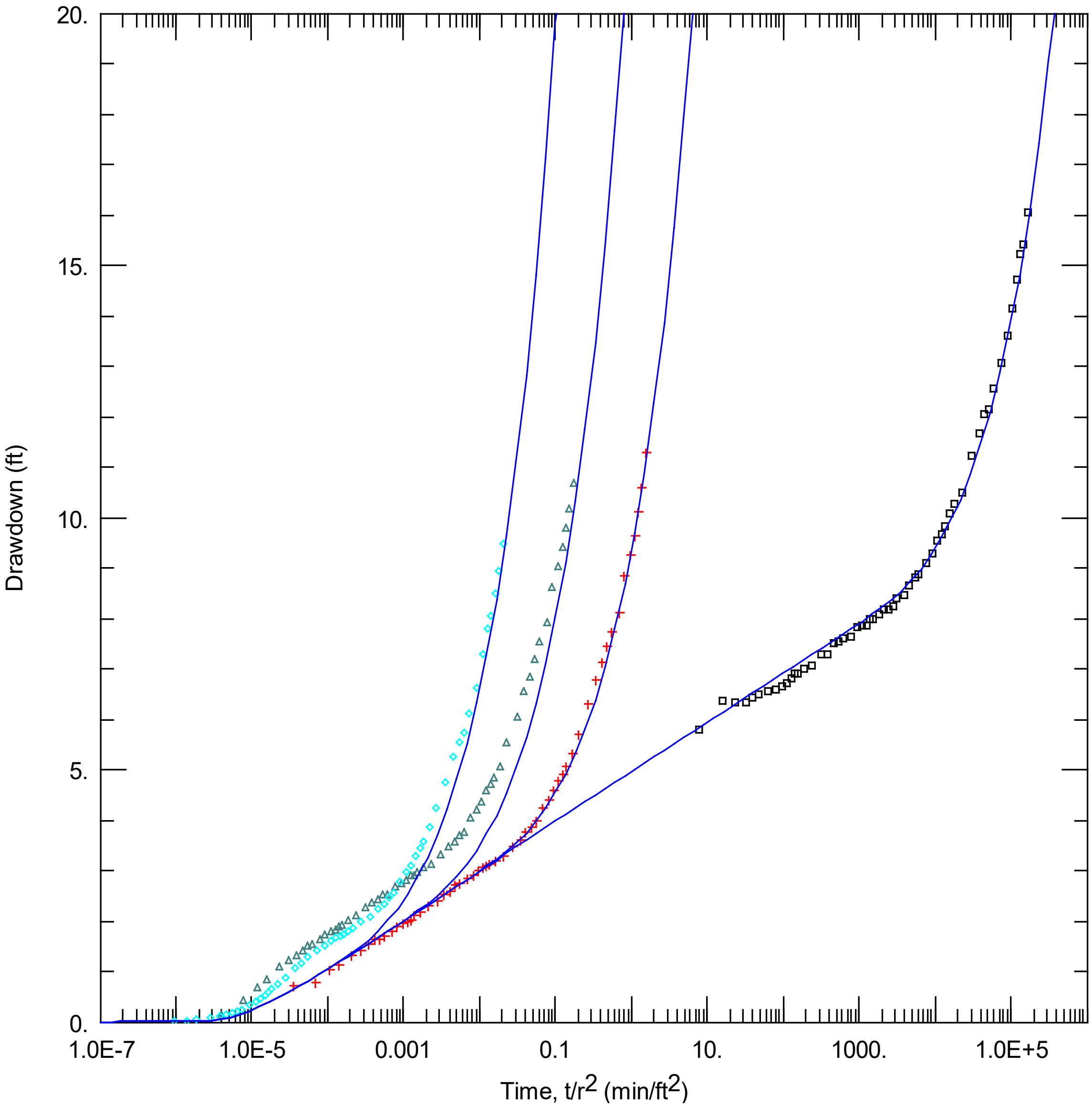

Figure 63. Buried-valley aquifer analysis of Estevan pumping test

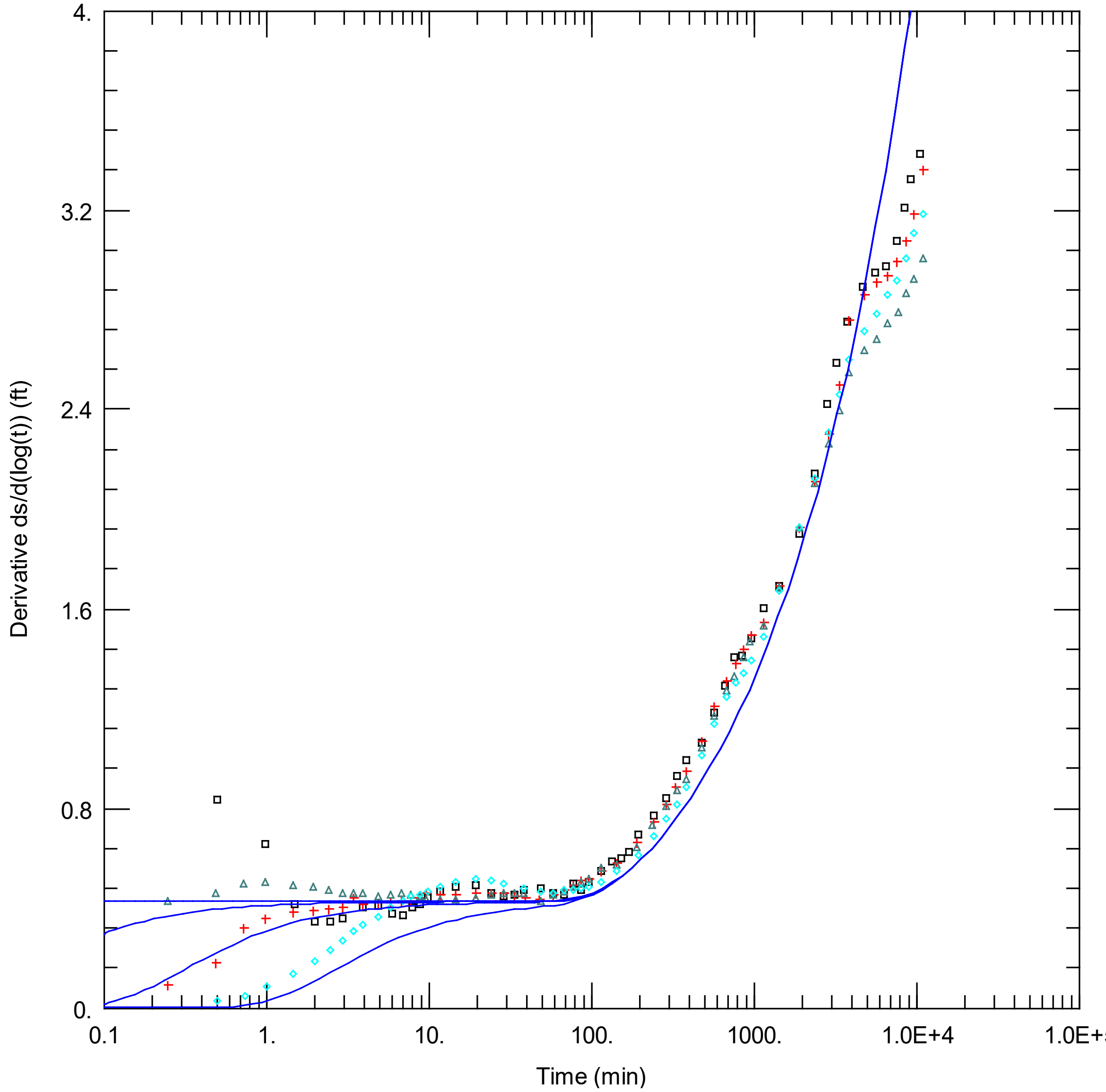

Figure 64. Drawdown Derivatives for buried-valley aquifer analysis

11.5. Estimation of the long-term capacity of the Estevan production well

In this section, the long-term yield of the Estevan well is estimated using three methods:

- Using the specific capacity estimated from the step test;
- The Q_{20} Method; and
- The Modified Moell Method.

1. Estimation of the well capacity from the step-test data

The maximum capacity of the production well is estimated according to:

$$Q_{max} = SC \times s_{w-max}$$

Here *SC* is the specific capacity inferred from the step test and $s_{\text{w-max}}$ is the maximum allowable drawdown for the production well.

- Referring to Figures 54 and 55, the specific capacity inferred from the step test is **67 igpm/ft**.
- According to Maathuis and van der Kamp (2006; p. 35), the allowable drawdown at the location of the Estevan 1965 pumping test is **73 m**.

The capacity of the production well is therefore:

$$Q_{max} = \left(67\ \frac{\text{igpm}}{\text{ft}}\right) \times (73\ \text{m}) \left|\frac{3.281\ \text{ft}}{\text{m}}\right| \left|\frac{\text{m}^3}{219.969\ \text{igallons}}\right| \left|\frac{1440\ \text{min}}{\text{d}}\right| = \mathbf{105{,}000\ m^3/day}$$

2. Estimation of the long-term well capacity with the Q_{20} method

The safe yield is estimated with Q_{20} method according to:

$$Q_{20} = 0.7 \times 0.68\, T\, H_{\text{A}}$$

Here T is the transmissivity, and H_{A} is the allowable drawdown after 20 years of pumping. The leading coefficient of 0.7 is the "safety factor".

- The transmissivity estimated from the buried-valley analysis (Figure 63) is **21,200 ft²/day (1,970 m²/day)**.
- We will again use the Maathuis and van der Kamp (2006; p. 35) allowable drawdown of **73 m**.

Substituting the values for T and H_A into the Q_{20} calculation yields:

$$Q_{20} = 0.7 \times 0.68\ (1{,}970\ \text{m}^2/\text{d})\ (73\ \text{m})$$

$$= \mathbf{68{,}400\ m^3/d}$$

Maathuis and van der Kamp (2006; p. 35) report a higher estimate of 97,700 m^3/d. In their calculation, they used the transmissivity of 2,800 m^2/d reported in Walton (1970) from a Theis type-curve analysis of the first 20 minutes of the drawdowns at Observation Well #3, located 220 m from the production well.

The Q_{20} Method is developed from the extrapolation of the Cooper-Jacob straight-line analysis to 20 years of pumping. It is assumed implicitly that the drawdowns in the pumping well approximate a straight-line when plotted against the logarithm of time. It is clear from the semilog plot of the pumping well drawdowns that the aquifer eventually does not respond as an ideal "Theis" aquifer (Figure 61). In particular, the drawdowns accelerate after about 100 minutes. It is important to recognize immediately that in this setting, extending the straight-line portion of the response is likely to significantly underestimate the drawdowns after 20 years of pumping.

3. Estimation of the long-term well capacity with the Modified Moell method

The long-term capacity of a production well is estimated with the Modified Moell method according to:

$$Q_{20} = 0.7 \times \frac{Q\ H_A}{s_{100\ \mathrm{min}} + \left(s_{20\ \mathrm{yrs}} - s_{100\ \mathrm{min}}\right)_{\mathrm{theo}}}$$

The following definitions are recalled:

Q_{20}	Well yield for 20 years of pumping (m^3/d);
Q	Actual discharge rate during the pumping test (m^3/d);
H_A	Available drawdown (m);
$s_{100\ \mathrm{min}}$	Measured drawdown after 100 minutes of pumping (m);
$s_{100\ \mathrm{min\text{-}theo}}$	Calculated theoretical drawdown after 100 minutes of pumping (m); and
$s_{20\ \mathrm{yrs\text{-}theo}}$	Calculated theoretical drawdown after 20 years of pumping (m).

The Province of Alberta *Guide to Groundwater Authorization* (2011) does not provide specific guidance on the estimation of the theoretical drawdowns for the Modified Moell method. It is indicated that the use of the Modified Moell method must be consistent with the appropriate aquifer model. Rationale for the chosen aquifer model must be provided with supporting data.

The model of a buried-valley aquifer yielded an excellent match to all of the observed drawdowns for the 11,520 minutes of the test (8 days). Therefore, for this case study the conceptual model inferred from the buried-valley analysis is used to predict the drawdowns after 20 years of pumping. It is important to note that regardless of the particular method used to estimate the long-term yield of the well, the estimation generally involves significant extrapolation. This is highlighted in Figure 65, in which the drawdowns observed in the pumping well are plotted with a time axis that extends to 20 years of pumping.

It is also important to note that the model of a buried-valley aquifer that has been adopted is relatively simple. The conceptual model is sufficiently simple that an analytical approach is still tractable, but the model nevertheless captures the essential elements of a buried channel aquifer system. The structure of typical buried-channel aquifer in a Canadian Prairie setting may be more complex. Under those circumstances the appropriate approach for estimating the long-term yield of a production well may involve the development of a numerical model. Indeed, at least two groundwater flow models have been developed to assess the long-term sustainability of groundwater resources in the Estevan area (Walton, 1970; p. 543; van der Kamp, 1985).

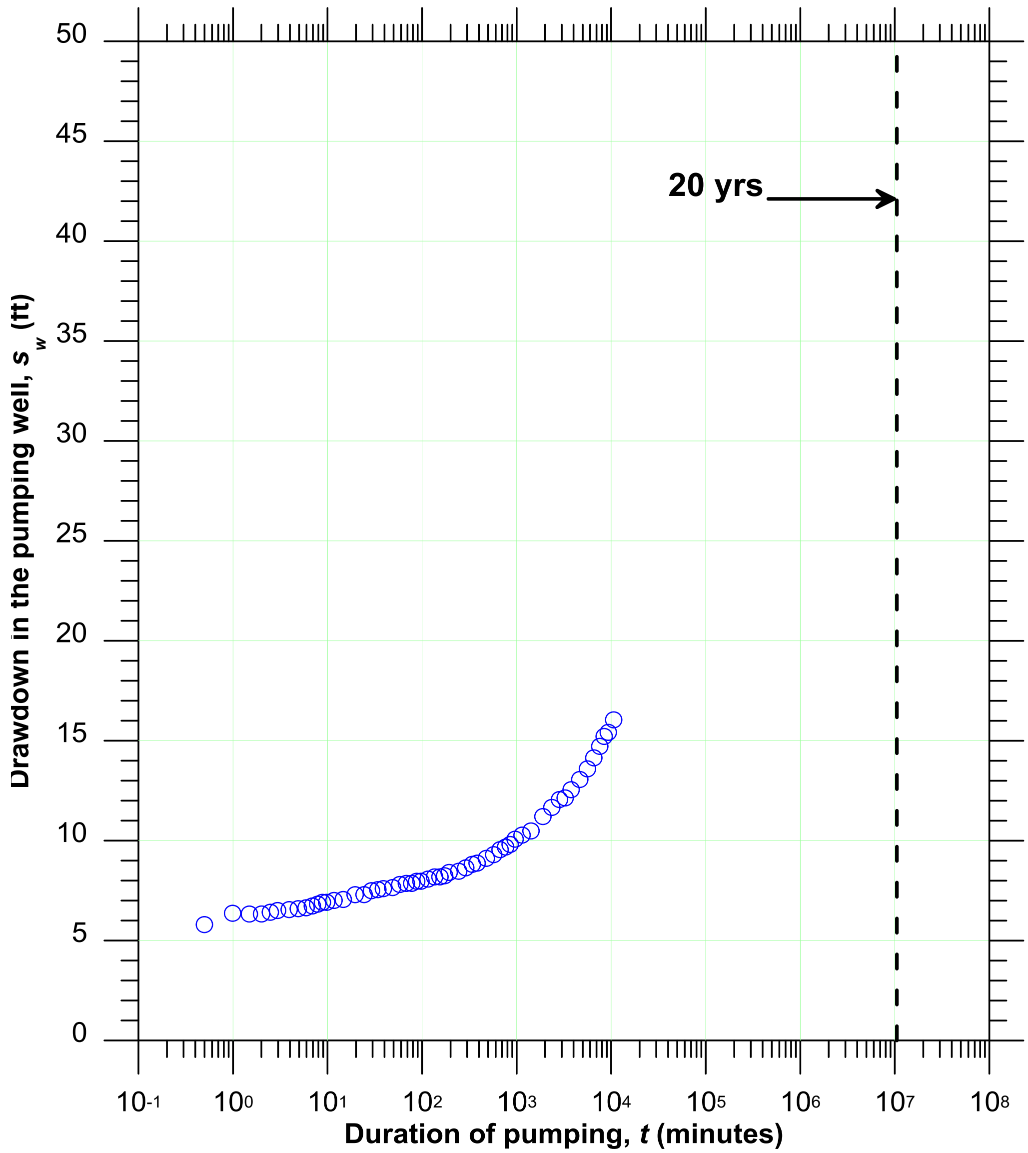

Figure 65. Pumping well drawdowns with time extended to 20 years

The drawdowns in the pumping well predicted after 20 years with the buried-valley model are plotted in Figure 66. In this plot, the drawdowns extend beyond the limits of the drawdown axis. To accommodate the entire range of drawdowns, the results are re-plotted in Figure 67 on log-log axes. As shown in the figure, a theoretical drawdown of 278 ft (84.7 m) is predicted after 20 years of pumping. This exceeds the allowable drawdown of 73 m, suggesting that the pumping rate during the constant-rate pumping test might not be sustainable over the long term.

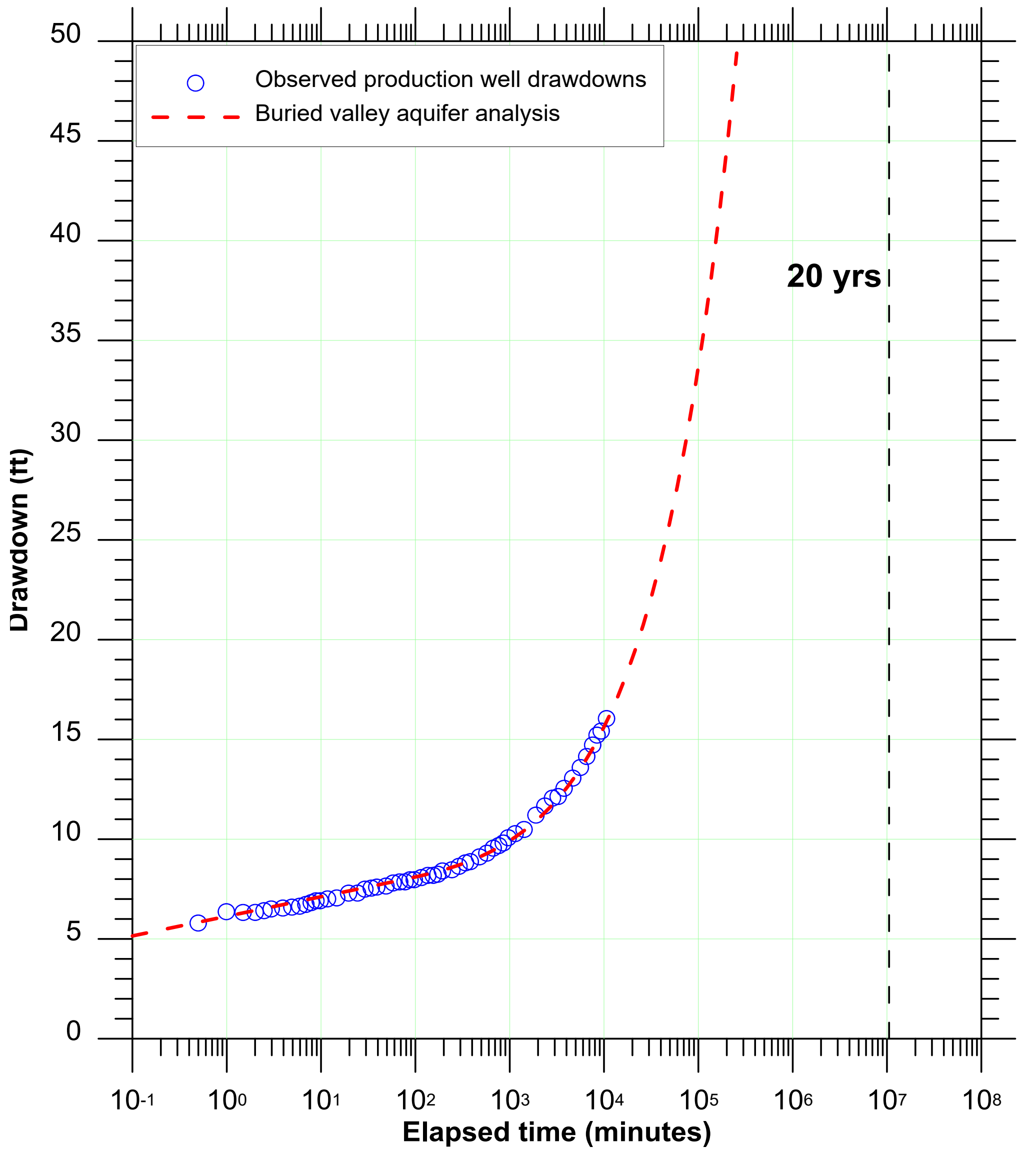

Figure 66. Long-term pumping well drawdowns predicted with the buried-valley model

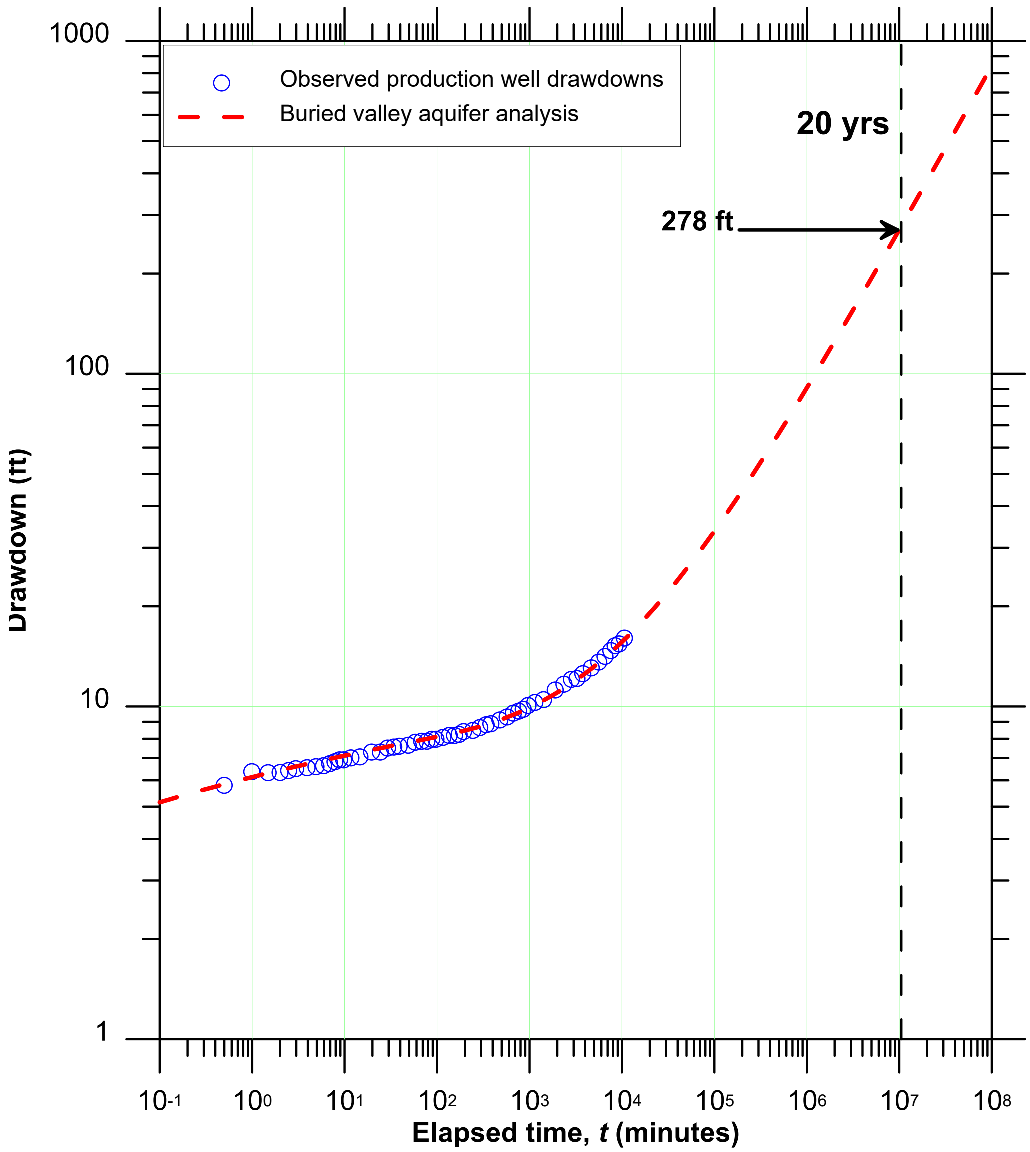

Figure 67. Long-term pumping well drawdowns predicted with the buried-valley model, logarithmic drawdown axis

The final step in the application of the Modified Moell method for the buried-valley aquifer model is to assemble the relevant drawdowns. The match to the pumping well drawdowns was obtained without invoking any additional drawdown processes; that is, all drawdowns in the pumping well are attributed to head losses in the formation. Therefore, the observed and theoretical drawdowns at 100 minutes are almost identical. The drawdowns for input to the Modified Moell method are:

$$s_{100\text{ min-theo}} = 7.99\text{ ft} = 2.44\text{ m}$$

$$s_{20\text{ years-theo}} = 278\text{ ft} = 84.73\text{ m}$$

Recalling that the allowable drawdown at the location of the Estevan 1965 pumping test is 73 m, the calculation with the Modified Moell Method yields:

$$Q = 0.7 \times \frac{(460\text{ Igpm})\,(73\text{ m})}{(2.43\text{ m}) + \left((84.73\text{ m}) - (2.44\text{ m})\right)_{theo}} \left|\frac{\text{m}^3}{219.97\text{ Igallons}}\right| \left|\frac{1440\text{ min}}{\text{day}}\right|$$

$$= \mathbf{1,820\ m^3/day}$$

11.6. Assessment of the estimates of the long-term capacity of the Estevan well

The estimates of the long-term yield of the Estevan well are summarized below.

Method	Estimated long-term yield (m^3/d)
Step test data	105,000
Q_{20} method	68,400
Modified Moell method	1,820

The long-term capacity of the Estevan well estimated with the Modified Moell Method is a relatively small fraction of the estimate developed with the Farvolden Q_{20} Method (1,820 m^3/d vs. 68,400 m^3/d) and an even smaller fraction of the value estimated from the step test.

It has been argued here that the Modified Moell method provides the most defensible estimate of the long-term sustainable yield of the Estevan well. The method is based on a conceptual model of the aquifer that is physically plausible and consistent with the hydrogeologic setting. The implementation of the conceptual model matches the complete drawdown and Derivative records for both the production well and the three observation wells.

Maathuis and van der Kamp (2003) reported the results of an analysis conducted in 1998, in which they evaluated the potential yield of the Estevan aquifer system based on the monitoring of drawdowns after 6 years of pumping followed by 3 years of recovery. They predicted that the sustainable yield of the Estevan valley aquifer ranged from 2,400 to 2,800 dam^3/yr (a dam^3 is 1,000 m^3). This corresponds to a pumping rate of between 6,600 to 7,600 m^3/d. This range exceeds the estimate developed here with Modified Moell method but is substantially smaller than the estimate developed with the Farvolden Q_{20} Method.

12. Key points

1. The estimation of the long-term capacity of a production well is a subtle task that requires professional judgement and critical thinking. Regardless of the approaches that are adopted, a big extrapolation from short-term data to long-term projections is involved.

2. Estimates of the capacity of a production well from the specific capacity and allowable drawdown are useful for reality-checks but should be treated with caution when long-term conditions are being considered.

3. Step tests are an essential component of hydrogeologic practice. Step tests are standard practice for supporting the design of a constant-rate pumping test. Step tests are usually too brief to support estimation of the long-term capacity of a well, but they do provide important insights into well conditions and how those conditions affect the drawdown in a production well.

4. The long-term capacity of production well is generally controlled by the response of the aquifer. Constant-rate pumping tests are essential for understanding that response. The key to pumping test interpretation is the inference of an appropriate conceptual model for the aquifer. In the Estevan case, the long-term drawdowns in the pumping well are controlled by the presence of the boundaries of the aquifer. The presence of these boundaries could only be inferred from a long-term constant-rate pumping test that was analyzed with consideration of the hydrogeologic setting.

13. References

Alberta Environment, 2011: Guide to Groundwater Authorization, Government of Alberta, March 2011.

Andriashek, L.D., and N. Atkinson, 2007: Buried Channels and Glacial-Drift Aquifers in Fort McMurray Region, Northeast Alberta, Alberta Geological Survey, EUB/AGS Earth Sciences Report 2007-01, March 2007.

Atkinson, N., and S. Slattery, 2011: The distribution and architecture of buried valley systems in Alberta, in Proceedings of *GeoHydro 2011*, Quebec City, August 28-31, 2011.

ASCE, 1998: Sustainability criteria for water resource systems, American Society of Civil Engineers Task Committee for Sustainability Criteria.

Bierschenk, W.H., 1964: Determining well efficiency by multiple step-drawdown tests, International Association of Scientific Hydrology, Publication No. 54 (General Assembly of Berkeley, Commission of Subterranean Waters), pp. 493-507.

Boonstra, J., 1989: **SATEM: Selected Aquifer Test Evaluation Methods**, ILRI Publication 48, International Institute for Land Reclamation and Improvement, Wageningen, The Netherlands.

Brown, R.H., 1963: The cone of depression and the area of diversion around a discharging well in an infinite strip aquifer subject to uniform recharge, in *U.S. Geological Survey Water-Supply Paper 1545C*, pp. C69-C85.

Bruin, J., and H.E. Hudson, Jr., 1955: Selected Methods for Pumping Test Analysis, Illinois State Water Survey, Report of Investigation 25, pp. 29-37.

Cambodia Construction & Engineering Co. Ltd. (CCEC), 2005: Design, Build and Lease of Water Supply Systems in Kandieng Reay Town, Svay Rieng Province, Summary Report on Water Source Investigation, Cambodia Provincial and Peri-Urban Water and Sanitation Project (CPPUWSP), Phnom Penh, Cambodia, June 25, 2005.

Cooper, H.H., Jr., and C.E. Jacob, 1946: A generalized graphical method for evaluating formation constants and summarizing well-field history, *Trans. American Geophysical Union*, vol. *27*, no. 4, pp. 526-534.

Cummings, D.I., H.A.J. Russell, and D.R. Sharpe, 2011: Buried-valley aquifers in the Canadian Prairies: A review, in Proceedings of *GeoHydro 2011*, Quebec City, August 28-31, 2011.

Driscoll, F.G., 1986: **Groundwater and Wells**, 2nd edition, Johnson Division, St. Paul, Minnesota.

Evans, D.J.A., and I.A. Campbell, 1995: Quaternary stratigraphy of the buried valleys of the lower Red Deer River, Alberta, Canada, *Journal of Quaternary Science*, vol. 10, no. 2, pp. 123-148.

Farvolden, R.N., 1959: Groundwater Supply in Alberta, Alberta Research Council, unpublished report, 9 p.

Farvolden, R.N., 1963: Bedrock channels of southern Alberta, in *Early Contributions to Groundwater Hydrology of Alberta*, Research Council of Alberta Bulletin 12, pp. 63-75.

Hantush, M.S., 1964: Hydraulics of wells, *Advances in Hydroscience*, vol. 1, pp. 281-433.

Herbert, R., and J.A. Barker, 1990: Predicting and interpreting well behaviour and well efficiency, in *Water Wells: Monitoring, Maintenance, Rehabilitation*, P. Howsam (ed.), E. & F.N. Spon, London, England.

Jacob, C.E., 1947: Drawdown test to determine effective radius of artesian well, *Transactions, American Society of Civil Engineers*, vol. 112, paper 2321, pp. 1047-1064.

Jagger Hims Ltd., 1998: Aquifer Performance Evaluation: Southeast Quadrant, reported submitted to the City of Guelph, November 1998.

Konikow, L.F., G.Z. Hornberger, K.J. Halford, and R.T. Hanson, 2009: Revised Multi-Node Well (MNW2) Package for MODFLOW Ground-Water Flow Model, United States Geological Survey, Techniques and Methods 6-A30.

Langguth, H.-R., and R. Voigt, 1980: **Hydrogeologische Methoden**, Springer-Verlag, Berlin, Germany.

Lennox, D.H., H. Maathuis, D. Pederson, 1988: Region 13: Western Glaciated Plains, in **The Geology of North America**, vol. O-2 , W. Back, J.S. Rosenshein, P.R. Seaber (eds.), The Geological Society of America, Boulder, Colorado.

Libby, R., 1979: Estimating Sustainable Yield to a Well in Heterogeneous Strata, Alberta Research Council, Bulletin 37, Edmonton, Alberta.

Maathuis, H., and G. van der Kamp, 2003: Groundwater resource evaluations of the Estevan Valley aquifer in southeastern Saskatchewan: A 40-year historical perspective, in *Proceedings of the 56th Canadian Geotechnical and 3rd Joint IAH-CNC and CGS Conference*, Winnipeg, Manitoba, 4 p.

Maathuis, H., and G. van der Kamp, 2006: The Q_{20} Concept: Sustainable Well Yield and Sustainable Aquifer Yield, prepared for Alberta Environment, Saskatchewan Watershed Authority, Prairie Farm Rehabilitation Administration, Prairie Provinces Water Board, Saskatchewan Research Council, SRC Publication No. 10417-4E06, July 2006.

Ramey, H.J., 1982: Advances in practical well-test analysis, *Journal of Petroleum Technology*, vol. 34, no. 7, pp. 650-659.

Theis, C.V., 1935. The relation between the lowering of the piezometric surface and the rate and duration of discharge of a well using groundwater storage, *American Geophysical Union Transactions*, vol. 16, pp. 519-524.

van der Kamp, G., 1985: Brief quantitative guidelines for the design and analysis of pumping tests, presented at the 18th Congress of the International Association of Hydrogeologists, September 8-13, 1985, Cambridge, U.K.

van der Kamp, G., and H. Maathuis, 2002: The peculiar groundwater hydraulics of buried-channel aquifers, in *Ground and Water: Theory to Practice*, Proceedings of the 55th Canadian Geotechnical and 3rd Joint IAH-CNC and CGS Groundwater Specialty Conference, Niagara Falls, Ontario, pp. 695-698.

van der Kamp, G., and H. Maathuis, 2005: The applicability of "Q20" methods for determining sustainable groundwater yields, in *Proceedings of the 58th Canadian Geotechnical Conference and 6th Joint IAH-CNC Groundwater Specialty Conference*, Saskatoon, Saskatchewan, September 18-21, 2005.

van der Kamp, G., and H. Maathuis, 2006: Groundwater sustainability in the Prairies – Some examples, in *Proceedings of the 59th Canadian Geotechnical Conference/4th Joint IAH-CNC/CGS Conference*, Vancouver, British Columbia, p. 1288-1293.

van der Kamp, G., and H. Maathuis, 2012: The unusual and large drawdown response of buried-valley aquifers to pumping, *Ground Water*, vol. 50, No. 2, pp. 207-215.

Walton, W.C., 1965: Potential Yield of a Sand and Gravel Aquifer in a Buried Valley near Estevan, Saskatchewan, report prepared for the Saskatchewan Research Council, Saskatoon, Saskatchewan.

Walton, W.C., 1970: **Groundwater Resource Evaluation**, McGraw-Hill, New York, New York.

Weyer, K.U., 2003: Determination of hydrogeological parameters from pumping of water wells in Alberta, WDA Consultants Inc., Calgary, Alberta, March 2003, 10 p.